



ASSESSING THE POTENTIAL FOR CARBON SEQUESTRATION IN DEPLETED HEAVY OIL RESERVOIRS USING ACOUSTIC LOGGING

Mumuni Amadu^[a] and Adango Miadonye^[b]

Keywords: carbon sequestration, heavy oil reservoir, heat transfer, acoustic logging, carbon dioxide emission.

As global warming due to anthropogenic greenhouse gases, notably carbon dioxide threatens to take a catastrophic dimension, geological storage of carbon dioxide has been widely accepted as a technically and economically viable remediation strategy. Consequently, targeted geological repositories are saline aquifers, salt caverns, deep unmineable coal seams and depleted oil and gas reservoirs. For storage in depleted oil reservoirs, the stratigraphic trapping capability of overlying low permeability shale is the principal motivating factor for long term containment of anthropogenic gas in oil reservoir until its dissolution and final immobilization by mineral carbonation reactions. Consequently, where the development of the oil reservoir by thermal recovery can lead to thermal pressurization of the cap rock layer, the ability of such a depleted reservoir to contain anthropogenic carbon dioxide must be thoroughly investigated to assess its competency as a proposed geological repository. In this study, seismic theory coupled with that of heat transfer has been used to derive interval velocity for a heavy oil reservoir under thermal recovery. The resulting equation has been validated using published works from literature sources.

* Corresponding Authors

E-Mail: adango_miadonye@cbu.ca

- [a] Department of Process Engineering and Applied Science,
Dalhousie University, Halifax, NS, Canada
[b] School of Science and Technology, Cape Breton University,
P.O. Box 5300, Sydney, NS, Canada.

Introduction

The capture and isolation of anthropogenic carbon dioxide in suitable geologic media have been universally acclaimed as a suitable global warming mitigation step. These geologic repositories could be depleted oil and gas reservoirs, salt caverns, deep unmineable coal seams and deep saline aquifers. In seeking to isolate carbon dioxide in depleted oil and gas reservoirs and deep saline aquifers one fundamental requirement is of technical importance. The reservoir or saline aquifer must be capped by a low permeability geological formation capable of providing long term hydrodynamic trapping mechanism in order to safely contain the injected gas until ultimate dissolution occurs under the subsurface environment. This crucial hydrodynamic trapping mechanism must be effective during injection and post injection periods.¹

Among the depleted oil reservoirs are those that were produced using thermal recovery techniques. Where these reservoirs are found at depths capable of sustaining injected carbon dioxide under supercritical conditions such as in China and Venezuela they are possible candidates for carbon geosequestration. However, in view of excessive heating environment connected to their development these deep depleted heavy oil reservoirs need to be thoroughly evaluated for cap rock geomechanical integrity before being included in the inventory of suitable depleted oil reservoirs.²⁻⁴ This technical evaluation is necessary because the high temperature of hot water or steam used in thermal oil recovery methods result in heat transfer from the

reservoir into the overlying cap rocks. The geomechanical implication of this heat transfer is seen in possible thermal pressurization of the resident brine in the cap rock. The low permeability nature of these cap rocks makes it difficult to diffuse excess pore pressure resulting in pore pressure levels exceeding limits required for tensile or shear failure. To obtain an idea about cap rock long term geomechanical integrity there is the need to monitor cap rock performance during thermal operations of deep heavy oil reservoirs. This requires time lapse seismic or acoustic monitoring, which consists of using base line seismic or acoustic survey results as a standard for comparison against current survey results. The aim of this paper is to analytically derive an equation that will link interval velocity to depth temperature during thermal operation designed to produce deep heavy oil reservoirs. Such an equation will enable the calculation of temperature change from acoustic monitoring data where interval velocity versus depth is measured from time to time during thermal operations of deep heavy oil reservoirs.

Theoretical Derivation

The most common approach for linking acoustic interval velocity to pore pressure is the famous Eaton's empirical equation given as follows:^{5,8}

$$P_p = P_{obs} - (P_{obs} - P_{hyd}) \left(\frac{V_i}{V_n} \right)^3 \quad (1)$$

Isolating the interval velocity in equation 1 gives:

$$V_i = \left[\frac{(P_{obs} - P_p) V_n^3}{(P_{obs} - P_{hyd})} \right]^{\frac{1}{3}} \quad (2)$$

Assuming a temperature change from initial value T_0 to T in the cap rock due to heat transfer from the injected fluid induces a pore pressure change due to aquathermal pressurization the pressure change and temperature change are related by.⁶

$$\Delta P_p = \frac{[\alpha_s(1-\phi) + \phi\alpha_f]}{c_w\phi} \Delta T \quad (3)$$

Integration of equation 3 within appropriate limits gives:

$$\int_{P_{pi}}^{P_p} dP_p = \frac{[\alpha_s(1-\phi) + \phi\alpha_f]}{c_w\phi} \int_{T_0}^T dT = \lambda \int_{T_0}^T dT \quad (4)$$

$$\lambda = \frac{[\alpha_s(1-\phi) + \phi\alpha_f]}{c_w\phi} \quad (5)$$

$$P_p - P_{pi} = \lambda(T - T_0)$$

$$P_p = \lambda(T - T_0) + P_{pi} \quad (6)$$

The following quantities will be defined:

$$\rho = \frac{V_n^3 P_{dcs}}{P_{dcs} - P_{hyd}} \quad (7)$$

$$\mu = \frac{V_n^3}{P_{dcs} - P_{hyd}} \quad (8)$$

Equation 2 can be written as:

$$V_i = (\rho - \mu P_p)^{\frac{1}{3}} \quad (9)$$

Assuming:

$$U = (\rho - \mu P_p) \quad (10)$$

Equation 9 can be written as:

$$V_i = U^{1/3} \quad (11)$$

U is a function of pressure so:

$$V_i = V_i(U(P_p)) \quad (12)$$

Differentiating equation 11 with regard to pore pressure gives:

$$\frac{dV_i}{dP_p} = \frac{dV_i}{dU} \frac{dU}{dP_p} = \frac{1}{3} U^{-2/3} \frac{dU}{dP_p} \quad (13)$$

From equation 10:

$$\frac{dU}{dP_p} = -\mu \quad (14)$$

Substituting equation 14 into equation 13 gives:

$$\frac{dV_i}{dP_p} = -\frac{1}{3} U^{-2/3} \mu = -\frac{\mu}{3} (\rho - \mu P_p)^{-2/3} \quad (15)$$

$$dV_i = -\frac{1}{3} U^{-2/3} \mu = -\frac{\mu}{3} (\rho - \mu P_p)^{-2/3} dP_p \quad (16)$$

Substituting for dP_p from equation 8 into equation 16 gives:

$$dV_i = -\frac{\mu}{3} (\rho - \mu P_p)^{-2/3} [\alpha_s(1-\phi) + \phi\alpha_f] dT \quad (17)$$

Substituting for pore pressure from equation 6 into equation 17 gives:

$$dV_i = -\frac{\mu}{3} [\rho - \mu \{\lambda(T - T_0) + P_{pi}\}]^{-2/3} [\alpha_s(1-\phi) + \phi\alpha_f] dT \quad (18)$$

$$\int_0^{V_i} dV_i = -\frac{\mu\gamma}{3} \int_{T_0}^T [\rho - \mu \{\lambda(T - T_0) + P_{pi}\}]^{-2/3} dT$$

$$V_i = -\frac{\mu\gamma}{3} \int_{T_0}^T [\rho - \mu \{\lambda(T - T_0) + P_{pi}\}]^{-2/3} dT = -\frac{\mu\gamma}{3} \int_{T_0}^T \frac{1}{[(\mu T_0 - \mu P_{pi} + \rho) - \mu T]^{2/3}} dT$$

$$V_i = -\frac{\mu\gamma}{3} \int_{T_0}^T [\rho - \mu \{\lambda(T - T_0) + P_{pi}\}]^{-2/3} = -C \int_{T_0}^T \frac{1}{[A - B]^{2/3}} \quad (19)$$

where:

$$A=(\mu l T_0 - \mu P \rho i + \rho); B=\mu l T; C=\frac{\mu l}{3} \quad (20)$$

Integration using maple program gives:

$$V_i = \frac{C(T_0 - T)}{(A - BT)^{2/3}} \quad (21)$$

Equation 21 finally links the interval velocity of acoustic wave to temperature. It shows an imminent decrease of velocity with temperature increases in thermal operations related to steam or water injection when temperature in the cap rock changes due to heat transfer from the reservoir.

Interval velocity is a function of depth in the sedimentary basin during well logging. Equation 21 can therefore be written in functional notation as:

$$V_i(Z) = \frac{C(T_0 - T(Z))}{(A - BT(Z))^{2/3}} \quad (22)$$

where:

$$V_i(Z) = F(Z) \quad (23)$$

Z= depth in the sedimentary basin

Derivation of Interval Velocity with Temperature Change

Where there is porosity change as a result of thermal pressurization, the relationship between porosity and transit time or slowness is given by the equation.¹⁴

$$\phi = \frac{\Delta t_{\text{obs}} - \Delta t_{\text{m}}}{\Delta t_{\text{f}} - \Delta t_{\text{m}}} = \frac{\Delta t_{\text{obs}}}{\Delta t_{\text{f}} - \Delta t_{\text{m}}} - \frac{\Delta t_{\text{m}}}{\Delta t_{\text{f}} - \Delta t_{\text{m}}} \quad (24)$$

Transit time or slowness is reciprocal of interval velocity thus observed interval velocity is given by:

$$V_i = \frac{1}{\Delta t_{\text{obs}}} \quad (25)$$

Equation 24 can be written as:

$$\phi = \frac{\Delta t_{\text{obs}} - \Delta t_{\text{m}}}{\Delta t_{\text{f}} - \Delta t_{\text{m}}} = \frac{1}{\Delta t_{\text{f}} - \Delta t_{\text{m}}} V_i^{-1} - \frac{\Delta t_{\text{m}}}{\Delta t_{\text{f}} - \Delta t_{\text{m}}} \quad (26)$$

Differentiating equation 25 with respect to interval velocity gives:

$$d\phi = \frac{\Delta t_{\text{obs}} - \Delta t_{\text{m}}}{\Delta t_{\text{f}} - \Delta t_{\text{m}}} = -\frac{1}{\Delta t_{\text{f}} - \Delta t_{\text{m}}} V_i^2 dV_i \quad (27)$$

For pore change resulting from thermal pressurization pore pressure change is related to temperature change as given in equation 3:

$$dP_p = \frac{[\alpha_s(1-\phi) + \phi\alpha_f]}{c_w\phi} dT \quad (28)$$

Thus:

$$\frac{dP_p}{dT} = \frac{[\alpha_s(1-\phi) + \phi\alpha_f]}{c_w\phi} \quad (29)$$

Assuming thermal pressurization of pore fluid results in a deformation that translates into a porosity change this will be given by:⁷

$$d\phi = -\phi C_s dP_p - (1-\phi)\alpha_s dT \quad (30)$$

From equation 30 the following can be written:

$$\frac{d\phi}{dT} = -\phi C_s \frac{dP_p}{dT} - (1-\phi)\alpha_s \quad (31)$$

This implies:

$$\frac{dP_p}{dT} = -\frac{\frac{d\phi}{dT} + (1-\phi)\alpha_s}{\phi C_s} \quad (32)$$

Equating equation 32 to equation 28 gives:

$$\left[\frac{\alpha_s(1-\phi) + \phi\alpha_f}{\phi c_w} \right] = -\frac{\frac{d\phi}{dT} + (1-\phi)\alpha_s}{\phi C_s} \quad (33)$$

This gives the temperature derivative of porosity as:

$$\frac{d\phi}{dT} = (1-\phi)\alpha_s - \phi C_s \left[\frac{\alpha_s(1-\phi) + \phi\alpha_f}{\phi c_w} \right] \quad (34)$$

Thus:

$$\left[\frac{1}{\left(\alpha_s - \frac{\alpha_f C_s}{c_w} \right) + \phi \left(\frac{\phi C_s \alpha_s}{c_w} \right)} \right] d\phi = dT \quad (35)$$

The following quantities will be defined:

$$\Pi = \left(\alpha_s - \frac{\alpha_f C_s}{c_w} \right)$$

$$\Omega = \left(\frac{\phi C_s \alpha_s}{c_w} \right)$$

Equation 35 becomes:

$$\frac{1}{[\Pi + \Omega\phi]} d\phi = dT \quad (36)$$

Integration gives:

$$\frac{1}{\Omega} \int_{\phi}^{\phi} \frac{1}{(\Pi + \Omega\phi)} d\phi = \int_{T_0}^T dT \quad (37)$$

$$\frac{1}{\Omega} \ln(\Pi + \Omega\phi) - \frac{1}{\Omega} \ln(\Pi - \Omega\phi) = T - T_0 \quad (38)$$

Thus:

$$\ln \left[\frac{\Pi + \Omega\phi}{\Pi - \Omega\phi} \right] = \Omega(T - T_0) \quad (39)$$

$$\phi = \frac{1}{\Omega} \left[(\Pi + \Omega\phi) \exp \Omega(T - T_0) - \Pi \right] \quad (40)$$

Equation 27 gives:

$$\phi = \frac{\Delta t_{obs} - \Delta t_{m}}{\Delta t_f - \Delta t_{m}} = \frac{1}{\Delta t_f - \Delta t_{m}} \frac{1}{V_i} - \frac{\Delta t_{m}}{\Delta t_f - \Delta t_{m}} \quad (41)$$

Substituting for porosity from equation 27 into equation 39 gives:

$$\frac{1}{V_i} = \frac{1}{\Omega} \left[(\Pi + \Omega\phi) \exp \Omega(T - T_0) - \Pi \right] (\Delta t_f - \Delta t_{m}) + \Delta t_{m} \quad (42)$$

Thus:

$$\phi = \frac{\Delta t_{obs} - \Delta t_{m}}{\Delta t_f - \Delta t_{m}} = \frac{1}{\Delta t_f - \Delta t_{m}} \frac{1}{V_i} - \frac{\Delta t_{m}}{\Delta t_f - \Delta t_{m}} \quad (43)$$

$$= \frac{1}{\Omega} \left[(\Pi + \Omega\phi) \exp \Omega(T - T_0) - \Pi \right]$$

This gives the relationship between interval velocity and temperature as:

$$V_i = \frac{1}{\Omega^{-1} \left[(\Pi - \Omega\phi) e^{\Omega(T - T_0)} \right] (\Delta t_f - \Delta t_{m}) + \Delta t_{m}} \quad (44)$$

In equation 44 the interval transit time for fluid and matrix are constants. All other quantities in the equation on the right hand side are constants except temperature. The equation therefore shows that as temperature increases the denominator increases and the effect is to decrease interval transit time as proven earlier.

Experimental Validation

The experimental validation of this equation requires laboratory measurement of acoustic wave velocity under reservoir conditions where *in situ* formation stresses are provided in the measuring system. For this paper the experimental validation of the equation will be sought by using experimental results from published literature sources. Equation 18 shows that by using log derived interval velocity the temperature at the given depth can be calculated and this can form the basis of time lapse acoustic monitoring in thermal operations. The parameter A in equation 21 contains pore pressure. Figure 1 shows a theoretical plot of this velocity trend with different pore pressures.

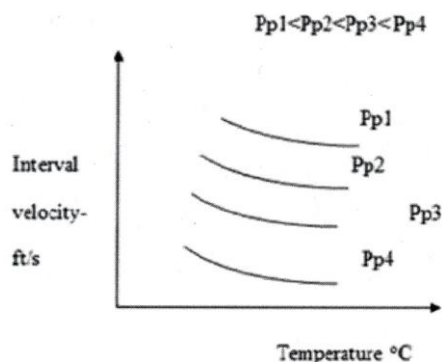


Figure 1. Theoretical plot of Eqn. 22 for different pore pressures

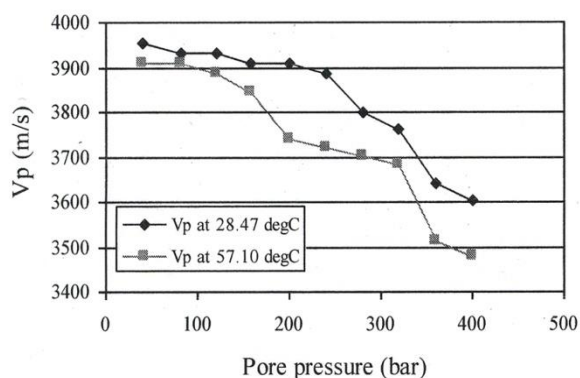


Figure 2. The effect of pore pressure on compressional wave velocity at different temperatures⁹

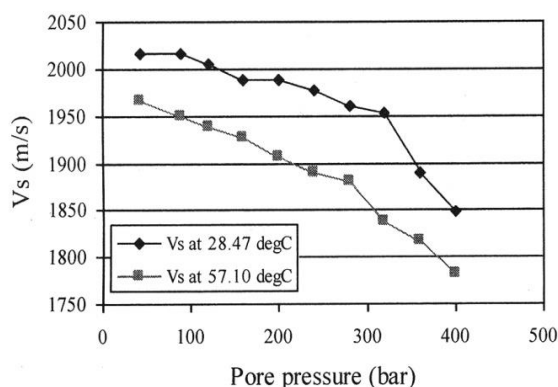


Figure 3. The effect of pore pressure on shear wave velocity at different temperatures⁹.

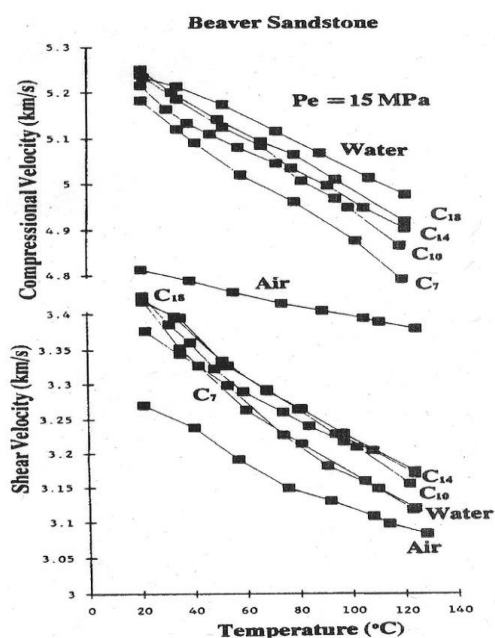


Figure 4. Then effect of temperature on compressional (top) shear (bottom) wave velocities for for different fluid contents Beaver sandstone¹²

Discussion

The demand for coal (hard coal, brown coal, lignite) has grown by 62 % over the past thirty years. The International Energy Administration (IEA), in its reference scenario, expects coal demand to grow by another 53 % up to 2030 with a possible decline in the market after this period due to carbon constraints in economies (Klaus Brendau).¹¹

This means that anthropogenic emission of carbon is supposed to reflect this growth in energy consumption trend. Since geological sequestration has been accepted by the intergovernmental panel on Climate Change as the most technically feasible mitigating step in reducing global warming, due to anthropogenic carbon dioxide emission, more geological repositories will be required to achieve this environmental remediation objective.

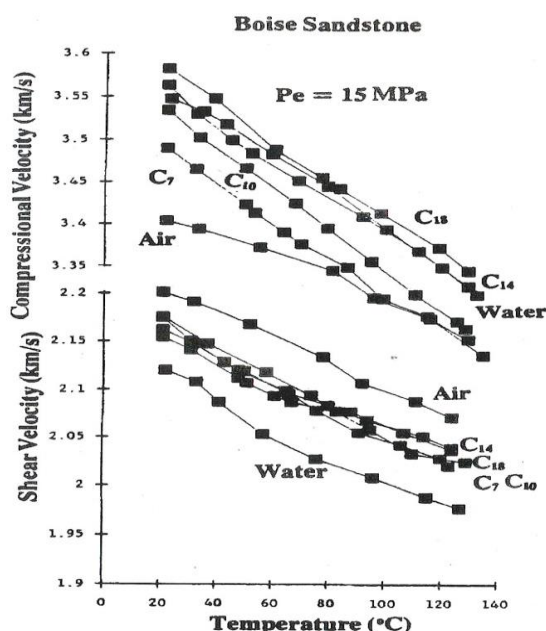


Figure 5. Then effect of temperature on compressional (top) and shear (bottom) wave velocities for different fluid contents of Boise sandstone¹²

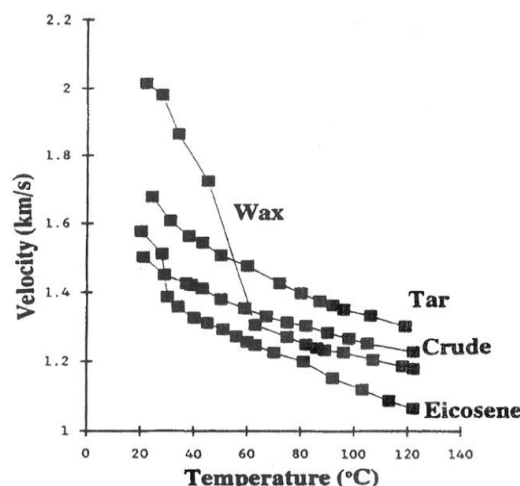


Figure 6. The effect of temperature on compressional (left) and shear (right) wave velocities for different fluid contents for Ottawa and Boise sands respectively¹²

This means that all the target geological repositories, depleted oil and gas reservoirs, salt caverns, deep unmineable coal seams and saline aquifers need to be geologically and technically evaluated for anthropogenic carbon dioxide sequestrations projects on global basis. In line with this objective deep depleted heavy oil reservoirs that have had their cap rocks subjected to excessive heat flow need to be thoroughly evaluated geomechanically during and after thermal operations. This is necessary to ensure that thermal pressurization of resident pore fluid in low permeability geologic formation that has the potential to induce shear and tensile failure did not reduce the hydrodynamic trapping capability of these cap rocks by impacting their capillary entry pressures and their required low permeabilities.

To be able to carry out this assessment there is the need to be able to obtain information about the heat transfer characteristic of the cap rock and the temperature evolution during thermal operation. Two approaches are possible. One an indirect method and it is based on the mathematical modelling of heat transfer in the cap rock reservoir system and solution of the temperature evolution for both reservoir and cap rock. In the hydrogeological industry this approach has been used to obtain the temperature field of the system in matters related to aquifer thermal energy storage for seasonal exploitation. In this paper an alternative approach base on a direct method of the time lapse acoustic monitoring of deep heavy oil reservoir thermal exploitation is proposed. This has to do with the time to time measurement of a seismic attribute which is the interval velocity. To be able to achieve this objective an equation that links interval velocity to temperature change has been presented. Since acoustic data such as interval velocity is depth related the corresponding temperature will be the temperature at the depth following thermal operation. The difference between this and the initial temperature imposed by the local geothermal gradient will be the temperature change since thermal operation began. Due to lack of laboratory resource experimental validation of the equation was not possible but interpretation of the equation by comparison with experimental data and graphical plots from literature sources shows that the equation is capable of predicting similar experimentally determined trends. In this regard, Figures 2 to 6 indicate a decrease in interval velocity for primary and shear waves with temperature increase which has been theoretically established by this work.

Application to thermal monitoring of critical interval velocity

Time lapse seismic or acoustic monitoring involves the time to time measurement of seismic or acoustic attributes of the earth related to saturation change resulting from fluid injection, change in bulk density resulting from hydraulic fracturing, change in interval velocity resulting from temperature change accompanying heat injection etc. and comparing these surveys with a base line survey acquired before any operations began. For a cap rock submitted to heat accumulation due to heat transfer from an injected fluid, the critical temperature resulting in tensile failure due to thermal pressurization of pore fluid will result in a critical interval velocity as given by equation 22:

$$V_i(Z) = \frac{C(T_i - T(Z))}{(A - BT(Z))^2} = F(Z)$$

The temperature at which this occurs is given by substituting critical temperature for temperature in equation 22. This temperature will be a function of depth as predicted by equation 22.

Figure 7 gives the observed sonic log velocities versus travel time (a) prior to heating as against hypothetical sonic log velocities (b) after heating of the reservoir. The figure shows that prior to heating the average elastic wave velocity between 120 and 150 meters was about 2400 m/s. After heating the average elastic wave velocity over the same

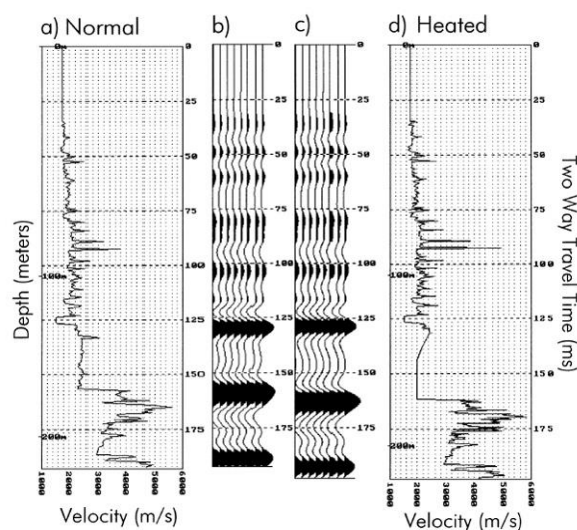


Figure 7. Comparison of logging data before and after heating¹⁰

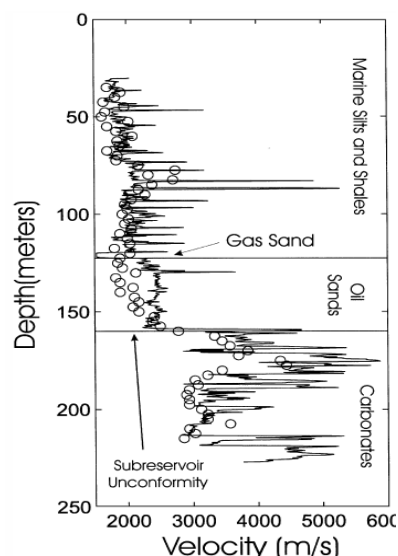


Figure 8. Sonic log showing characteristic interval velocity (line and open interval velocity after thermal recovery open circle)¹⁰

depth interval is seen to be about 2100 m/s (Figure 7(b) and (c)). The figure clearly shows a shift of the interval velocity after thermal recovery to the left, a clear evidence of decrease in interval velocity after thermal operations. This shows that by using log derived data such as the interval velocity the temperature of the cap rock interval corresponding to these time lapse acoustic log can be deduced using relevant thermophysical parameters together with the equation 22.

Figure 8 also shows a graphical plot of sonic log characteristic interval velocity of a heavy oil reservoir (line) consisting of sand and with an overlying marine silt and clay cap rock and the characteristic interval velocity after thermal recovery. It clearly shows a shift of the interval velocity after thermal recovery to the right in both the reservoir and the cap rock, a clear evidence of decrease in interval velocity after thermal recovery of heavy oil. This shows that by using log derived data such as the interval velocity the temperature of the cap rock interval corresponding to these time lapse acoustic log can be deduced using relevant thermophysical parameters together with equation presented by this work.

Application to Thermal monitoring of Critical State Properties

Monitoring of subsurface operations refers to the systematic measurements and detection of subsurface property changes in response to subsurface related processes such as temperature and stress changes. These are invariably related to thermal operations in tertiary enhanced oil recovery of heavy oils or the injection of fluid into petroleum reservoirs as encountered in secondary oil recovery and carbon dioxide injection into saline aquifers. Each of these activities has the potential to perturb subsurface pressure and temperature regimes. In either of these operations there are two types of monitoring objectives.¹³ Deep monitoring of the reservoir or geologic repository integrity and most importantly plume evolution for the case of carbon geosequestration and near surface monitoring is designed to ensure public safety and environmental health. These two principal aims underlie traditional monitoring operations of subsurface operations but in the case of carbon geosequestration where cap rock (low permeability overlying) formation with hydrodynamic trapping capability is fundamental to long term safe geological isolation of the gas, monitoring of this formation deserves to be considered and is the key focus of this work. In this regard, while thermal and fluid injection operations change the pressure and temperature regimes of the reservoir and therefore stress regimes, these two operations will not cause flow in the cap rock but will induce similar stress changes through heat transfer and pressure build up in the reservoir particularly in the vicinity of the injection wells. Heat transfer from the injected fluid into the cap rock causes thermal loading of the resident fluid with attendant excess pore pressure build ups while fluid pressure at the base of the cap rock induces bending in the cap rock with attendant stress problems. To assess the potential of the cap rock for carbon sequestration, therefore, requires monitoring the cap rock and making sure critical pressures and stresses are not exceeded to cause failure and undermined the geomechanical integrity.

Conclusion

Global warming due to anthropogenic emission of carbon dioxide has reached unprecedented levels. To mitigate global warming effects due to this gas geological storage of anthropogenic carbon dioxide is the most technically feasible and affordable solution from both immediate and long term planning perspectives. To achieve this, depleted oil reservoirs are good candidates for geologic repositories. Among these reservoirs there those that containing oils that cannot be produced without heat inputs. These are deep heavy oil reservoirs where carbon dioxide can exist under supercritical conditions. The occurrence of these reservoirs has been reported in China where anthropogenic carbon dioxide emissions are at record levels. The implication is that the excessive heat inputs can render the cap rocks of these reservoirs geomechanically unsuitable for carbon sequestration purposes. To be able to determine their suitability therefore requires monitoring their thermal operations. One way to do this is to use time lapse seismic or acoustic monitoring. It consists of measuring seismic attributes such as velocity or acoustic impedance from time to time and a comparison of this with base line survey results.

To be able to achieve this objective this paper has presented an equation that links interval velocity to temperature during thermal operation designed for heavy oil exploitation. Although lack of acoustic logging data for such purposes are not available for testing the equation the observation is that it theoretically predicts experimental trends reported in literature works and can be used to aid temperature computations using acoustic logging data and inputs of petrophysical and thermophysical property data.

Greek Symbols and Nomenclatures

P_p =Pore pressure, psi

P_{obs} =Overburden pressure, psi

P_{hyd} =Hydrostatic pressure, psi

V_i = Interval velocity, ft s⁻¹

V_n = Normally compacted shale interval velocity, ft/s

Φ = porosity change,

Φ_0 = initial porosity,

C_s = grain compressibility,

P_p = pore pressure

References

- ¹Durk-Jan Peet (Editor):" *Geotechnology and Sustainable Development: Challenges for the Future*" **2008**, ISBN 978-90-5972-293-4
- ²Liu Wenzhang Research Institute of Petroleum Exploration and Development, CNPC, China:" *Thermal Recovery Status and Development Prospect for Heavy Oil in China*" UNITAR Centre for Heavy Crude and Tar Sands. No.198, **1998**
- ³Head, I. M., Jones, D. M. and Larter, S. R., *Nature*, **2003**, 426(20), 344. www.nature.com/nature

- ⁴Eremenko, E., Kochanova, S., Kourenko, M., Perevozchikov, S., "Simulation of a Sector Model of the Heavy Oil Thermal Recovery" Society of Petroleum Engineers, **2004**.
- ⁵Eaton, B. A., *World Oil*, **1972**, 182, 51-56.
- ⁶Shi, Y.-L. and Wang, C.-Y., *J. Geophys. Res.*, **1986**, 91(B2), 2153-2162.
- ⁷Ghabezloo, S. and Sulem, J., *Ital. Geotechn. J.*, **2012**, 1, 29-43.
- ⁸Chopra, S. and Huffman, A., "Velocity determination for pore pressure prediction" 28 CSEG RECORDER, April **2006**
- ⁹Setyowiyoto, J. and Samsuri, A., *Int. J. Eng. Technol., IJET*, **2009**, 9(10), 80-93.
- ¹⁰Schmitt, D. R., *Geophysics*, **1999**, 64(2), 368-377.
- ¹¹Klaus Brendow, "World Coal Perspectives to 2030" World Energy Council, Geneva/London, **2004**.
- ¹²Wang, Z. and Nur, A., *Geophysics*, **1990**, 55(10), 723-733.
- ¹³Wielopolski, L., *Int. J. Environ. Res. Public Health*, **2011**, 8, 818-829.
- ¹⁴Raymer, L. L., Hunt, E. R., and Gardner, J., S., *An Improved Sonic Transit Time-to-Porosity Transform*, SPWLA Twenty-First Annual Logging Symposium, July, 8-11, 1980.

Received: 09.09.2014.

Accepted: 04.11.2014.



AGGREGATION AND COMPLEX FORMATION OF COBALT(II) SULFONATED PHTHALOCYANINE WITH 1,4- DIAZABICYCLO[2.2.2]OCTANE IN WATER-ORGANIC MEDIUM

Anna Filippova,^[a] Alena Voronina,^[a] Natalya Litova,^[a] Mikhail Razumov,^[a] Artur Vashurin^{[a]*}
and Svetlana Pukhovskaya^[a]

Keywords: cobalt(II) tetrasulfophthalocyaninate, solution, self-association, water, ethanol, DABCO

Self-association of water-soluble Co(II)-phthalocyanine has been studied. Influence of axial coordination of DABCO and nature of solvent on self-association of metallophthalocyanines is shown. Features of solvation interaction of cobalt(II) tetrasulfophthalocyaninate in water and water-ethanol mixture are identified.

* Corresponding Authors

E-Mail: asvashurin@mail.ru

[a] Ivanovo State University of Chemistry and Technology,
Ivanovo, 153000 Sheremetevsky str. 7, Russia

Introduction

The relevance of present study emanates from the use of cobalt(II) tetrasulfophthalocyanine as catalyst for mild oxidation processes of organic compounds.¹⁻³ It is known that the homogeneous catalytic process is accompanied by self-association processes of the phthalocyanine catalyst.⁴⁻⁷

Influence of self-association of metallophthalocyanines on their catalytic properties is ambiguous. On one hand the activity of phthalocyanine as catalyst decreases, on other hand, self-association processes favors the formation of phthalocyanine supramolecular structures⁸⁻¹⁰ that can result in increased output of the target product of catalysis in the synthesis.

To decrease aggregation and increase catalytic activity of metallophthalocyanines, a procedure of macrocycle heterogenization on the surface of solid-phase carrier need to be carried out.¹¹⁻¹⁵ It leads to increased chemical bonding of macrocycle and polymer surface.

However, presently there is no way to control the processes of association and increase catalytic activity of metallophthalocyanines in homogenous medium. Research directed to use various alloying supplements in homogenous catalysis is mainly empirical and often have random nature. Such supplements, casually represented by axial ligands, are considered as part of models, imitating active site of mono- and dioxygenases enzymes. As of now there are many examples of catalytic reactions, when a small amount of specific supplement increases the rate of reaction but not output. Usually unproved mechanisms of supplementary action has been suggested by the authors.¹⁶

Hence the possibility to control the self-association of metallophthalocyanines due to axial coordination processes and variation of solvating power of medium to create catalytic active liquid-phase systems is promising. Accessibility of metallophthalocyanines reaction center for bonding of additional ligand during axial coordination is very important.

There is almost no works about association in the presence of bidentate axial ligands in the literature. However, it is known, that formation of molecular associates with polydentate ligands can change coordination ability of macroheterocycles and type of metallophthalocyanines associates in solution.¹⁷⁻²⁰ Besides interaction between metallophthalocyanines and polydentate ligands is interesting for fundamental studies of supramolecular liquid-phase systems formation also.

The possibility to control the monomer-dimer associative equilibrium for cobalt(II) tetrasulfophthalocyaninate due to molecular complex formation with 1,4-diazabicyclo[2.2.2]octane (DABCO) and variation of solvating power of medium is considered in this work.

Experimental

Cobalt(II) tetrasulfophthalocyaninate (CoPc) was synthesized and purified by a known direct sulfonation method.²¹

Its composition and structure is confirmed by electron-absorption (UV-Vis) spectroscopy, IR spectroscopy and elemental analyzes. IR-spectra were recorded on the Avatar 360 FT-IR spectrophotometer using KBr tablets. There are intense bands at 700, 1032-1035, 1192-1197 cm^{-1} , it is caused by presence of sulfonic groups. Oscillation in 839-855 cm^{-1} is caused by C-H vibrations of three-substituted benzene nuclei connecting with porfirazine ring. IR-spectra matched with literature data.¹⁸

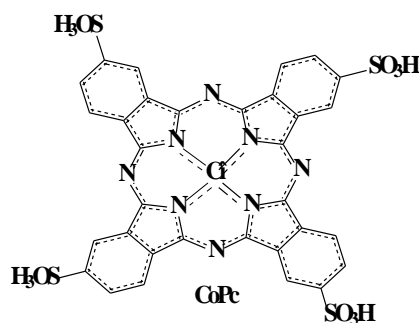


Figure 1. Cobalt(II) tetrasulfophthalocyaninate

1,4-Diazabicyclo[2.2.2]octane (DABCO) was commercial product (Sigma-Aldrich) with 99.98% purity and was used as received.

Degassed distilled water was used for preparing the solutions. Solvents, used for the work, was purified by known methods.^{22,23} Water content in ethanol was determined by potentiometric titration according to Fisher's method.²³

Coordination of DABCO with CoPc was studied by spectrophotometric method. UV-Vis spectra were registered with UNICO-2800 spectrophotometer. Investigations were carried out at 298.15 K in quartz cell with depth of absorbing layer of 10 mm, placed in a thermostatic cell.

To calculate stability constants of molecular complexes analytical wavelengths from UV-Vis spectra were used.

$$K_y = \frac{[LCoPc]}{[CoPc][L]} \quad (1)$$

Equilibrium concentration of molecular complex was calculated according to eqn. (2)

$$c_{LCoPc} = c_{CoPc}^0 \cdot \frac{(A_b - A_p)}{(A_b - A_k)} \quad (2)$$

where c_{LCoPc} is equilibrium LCoPc concentration, c_{CoPc}^0 is an initial CoPc concentration, A_0 , A_p and A_k are initial, equilibrium and final optical density of the solution respectively.

Concentration of unbonded ligand was calculated according to the Eqn. (3).

$$c_L = c_L^0 - c_{CoPc}^0 \cdot \frac{(A_b - A_p)}{(A_b - A_k)} \quad (3)$$

Combination of equations (1) and (3) leads to equation (4), which enables one to calculate the equilibrium constant.

$$K_y = \frac{[(A_b - A_p)/(A_p - A_k)]}{[c_L^0 - c_{CoPc}^0 \cdot (A_b - A_p)/(A_b - A_k)]} \quad (4)$$

Investigation was carried out with a hundredfold excess of the ligand to relative CoPc, therefore the equilibrium concentration of the ligand was taken as its initial concentration. It simplified the calculation of K_y equation (5).

$$K_y = \frac{(A_b - A_p)}{(A_b - A_k) \cdot c_L^0} \quad (5)$$

Results and Discussion

We have investigated the self-association processes of CoPc in water previously.⁶ Earlier data showed that in concentration range of $2 \times 10^{-5} - 2 \times 10^{-4} \text{ mol L}^{-1}$, the phthalocyanine is mostly dimerized, caused by π - π interaction between macrocycles molecules. π - π Dimers are formed due to π - σ -contraction and π - π -repulsion of macrocycles electron systems.²⁴ Variation in the solvents' solvation properties lead to a shift in the monomer-dimer equilibrium (6) and hence in the catalytic activity of CoPc.



Introduction of strong electron donors in the system, for example pyridine that is able to form stable axial complexes²⁵ with CoPc, leads to shift of associative equilibrium (6) towards the monomeric form due to destruction of π - π - dimer and domination of π - π - repulsion of electrons systems of two macromolecules that causes changes in its solvation environment. The solvation power is reduced by lowering the dielectric constant of the medium (ϵ_{Py} 12.3; ϵ_{H_2O} 78.5)²⁶ of mixed solvent. However, it is amplified by specific solvation electron-donor properties of an organic solvent (DN_{Py} 33.1; DN_{H_2O} 18).²⁶

Pyridine, displacing water from the near solvation field of metal cation in phthalocyanine, forms stable axial complex (K_y $800 \pm 20 \text{ L mol}^{-1}$). It is not a favorable factor. Mechanisms of oxidation of certain organic compounds with phthalocyanines complexes suggest easy removal of solvent from inner coordination sphere of CoPc, freeing it for substrate. Herewith molecules of CoPc must not aggregate.²⁷⁻³¹

The principle of chemical transformations acceleration, based on favorable orientation of reagent, provided by hydrogen bonds or hydrophobic interactions of environment, is known as characteristics of enzymatic catalysis.³²

Thus, the solvent for catalytically active liquid-phase system must be able to solvate CoPc and to form labile molecular complexes due to specific solvation (ϵ from 20 to 50; $DN < 25$). Probably use of mixed solvents, allowing the fine tuning of these parameters, is the most promising.

Based on foregoing, water-organic mixtures, for example water-ethanol, are chosen as medium for liquid-phase modeling of catalytic process with coordinated metallophthalocyanines. Ethanol is miscible with water in different molar ratios and have the necessary solvation characteristics (ϵ 24.3; DN 19.6)²⁶, that allows control of monomer-dimer equilibrium for CoPc.

Figure 2 depicts the changes in the optical density of CoPc as observed in the electronic absorption spectrum at different concentration of ethanol.

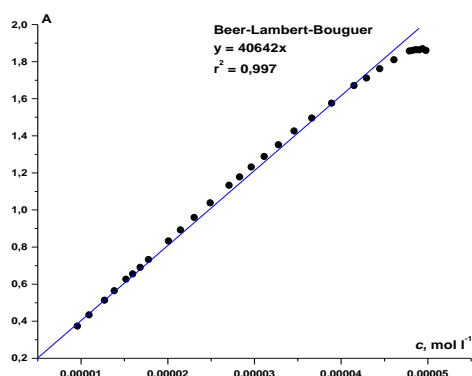


Figure 2. Dependence of optical density (*Q*-band λ 669 nm) of CoPc's ethanol solution on concentration, at 298.15 K

Data in figure 1 show that dependence of CoPc's absorption in *Q*-band, in the range of ethanol concentration from 0 to 4.7×10^{-5} mol L⁻¹ obeys Beer-Lambert-Bouguer law, indicating the existence of monomeric form of CoPc. Obviously, equilibrium (6) is shifted to the left. Value of molar extinction coefficient (ϵ) for *Q*-band is 40600 ± 50 L (mol cm)⁻¹. Probably, it will favor the catalytic activity of CoPc.

Figure 3 shows UV-Vis spectra for solutions of CoPc in water and ethanol.

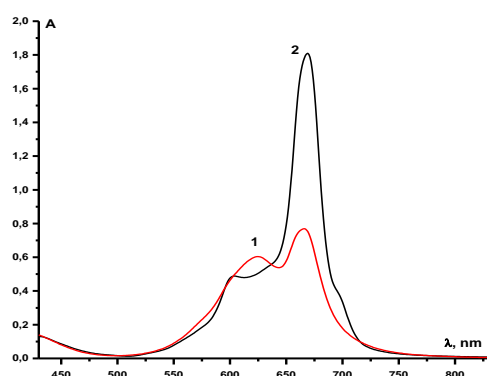


Figure 3. UV-Vis spectra of CoPc's solution with concentration of 4.61×10^{-5} mol L⁻¹, at 298.15 K in (1) water, (2) ethanol.

Data in figure 2 shows differences between CoPc's spectra in water and ethanol. Perusal of spectra indicates the presence of associated forms of CoPc in solution. Wide absorption peaks in the visible region of the spectrum is characteristic of aqueous solution of CoPc. Absorption bands of almost equal intensity in area of 627 nm (dimeric form of CoPc) and *Q*-band in area of 670 nm (monomeric

form of macrocycle) are recorded in the UV-Vis spectra. In ethanol, for CoPc, intensive *Q*-band in area of 669 nm and negligible absorption in area of 595 nm are obtained. These data let us to suggest that the extent of dimerization of the macrocycle in ethanol is rather lower than that in water solution. Probably, it caused by presence of equilibrium (7) in system, induced by the formation of molecular complexes due to axial coordination of solvent molecule.



From the point of view of green chemistry and technology, water is preferable to ethanol. Hence, the catalysis is implemented technologically in the water. Based on this, influence of the addition of ethanol on the association process of CoPc was studied.

Figure 4 shows alteration in UV-Vis spectra of aqueous solution of CoPc, when 4.91×10^{-5} mol L⁻¹ of ethanol is added.

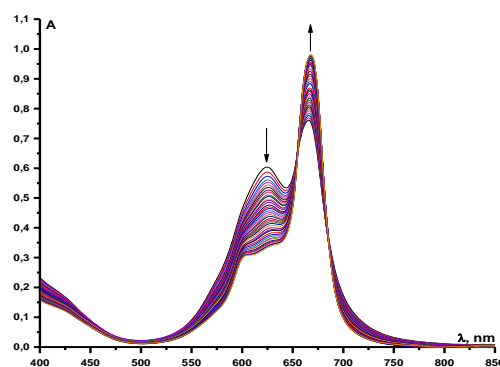


Figure 4. Alteration of UV-Vis spectra of aqueous solution CoPc at 298.15 K when ethanol is added.

There are significant spectral changes by the addition of ethanol to the aqueous solution of CoPc. Absorption band in area of 670 nm is increased, dimeric form band (627 nm) is decreased and showed a hypsochromic shift of 30 nm. These data suggest dissociation of CoPc-dimers due to formation of axial complexes with ethanol ($K_y = 107 \pm 8$ L mol⁻¹), which, however, are not as stable as the complexes with pyridine. Calculations by the method of Bent-French³³ indicated axial coordination of one ethanol molecule only. Back titration does not cause significant spectral changes. These data show there is a low competition for water molecules by cobalt cation of the phthalocyanine. The results demonstrate the possibility of variation in the associative equilibrium of CoPc in water by an addition of ethanol.

Interchange of axial ligands, containing different heteroatoms, forms the basis of metallophthalocyanines catalysis. However, the usefulness of replacing ethanol from amine derivatives of phthalocyanine is limited because of possibility of association.³⁴

Therefore, we studied possibility of ligand exchange in CoPc by displacement of solvent from coordination cavity of macrocycle with another ligand in the next stage of the work. The complex formation of CoPc with DABCO was studied for these purposes. This process simulates the exchange of coordinated solvent molecules on the substrate during the catalysis.

Introduction of DABCO in ethanol solution of CoPc causes consistent increase in the intensity of absorption Q -band region ($\Delta_{\max}A$ 0.483) (Figure 5). It is due to the axial coordination of DABCO on the central metal cation of CoPc.

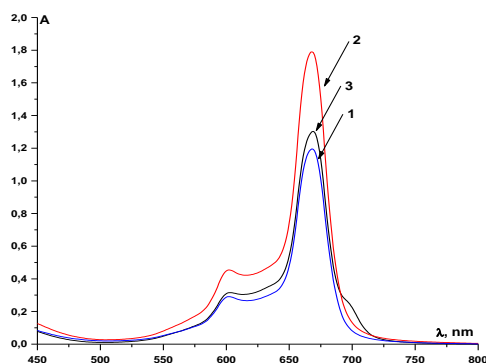


Figure 5. UV-Vis spectra of CoPc solution (c $4.98 \cdot 10^{-5}$ mol L $^{-1}$) in ethanol at 298.15 K, 1) without DABCO; 2) n (DABCO) $3.46 \cdot 10^{-5}$ mol; 3) n (DABCO) $17.35 \cdot 10^{-5}$ mol.

An isosbestic point is obtained in the UV-Vis spectra. It indicates the formation of new chromophore in solution. Obviously, the chromophore is molecular complex, L-CoPc, with DABCO in the ratio of 1:1. Stability constant of this complex ($K_y = 280 \pm 8$ L mol $^{-1}$), calculated by the equation (5), is more than twice of the stability constant of complex with ethanol. Further, it should be noted that complex CoPc-DABCO in aqueous solution is rather stable. It indicates influence of solvation processes on complex formation and dimerization. Probably it is caused by the effect of donor-acceptor interaction of DABCO and the solvent on the DABCO molecular associate formation.³⁵

When the ratio [CoPc]:[DABCO] reaches 1:0.0139, there is a decrease in intensity of Q -band absorption ($\Delta_{\max}A$ 0.592) and a shift of the isosbestic point.

Probably, these alterations are connected with the coordination of second metalophthalocyanines molecule and the formation of sandwich-type dimers CoPc-DABCO-CoPc (Figure 6). Thermodynamic stability constant of sandwich-type dimer is 50 ± 4 L mol $^{-1}$.

Thus, this work shows that there are possibilities of controlling the associative monomer-dimer equilibrium for CoPc in solutions by molecular complex formation and varying the solvating power of the medium.

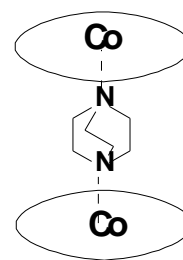


Figure 6. Scheme of sandwich dimer of CoPc-DABCO-CoPc

Acknowledgments

The work was financially supported by the Ministry of Education and Science of the Russian Federation (state assignment) and Russian Foundation for Basic Research (research projects No. 13-03-00615-a and 13-03-01343-a).

References

- Sorokin, A. B., *Chem. Rev.*, **2013**, *113*, 8152
- Basu, B., Satapathy, S., Bhatnagar, A. K., *Catal. Rev.: Sci. Eng.*, **1993**, *35*, 571
- Das, G., Sain, B., Kumar, S., *Catal. Today*, **2012**, *198*, 228
- Schelly, Z. A., Harvard D.J., Hemmes, P., Eyring E. M., *J. Phys. Chem.*, **1970**, *74*, 3040
- Yang, Yu-Ch., Ward, J. R., Seiders, R. P., *Inorg. Chem.*, **1985**, *24*, 1765
- Voronina, A. A., Kuzmin, I. A., Vashurin, A. S., Shaposhnikov, G. P., Pukhovskaya, S. G., Golubchikov, O. A. *Russ. J. Gen. Chem.*, **2014**, *84*, 1777
- Iliev, V., Alexiev, V., Bilyarska, L., *J. Mol. Catal. A: Chem.*, **1999**, *137*, 15
- Beletskaya, I., Tyurin, V. S., Tsvadze, A. Y., Guillard, R., Stern, C., *Chem. Rev.*, **2009**, *109*, 1659
- Tong, S.-L., Zhang, J., Yan, Ya., Hu, Sh., Yu, J., Yu, L., *Solid State Sci.*, **2011**, *13*, 1967
- Ishikawa, N., Kaizu, Y., *Coord. Chem. Rev.*, **2002**, *226*, 93
- Wu, S.-H., Wu, J.-L., Jia, Sh.-Y., Chang, Q.-W., Ren, H.-T., Liu, Yo., *Appl. Surf. Sci.*, **2013**, *287*, 389
- Sharma, R. K., Gulati, S., Pandey, A., *Inorg. Chim. Acta*, **2013**, *397*, 21
- Marfin, Yu. S., Vashurin, A. S., Rummyantsev, E. V., Puhovskaya, S. G., *J. Sol-Gel Sci. Technol.*, **2013**, *66*, 306
- Voronina, A. A., Tarasyuk, I. A., Marfin, Yu. S., Vashurin, A. S., Rummyantsev, E. V., Pukhovskaya, S. G. *J. Non-Cryst. Solids*, **2014**, *406*, 5
- Voronina, A., Kuzmin, I., Vashurin, A., Pukhovskaya, S., Futerman, N., Shepelev, M., *Eur. Chem. Bull.*, **2014**, *3*, 187
- Shul'pin, G. B., *J. Mol. Catal. A: Chem.*, **2002**, *189*, 39
- Lebedeva, N., Pavlycheva, N., Petrova, O., Vyugin, A., Kinchin, A., Parfenyuk, E., Mayzhlish, V., Shaposhnikov, G., *Mend. Commun.*, **2003**, *13*, 237
- Palewska, K., Sworakowski, J., Lipinski, J., *Opt. Mater.*, **2012**, *34*, 1717

- ¹⁹Palewska, K., Sworakowski, J., Lipinski, J., *J. Photochem. Photobiol. A: Chem.*, **2011**, *223*, 149
- ²⁰Günzel, A., Yarasir M. N., Kandaz, M., Koca, A., *Polyhedron*, **2010**, *29*, 3394
- ²¹Kulinich, V. P., Shaposhnikov, G. P., Badaukaite, R. A., *Macroheterocycles*, **2010**, *3*, 23
- ²²Weissberger, A., Proskauer, E. S., Riddick, J. A., Toops, E. E. *Organic solvent: physical properties and methods of purification*, Interscience Publishers Inc, New York **1955**.
- ²³Gordon, J. A., Ford, R. A. *The Chemist's Companion: A Handbook of Practical Data, Techniques, and References*, John Wiley & Sons, New York, **1972**
- ²⁴Snow, A. W., *The Porphyrin Handbook. Phthalocyanines: Properties and Materials*, Elsevier Science, Amsterdam, **2003**, *17*, 129
- ²⁵Berezin, B. D. *Coordination compounds of porphyrins and phthalocyanines*, John Wiley, Toronto, **1981**
- ²⁶Moskva, V. V., *Soros Educ. J.*, **1999**, *4*, 44 (in Russ))
- ²⁷Hoffman, M., *The sciences of the Total Environmental*, **1987**, *64*, 99
- ²⁸Borisenkova, S. A., *Russ. J. Petrol. Chem.*, **1991**, *31*, 391
- ²⁹Fischer, H., Schulz-Ekloff, G., Wohrle, D., *Chem. Eng. Technol.*, **1997**, *20*, 624
- ³⁰Buck, T., Bohlen, H., Wöhrle, D., Schulz-Ekloff, G., Andreev, A., *J. Mol. Catal.*, **1993**, *80*, 253
- ³¹Tyapochkin, E. M., Kozliak, E. I., *J. Mol. Catal. A: Chem.*, **2005**, *242*, 1
- ³²Nekipelov, V. M., Zamaraev K. I., *Coord. Chem. Rev.* **1985**, *61*, 185
- ³³Bent, H. E., French, C. L., *J. Am. Chem. Soc.*, **1941**, *63*, 568
- ³⁴Zaichikov, A. M., Krestyaninov M. A., Antonova O. A., *J. Therm. Anal. Calorim.*, **2014**, *115*, 1857
- ³⁵Zhiltsova, E. P., Pashirova, T. N., Kashapov, R. R., Lukashenko, S. S., Voloshina, A. D., Kulik, N. V., Zobov, V. V., Zakharova, L. Ya., Kononov, A. I., Gaisin, N. K., Gnezdilov, O. I., *Russ. Chem. Bull.*, **2011**, *61*, 113

Received: 14.10.2014.

Accepted: 22.11.2014.



D-ARABINO-HEX-1-ENITOL FROM THE INACTIVE FRACTION OF *ACALYPHA WILKESIANA* VAR. *LACE-ACALYPHA* (MUELL & ARG.)

Olawale H. Oladimeji^{[a]*} and Francis I. Udom^[a]

Keywords: *A. wilkesiana* var. *lace-acalypha*; inactive fraction; chromatography; antibacterial; 1,5-anhydro-2-deoxy-D-enopyranose-arabino-hex-1-enitol.

Different herbal preparations of *Acalypha wilkesiana* var. *lace-acalypha* (Muell & Arg.) are employed in traditional medicine for the treatment and management of disease conditions such as wounds, tumors, hypertension, inflammations, skin infections, gastroenteritis and many others. Ethyl 3,4,5-trihydroxybenzoate (ethyl gallate) and 1,2,3-benzenetriol (pyrogallol) had previously been isolated from the active fractions of this plant. However, this present study was done to isolate compound(s) from one of the inactive fractions. Hence, a short silica-gel column chromatography of the inactive fraction (5A) furnished a compound designated as **3** [R_f 0.15; $[n]^{20}_D$ 1.0300]. The structure of **3** has been established to be D-arabino-hex-1-enitol-1,5-anhydro-2-deoxy (1,5-anhydro-2-deoxy-D-enopyranose-arabino-hex-1-enitol) by a combination of 1H NMR, ^{13}C NMR, MS and IR spectral techniques. Compound **3** recorded no antibacterial activity against *B. subtilis*, *S. aureus* and *Ps. aeruginosa*. However, it demonstrated very weak antibacterial activities against *E. coli* and *S. typhi*, which were slightly better than the activity furnished by 5A. Furthermore, it was observed that **3** was inactive against *C. albicans*. Surprisingly, the crude extract and butanol fraction generally demonstrated comparably stronger antimicrobial activities than **3** implying that the purification of the crude extract and 5A did not improve the activity demonstrated by **3**.

Corresponding Author*

Fax: +2347038916740

E-Mail: olawaleoladimeji@hotmail.com,

wale430@yahoo.co.uk; hakeemoladimeji@uniuyo.edu.ng

[a] Department of Pharmaceutical and Medicinal Chemistry, Faculty of Pharmacy, University of Uyo, Uyo, Nigeria.

EXPERIMENTAL

Isolation

Sample 5A (1.5 g, inactive, dirty, viscous yellow substance), a semi-pure residue had been obtained previously from the chromatographic separation of the butanol fraction of the plant.¹⁴ It was purified on a much shorter silica-gel 254 column (Pyrex, USA; 7 g pre-swollen in 100 % toluene; 4 g concentration zone + 6 g separation zone; 11 x 3 cm) by eluting successively with 100 % toluene (110 mL) and 10 % (CH₃)₂CO:toluene (60 mL). Fractions of 5 mL each were collected, monitored on silica plates (Merck, Germany) in (CH₃)₂CO:toluene:H₂O (10:20:1) and (CH₃)₂CO:EtOAc (40:60) using FeCl₃/CH₃OH and vanillin-H₂SO₄ as spray reagents. Hence, two sub-fractions coded 5A-I and 5A-II with similar TLC characteristics (R_f values, reaction with FeCl₃ reagent or vanillin-H₂SO₄ spray) were bulked.

Further TLC examinations of the sub-fractions in (CH₃)₂CO:toluene:H₂O (10:20:1) and (CH₃)₂CO:EtOAc (40:60) indicated no materials especially in 5A-I. However, spectral analyses identified 5A-II to be D-arabino-hex-1-enitol-1,5-anhydro-2-deoxy (1,5-anhydro-2-deoxy-D-enopyranose-arabino-hex-1-enitol) and designated as compound **3** (light yellow oil; R_f (0.15); 93 mg). Initially, the refractometer (WAY-15 Abbe, England) was zeroed and the refractive index of **3** was measured at the wavelength (λ) of Na-D line (589.3 nm) at 20.5 °C.¹⁵⁻¹⁷

INTRODUCTION

Euphorbiaceae is one the largest families in the plant kingdom¹⁻³ to which the genus, *Acalypha* belongs.^{4,5} Extracts of *Acalypha* species are employed in traditional medicine in countries around the world and a few are well documented in homopathic pharmacopoeia.^{6,7}

Acalypha wilkesiana var. *lace-acalypha* is an ornamental plant which had been introduced to tropical West Africa from other parts of the world and now cultivated as a foliage plant in garden, orchards, greenhouse and parks.⁸ Different herbal preparations of this plant are used to treat headaches, fever, skin-fungal infections, mycoses, gastroenteritis,⁹⁻¹¹ breast tumors, wounds, inflammations and hypertension.^{12,13}

Prior to this present study, two polyphenols, ethyl gallate and pyrogallol had been isolated from the active fractions of this plant.¹⁴ It is imperative that the inactive fractions should equally be investigated with the aim of isolating any compound(s) therein which would be used to chemotaxonomically mark this species and variety in particular and the genus, *Acalypha* in general respectively.

Table 1. Antimicrobial screening of crude extract, butanol fraction, 5A and isolate **3** at different concentrations on test microbes in 100 % MeOH

Test microbe	LA 20 mg L ⁻¹	BU 10 mg mL ⁻¹	5A 5 mg mL ⁻¹	3 2 mg L ⁻¹	Streptomycine 10 µg mL ⁻¹	Nystatin 1 mg mL ⁻¹	100 % MeOH
<i>B.subtilis</i> (NCTC 8853)	14	14.5	5	5	23	5	5
<i>S. aureus</i> (NCTC 6872)	14	20	5	5	36.5	5	5
<i>E.coli</i> (NCTC 10764)	5	5	6	7	19	5	5
<i>P. aeruginosa</i> (ATCC 2654)	18	18	5	5	5	5	5
<i>S. typhi</i> (NCTC 5438)	13	7	6	6.5	18	5	5
<i>C. albicans</i> (NCYC 436)	11	5	5	5	5	26	5

Key: The zone diameter recorded is zone of inhibition + size of cup (zone of inhibition +5) mm; LA = Crude ethanolic extract; BU = Butanol fraction; 5A = Semi-pure residue obtained from BU which furnished compound **3**; **3** = D-arabino-hex-1-enitol-1, 5-anhydro-2-deoxy (1, 5-anhydro-2-deoxy-D-enopyranose-arabino-hex-1-enitol); NCTC - National Collection of Type Cultures, Central Public Health Laboratory, Colindale Avenue, London NW9, UK; NCYC- National Collection of Yeast Cultures, UK; ATCC- American Type Culture Collection, Washington, DC

Antimicrobial screening

The micro-organisms used in this investigation included *Bacillus subtilis* (NCTC 8853), *Staphylococcus aureus* (NCTC 6872), *Escherichia coli* (NCTC 10764), *Pseudomonas aeruginosa* (ATCC 2654), *Salmonella typhi* (NCTC 5438) and *Candida albicans* (NCYC 436). They were clinically isolated from specimens of diarrheal stool, abscesses, necrotizing fasciitis, osteomyelitis, urine, wounds and vaginal swabs obtained from the Medical Laboratory, University of Uyo Health Centre, Uyo. The clinical isolates were collected in sterile bottles, identified and typed by convectional biochemical tests^{18,19} and then refrigerated at – 5 °C at the Microbiology and Parasitology Unit, Faculty of Pharmacy prior to use.

The agar diffusion method was used observing standard procedure with Nutrient Agar CM003, Mueller Hinton CM037 (Biotech Limited, Ipswich, England) and Sabouraud Dextrose Agar (Biomark, India) for the bacteria and fungus respectively. The inoculum of each micro-organism was introduced into each petridish (Pyrex, England). Cylindrical plugs were removed from the agar plates by means of a sterile cork borer (Simax, England) to produce wells with diameter of approximately 5 millimetres. The wells were equidistant from each other and the edge of the plate.^{20,21}

Concentrations of 20 mg mL⁻¹ of crude extract, 10 mg mL⁻¹ of butanol fraction, 5 mg mL⁻¹ of 5A and 2 mg mL⁻¹ of **3** were introduced into the wells. Also, different concentrations of 10 µg mL⁻¹ streptomycin (Fidson Chemicals, Nigeria), 1 mg mL⁻¹ of nystatin (Neimeth Plc, Nigeria) and 100 % methanol were introduced into separate wells as positive and negative controls respectively.²²⁻²⁵ The experiments were carried out in triplicates. The plates were left at room temperature for 2 h to allow for diffusion. The plates were then incubated at 37± 2 °C for 24 h. Zones of inhibition were measured in millimetre (mm).

Spectroscopic data

The spectroscopic data were obtained on: ES⁺-MS on Kratos MS 80, IR on Perkin-Elmer FT-IR 8400S, ¹H and ¹³C NMR on Bruker AC 250 operating 300 MHz for proton and 75 MHz for carbon-13 using CD₃OD as solvent and TMS as internal standard.

RESULTS AND DISCUSSION

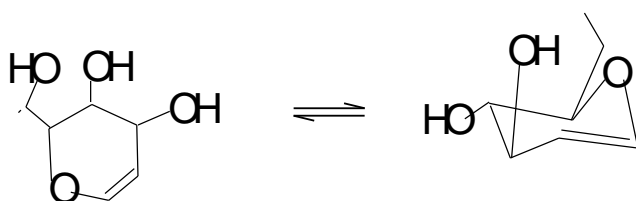
Compound **3**: C₆H₁₀O₄; light yellow oil; *R_f* (0.15); [*n*]_D²⁰ (1.0300); MS [ES⁺-MS] *m/z* (relative intensity): 146 [M]⁺ (5.26 %), 128 [M-H₂O]⁺ (2.44 %), 115 [M-CH₂OH]⁺ (1.27 %), 97 [M-CH₂OH-H₂O]⁺ (8.52 %), 73 [M-CH₂OH-2H₂O-6H]⁺ (100.00 %) (base peak), 55 [M-C₆H₃O]⁺ (52.83 %) and 29 [M-C₆H₉O₃]⁺ (40.32 %); IR [FTIR] cm⁻¹: 1061 (C-O), 1653 (CH=CH) and 3526 (OH); ¹H NMR δ (ppm): 1.45 and 5.15 (olefinic proton); ¹³C NMR δ (ppm): 32.76 (methylene-C), 105.13, 105.34 (hydroxylated-C) and 121.22 (C=C).

Elucidation of the chemical structure of compound **3**

The determinations of physical parameters are important in identifying compounds. Physical constants such as optical rotation, optical density and refractive index are used in the qualitative and quantitative analyses of substances. Also, these parameters are employed to confirm the purity, identity, integrity of active substances and as well as monitor the progress of reactions.¹⁵⁻¹⁷ The physical examination of compound **3** showed that it was an oily substance. In this study, only the refractive index was measured at the wavelength (λ) of Na-D light (589.3 nm) and a temperature of 20.5 °C. The measured refractive index of compound **3** is 1.0300. The refractive index of a substance is an indication of the number, type of atoms and chemical groups (species) in the substance. Each atom or group in the substance contributes to its refractivity which

adds eventually to the refractive index of the substance. Furthermore, refractive index can be used to monitor the progress of chromatographic separation by measuring the refractive indices of the effluent solvents employed.¹⁵⁻¹⁷ The structure of **3** was established by a combination of above-mentioned spectroscopic techniques. The obtained MS data were matched with library data of organic compounds.²⁶

Hence, compound **3** was identified to be D-arabino-hex-1-enitol-1, 5-anhydro-2-deoxy (1, 5-anhydro-2-deoxy-D-enopyranose-arabino-hex-1-enitol). The ES⁺-MS of **3** showed diagnostic fragmented peaks such as [M]⁺ at m/z 146 (5.26 %) while 126 (2.44 %), 115 (1.27 %) and 97 (8.52 %) represented the losses of water, methylene alcohol and water and methylene alcohol units respectively from the molecular ion. Furthermore, the ion at 73 (100 %) indicated the base peak while ions at 55 (52.83 %) and 29 (40.32 %) were quasi-peaks.^{17,27-30} The IR spectrum of the **3** showed diagnostic absorption stretchings at 1653 and 3526 cm⁻¹ representing the -CH=CH and -OH functional groups respectively. In addition, the -C-O absorption (ether linkage) at 1061 cm⁻¹ was equally very diagnostic. Though, the ¹H and ¹³C NMR spectra could not readily be used to identify **3** but the ¹H signal at 5.15 ppm indicated the presence of olefinic proton while ¹³C signals at 105.13, 105.34 and 121.22 ppm showed the presence of hydroxylated-C and C=C (unsaturation) respectively. Compound **3** is presented both in the planar and chair conformations.³¹



Compound **3**.

Antimicrobial screening

The results of the antimicrobial tests displayed in Table 1 show that **3** recorded no antibacterial activity against *B. subtilis*, *S. aureus* and *Ps. aeruginosa*. However, it demonstrated very weak antibacterial activities against *E. coli* and *S. typhi*, which were slightly better than the activity furnished by 5A. Furthermore, it was observed that this compound was inactive against *C. albicans*. This particular observation was not surprising because fungal strains such as *Candida spp.* limit the permeation of substances because of their integral structures which are pleomorphic and facultative in nature hence, resembling those of higher plants.³²

CONCLUSIONS

In this study, D-arabino-hex-1-enitol-1, 5-anhydro-2-deoxy has been isolated from the inactive fraction of *A. wilkesiana* var. *lace-acalypha* (Muell & Arg.). It is expected that this compound would serve as a chemotaxonomic marker for this species and variety in particular and the

genus, *Acalypha* in general. However, the isolated compound was generally inactive against bacterial and fungal (candidal) strains.

ACKNOWLEDGEMENTS

The authors acknowledge the efforts rendered by B. Odjobo of the Federal Institute of Industrial Research, Oshodi (FIIRO) Lagos in obtaining the spectra of the compound. The assistance of E. Akpan, Principal Technologist, Pharmaceutical Microbiology Unit, Faculty of Pharmacy, University of Uyo, Uyo, Nigeria in the antimicrobial screening is equally appreciated.

References

- Dalziel, J. M., *Useful Plants of West Tropical Africa. Crown Agents for Overseas Governments and Administrations*, **1956**, 45.
- Sofowora, A., *Medicinal Plants and Traditional Medicine in Africa*. Spectrum Books Limited, **2008**, 85.
- Trease, A., Evans, W. C., *Pharmacognosy*. 4th edition, W. B. Saunders Company, **2009**, 54-58.
- Oliver, B., *Medicinal Plants in Nigeria I*. Nigerian College of Arts, Science and Technology, **1959**, 58.
- Oliver, B., *Medicinal Plants in Nigeria II*. Nigerian College of Arts, Science and Technology, **1960**, 45-46.
- THPUSA. 6th edition, Otis Chapp Inc., **1941**, 65.
- HPI. **1971**, 1, 79.
- Burkill, H. M., *The Useful Plants of West Tropical Africa*. 2nd edition, Royal Botanical Gardens, **1985**, 94-96.
- Oladunmoye, M. K., *Int. Trop. Med.*, **2006**, 1(3), 134-136.
- Akinyemi, K. O., Oladapo, O., Okwara, C. E., Ibe, C. C., Fasure, K. A., *Compl. Alter. Med.*, **2005**, 5(6), 886-890.
- Oloduro, A. O., Bakere, M. K., Omoboye, O. O., Dada, C. A., *Ife J. Sci.*, **2011**, 13, 23-25.
- Bussing, A., Stein, G. M., Herterich, A. I., Pfuller, U., *J. Ethnopharmacol.*, **1999**, 66, 301-309.
- Ikewuchi, J., Anyadiegwu, A., Ogono, E. Y., Okungbara, S. O., *Pak. J. Nutr.*, **2008**, 17(1), 130-132.
- Oladimeji, H. O., Tom, E. U., Attih, E. E., *Eur. Chem. Bull.*, **2014**, 3(8), 1-4.
- Olaniyi, A. A., *Essential Medicinal Chemistry*. 1st edition, Shaneson C. I. Limited, **1989**, 137-157.
- Olaniyi, A. A., Ogungbamila, F. O., *Experimental Pharmaceutical Chemistry*. Shaneson C. I. Limited, **1991**, 78-79.
- Olaniyi, A. A., *Principles of Quality Assurance and Pharmaceutical Analysis*. Mosuro Publishers, **2000**, 151-158, 216-217, 264-268 and 443-457.
- Gibson, L., Khoury, J., *Lett. Appl. Microbiol.*, **1986**, 3, 127-129.
- Murray, P., Baron, E., Pfaller, M., Tenover, F., Tenover, R., *Manual of Clinical Microbiology*. American Society of Microbiology Press, **1995**, 973.
- Washington, J., *The Agar Diffusion Method*. In: *Manual of Clinical Microbiology*, 4th edition, American Society of Microbiology Press, **1995**, 971-973.

- ²¹NCCLS. *Performance Standard for Antimicrobial Susceptibility Test*, 8th edition, Approved Standard, The Committee, **2003**, 130.
- ²²Oladimeji, H. O., *Bioactivity Guided Fractionation of Acalypha wilkesiana Muell & Arg.* M. Sc, Thesis, Obafemi Awolowo University, **1997**.
- ²³Adesina, S. K., Idowu, O., Ogundaini, A. O., Oladimeji, H., Olugbade, T. A., Onawunmi, G. O., Pais, M., *Phytother. Res.*, **2000**, *14*, 371-374.
- ²⁴Nia, R., *Isolation and Characterization of Antibacterial Constituents from Calliandra haematocephala Hassk and Cissus quadrangularis L.*, Ph. D. Thesis, Obafemi Awolowo University, **1999**.
- ²⁵Oladimeji, H. O., *Chemical and Biological Studies on Cyathula prostrata (L.)Blume*, Ph. D. Thesis, University of Uyo, **2012**.
- ²⁶Lopez-Avila, V., *Org. Mass Spect.*, **1987**, *22*, 557.
- ²⁷Beynon, J. H., Williams, A. E., *Thermal Analysis, Techniques and Applications*, Chapman and Hall, **1988**, 76-79.
- ²⁸Millard, R. J., *Quantitative Mass Spectra*. Clapton Moore Press, **1979**, 73.
- ²⁹Constantin, E., Schnell, A., *Mass Spectrometry*. Ellis Horwood Press, **1990**, 141-146.
- ³⁰RSC. *Specialist Reports on Mass Spectrometry*, **1999**, *1*, 57-59.
- ³¹Morrison, R. T., Boyd, R. N., *Organic Chemistry*, 12th edition, Allyn and Bacon Inc., **1977**, 299-300.
- ³²Brown, M. R., *Pharm. J.*, **1975**, *215*, 239-242.

Received: 23.07.2014.

Accepted: 25.11.2014.



SYNTHESIS AND REACTIONS OF SOME 2(3H)- AND 2(5H)-FURANONE DERIVATIVES: A COMPARATIVE STUDY

Ahmed I. Hashem,^[a] Wael S. I. Abou-Elmagd^[a] and Ahmed Abd-Elaziz^[a]

Keywords: 2(5H)-furanone, 2(3H)-furanone, nitrogen, nucleophiles, unfavored 1,4- addition, thiazolidine and tetrazole rings..

Early, it was found that benzoin condensed with ethyl cyanoacetate in the presence of ethoxide ion to give 3-cyano-3,4-diphenyl-2(5H)-furanone **1**. On reinvestigating this reaction, we were able to isolate **1** together with another product, in low yield, which was proved to be 3-cyano-3,4-diphenyl-2(3H)-furanone **2**. The latter is formed by isomerization of **1** under the basic conditions employed. Energy calculations revealed that the 2(5H)-furanone **1** is more stable than the 2(3H)-isomer by 24.5 KJ/mole. The behavior of the two furanones **1** and **2** towards some nitrogen nucleophiles viz. hydrazine hydrate, benzylamine and ammonium acetate is studied. The unfavored 1,4 addition of these nucleophiles to the α,β -unsaturated carbonyl moiety of **1** is explained in terms of steric and electronic effects of the phenyl group at position 4. The nitrile groups at position 3 of the furanones **1** and **2** were utilized to construct thiazolidine and tetrazole rings by the action of thioglycolic acid and sodium azide respectively. The structures of all the products obtained were illustrated from their analytical and spectral properties.

Corresponding Authors

Tel./Fax: +20224831836

E-Mail: waelmagd97@yahoo.com

[a] Chemistry Department, Faculty of Science, Ain Shams University, Abassia, Cairo, Egypt, post code 11566.

reactions were monitored by the thin layer chromatography using Merck Kiesel gel 60 F254 aluminum backed plates.

General procedure for condensation of benzoin with ethyl cyanoacetate.¹³

A mixture of (0.1 mol, 21.2 g) of benzoin in 70 ml of absolute alcohol there was added (0.1 mol, 11.3 ml) of ethyl cyanoacetate followed by 2.3 g of sodium dissolved in 70 ml of absolute alcohol. There was a momentary purple color on adding sodium and heat is developed. On shaking the benzoin dissolved to form a clear reddish solution. This was heated on the water bath under reflux condenser for three hours, after which it was poured into 800 ml of water. A small precipitate of unchanged benzoin was filtered off and the clear filtrate acidified. A granular semi-solid precipitate was filtered off, rubbed with a small amount of ether and the white crystals filtered from ether yield about 85 %. Recrystallization from methanol yielded 3-cyano-4,5-diphenyl-2(5H)-furanone **1**. Another precipitate was collected from ether layer and recrystallized from methanol to give 3-cyano-4,5-diphenyl-2(3H)-furanone **2**.

3-cyano-4,5-diphenyl-2(5H)-furanone, (1).

White crystals; m.p: 139-140 °C, yield 85 %. IR (KBr) (ν_{\max} , cm^{-1}): 2235 (CN), 1770 (C=O lactone), 1621 (C=C). ¹H-NMR (DMSO- d_6): δ_{H} (ppm) 6.17 (s, 1H, CH-Ph) 6.95-7.40 (m, 10H, ArH). MS, m/z (%): 261 (M^+ , 57), 217 (31), 91(24), 77 (100). Anal. Calcd. For $\text{C}_{17}\text{H}_{11}\text{NO}_2$ (261): C, 78.15; H, 4.24; N, 5.36. Found: C, 78.30; H, 4.33; N, 5.76.

3-cyano-4,5-diphenyl-2(3H)-furanone, (2).

Yellow crystals; m.p: 167-169 °C, yield 15 %. IR (KBr) (ν_{\max} , cm^{-1}): 2252 (CN), 1782 (C=O lactone), 1623 (C=C). ¹H-NMR (DMSO- d_6): δ_{H} (ppm) 4.23 (s, 1H, CH-CN) 7.09-7.47 (m, 10H, ArH). MS, m/z (%): 261 (M^+ , 39), 217 (54), 191(31), 77 (100). Anal. Calcd. For $\text{C}_{17}\text{H}_{11}\text{NO}_2$ (261): C, 78.15; H, 4.24; N, 5.36. Found: C, 77.96; H, 4.17; N, 5.56.

Introduction

Furanones represent a group of heterocyclic compounds of special importance. According to the relative positions of the carbonyl group and the double bond in the hetero ring, there are three types of furanones namely; 2(3H)-, 2(5H)- and 3(2H)-furanones. Compounds of the first type are characterized by facile ring opening to give acyclic products which can be recycled to give heterocyclic derivatives of synthetic and biological importance. The nucleus of the second type is the core skeleton in many natural products.

The chemistry of the first two types had been reviewed by one of us.^{1,2} Also, our research group were interested during the last decades in the utilization of 2(3H)-furanone derivatives in the construction of a variety of heterocyclic systems, viz. pyrrolinones,^{3,4} pyridazinones,^{5,6,7} isothiazolones,⁸ oxadiazoles,^{9,10} and triazoles.^{11,12}

Experimental section

General

Melting points were measured on a Gallen Kamp electric melting point apparatus. The infrared spectra were recorded using potassium bromide disks on FTIR Thermo Electron Nicolet 7600 (USA) infrared spectrometer. The ¹H-NMR spectra were run at 300 MHz on a GEMINI 300 BB NMR spectrometer using tetramethyl silane (TMS) as internal standard in deuterated dimethylsulphoxide (DMSO- d_6). The mass spectra were recorded on a shimadzu GC-MS QP-1000EX mass spectrometer operating at 70 eV. The

General procedure for the action of hydrazine hydrate on the 2(5H)-furanone (1)

a) Hydrazine hydrate (1.1 mmol) was added to a solution of the furanone **1** (1 mmol) in ethanol (20 ml). The reaction mixture was left at room temperature with occasional shaking. The product obtained was filtered off, washed with ethanol, and found to be the furanone **2**.

b) The same reaction was carried out at 80 °C in ethanol as solvent for 30 min. The product obtained was filtered off, washed with ethanol, and found to be the acid hydrazide derivative **5**.

c) The reaction mixture was heated under reflux for 3 h. The solvent was distilled off under reduced pressure. The solid obtained was washed thoroughly with ethanol, drained and recrystallized from ethanol to give the pyridazinone derivative **6**. The pyridazinone derivative **6** was also obtained by ring closure of the acid hydrazide **5** by refluxing with HCl/AcOH mixture (1:1).

d) The acid hydrazide and the pyridazinone derivatives **5** and **6** respectively were also obtained when the reaction was carried out on the 2(5H)-furanone **2**.

2-cyano-4-oxo-3,4-diphenyl butanhydrazide, (5).

White crystals; m.p: 265-266 °C, yield 60 %. IR (KBr) (ν_{\max} , cm^{-1}): 2250 (CN), 1708.1661 (C=O), 1623 (C=C). $^1\text{H-NMR}$ (DMSO- d_6): δ_{H} (ppm) 4.27 (s, 1H, CHCN), 4.53 (s, 1H, CHPh), 5.13 (br.s, 2H, NH₂), 6.67 (br.s, 1H, NHCO), 7.06-7.93 (m, 10H, ArH). MS, m/z (%): 293 (M^+ , 27), 262 (73), 195(38), 105(100), 91(86), 77(56). Anal. Calcd. For $\text{C}_{17}\text{H}_{15}\text{N}_3\text{O}_2$ (293): C, 69.61; H, 5.15; N, 14.33. Found: C, 69.95; H, 5.27; N, 5.56.

4-cyano-5,6-diphenyl-1,2,3,4-tetrahydropyridazine-3-one, (6).

Faint red powder; m.p: 230-232 °C, yield 65 %. IR (KBr) (ν_{\max} , cm^{-1}): 2279 (CN), 1678 (C=O cyclic amide), 1620 (C=C). $^1\text{H-NMR}$ (DMSO- d_6): δ_{H} (ppm) 3.45 (br.s, 1H, NH, exchangeable), 5.33 (s, 1H, CHCN), 7.08-7.72 (m, 10H, ArH), 10.38 (br.s, 1H, NHCO). MS, m/z (%): 275 (M^+ , 27), 273 (85), 257(76), 245(38), 232(43), 217(29), 91(23), 77(100). Anal. Calcd. For $\text{C}_{17}\text{H}_{13}\text{N}_3\text{O}$ (275): C, 74.17; H, 4.76; N, 15.26. Found: C, 74.55; H, 4.62; N, 15.47.

General procedure for the action of benzylamine on the 2(5H)- and 2(3H)-furanones, (1) and (2), respectively.

a) A solution of the furanone derivatives **1** or **2** (0.01 mol) in benzene and benzyl amine (0.02 mol) was refluxed for 3 h. The reaction mixture was left to cool at room temperature. The product obtained was filtered off, recrystallized from ethanol to give N-benzylamide derivative **7**.

b) On fusion of the furanone derivatives **1** and **2** (0.5 g) with benzylamine (1 ml) for 2 h, the product obtained was treated with methanol to give gray powder, filtered off, recrystallized from ethanol to give the pyrrolone derivatives **8** and **9**, respectively.

N-benzyl-2-cyano-4-oxo-3,4-diphenyl butanamide, (7).

White powder; m.p: 212-214 °C, yield 70 %. IR (KBr) (ν_{\max} , cm^{-1}): 3283(NH), 2360 (CN), 1682,1654 (C=O), 1625 (C=C). $^1\text{H-NMR}$ (DMSO- d_6): δ_{H} (ppm) 4.22 (d, 1H, CHCN, J= 6.6), 4.35 (d-d, 2H, NHCH₂, J=11.2), 4.51 (d, 1H, CHPh, J= 6.6), 7.24-7.87 (m, 15H, ArH), 9.27 (br.s, 1H, NHCO). MS, m/z (%): 368 (M^+ , 39), 291 (67), 262(71), 213 (52), 184 (56), 105(100), 91(87), 77(63). Anal. Calcd. For $\text{C}_{24}\text{H}_{20}\text{N}_2\text{O}_2$ (368): C, 78.24; H, 5.47; N, 7.60. Found: C, 78.75; H, 5.71; N, 7.43.

1-benzyl-3-cyano-4,5-diphenyl-2,5-dihydro-1H-pyrrole-2-one, (8).

Faint yellow crystals; m.p: 142-144 °C, yield 80 %. IR (KBr) (ν_{\max} , cm^{-1}): 2223 (CN), 1685 (C=O), 1620 (C=C). $^1\text{H-NMR}$ (DMSO- d_6): 4.25-5.29 (m, 2H, NCH₂), 5.32 (s, 1H, CHPh), 6.93-7.50 (m, 15H, ArH). MS, m/z (%): 350 (M^+ , 23), 245 (35), 217(47), 91(100), 77(87). Anal. Calcd. For $\text{C}_{24}\text{H}_{18}\text{N}_2\text{O}$ (350): C, 82.26; H, 5.18; N, 7.99. Found: C, 82.09; H, 5.23; N, 7.79.

1-benzyl-3-cyano-4,5-diphenyl-2,3-dihydro-1H-pyrrole-2-one, (9).

Faint yellow crystals; m.p: 148-150 °C, yield 55 %. IR (KBr) (ν_{\max} , cm^{-1}): 2271 (CN), 1687 (C=O), 1620 (C=C). $^1\text{H-NMR}$ (DMSO- d_6): 4.09 (s, 1H, CHCN), 4.19-4.23 (m, 2H, NCH₂), 7.11-7.76 (m, 15H, ArH). MS, m/z (%): 350 (M^+ , 52), 245 (42), 217(29), 180(100), 91(89), 77(83). Anal. Calcd. For $\text{C}_{24}\text{H}_{18}\text{N}_2\text{O}$ (350): C, 82.26; H, 5.18; N, 7.99. Found: C, 82.17; H, 5.07; N, 7.83.

General procedure for the action of ammonium acetate on the 2(5H)- and 2(3H)-furanones (1) and (2) respectively.

a) A mixture of the furanone derivatives **1** or **2** (0.01 mol) in acetic acid and ammonium acetate (0.1 mol) was refluxed for 3 h. The reaction mixture was left to cool at room temperature. The product obtained was filtered off, recrystallized from ethanol to give pyrrolone derivative **10** and **11**, respectively.

b) Fusion of the furanone derivatives **1** or **2** (0.5 g) with ammonium acetate (1 g) for 1h. The product obtained was treated with water to give gray powder, filtered off, recrystallized from ethanol to give the pyrrolone derivatives **10** and **11**, respectively.

3-Cyano-4,5-diphenyl-2,5-dihydro-1H-pyrrole-2-one, (10).

White powder; m.p: 232-234 °C, yield 40 %. IR (KBr) (ν_{\max} , cm^{-1}): 3185(NH), 2194 (CN), 1656 (C=O), 1602 (C=C). $^1\text{H-NMR}$ (DMSO- d_6): 4.33 (br.s, 1H, OH(lactim form), exchangeable), 5.53 (s, 1H, CHPh), 7.29-7.94 (m, 10H, ArH), 13.42(br.s, 1H, NH, exchangeable). MS, m/z (%): 260 (M^+ , 46), 217 (67), 129(86), 103(77), 91(79), 77(100). Anal. Calcd. For $\text{C}_{17}\text{H}_{12}\text{N}_2\text{O}$ (260): C, 78.44; H, 4.65; N, 10.76. Found: C, 78.59; H, 5.01; N, 10.53.

3-cyano-4,5-diphenyl-2,3-dihydro-1H-pyrrole-2-one (11).

Gray powder; m.p: 297-299 °C, yield 35 %. IR (KBr) (ν_{\max} , cm^{-1}): 2286 (CN), 1679 (C=O), 1605 (C=C). $^1\text{H-NMR}$ (DMSO- d_6): 4.12 (s, 1H, CHCN), 6.93-7.46 (m, 10H, ArH), 10.74 (br.s, 1H, NH, exchangeable). MS, m/z (%): 260 (M^+ , 35), 217 (59), 180(100), 77(93). Anal. Calcd. For $\text{C}_{17}\text{H}_{12}\text{N}_2\text{O}$ (260): C, 78.44; H, 4.65; N, 10.76. Found: C, 78.64; H, 4.87; N, 10.83.

General procedure for the action of thioglycolic acid on the 2(5H)- and 2(3H)-furanones, (1) and (2), respectively.

A mixture of 10 mmol of 2(5H)-furanone, thioglycolic acid (10 mmol) in pyridine (10 ml) was refluxed for 3 h. the solvent was removed under reduced pressure and the solid obtained was filtered off washed with ethanol and recrystallized from methanol/ dioxane mixture to give the thiazolidinone derivatives **12** and **13** respectively.

2-(4,5-diphenyl-2(3H)-furanone-3-yl)thiazol-4(5H)-one, (12)

Bright green crystals; m.p: 206-208 °C, yield 90 %. IR (KBr) (ν_{\max} , cm^{-1}): 3200-3418 (br.) (OH), 1754 (C=O lactone), 1620,1600 (C=N, C=C). $^1\text{H-NMR}$ (DMSO- d_6): 5.88 (s, 1H, CHPh), 7.25-7.55 (m, 11H, ArH), 10.88 (br.s, 1H, OH, exchangeable). MS, m/z (%):337 (M^+ +2, 4), 335 (M^+ , 49), 260 (67), 232(43), 188(35), 91(56), 77(100). Anal. Calcd. For $\text{C}_{19}\text{H}_{13}\text{NO}_3\text{S}$ (335): C, 68.04; H, 3.91; N, 4.18; S, 9.56. Found: C, 68.29; H, 3.75; N, 4.32; S, 9.72.

2-(4,5-diphenyl-2(5H)-furanone-3-yl)-5-hydroxythiazol, (13)

Bright red crystals; m.p: 212-214 °C, yield 85 %. IR (KBr) (ν_{\max} , cm^{-1}): 1768 (C=O lactone), 1712 (C=O thiazolidinone), 1630, 1620 (C=N, C=C). $^1\text{H-NMR}$ (DMSO- d_6): 3.18 (s, 1H, CHCO), 3.93 (s, 2H, CH_2 Thiazolidinone), 7.21-7.54 (m, 10H, ArH). MS, m/z (%):337 (M^+ +2, 3), 335 (M^+ , 51), 304 (23), 263(75), 240(43), 180(87), 161(31), 77(100). Anal. Calcd. For $\text{C}_{19}\text{H}_{13}\text{NO}_3\text{S}$ (335): C, 68.04; H, 3.91; N, 4.18; S, 9.56. Found: C, 67.76; H, 3.80; N, 4.07; S, 9.38.

General procedure for the action of sodium azide on the 2(5H)- and 2(3H)-furanones, (1) and (2), respectively.

0.01 mol of the furanones **1** or **2**, sodium azide (6 mmol) and NH_4Cl (6 mmol) in 15 ml acetic acid were refluxed for 5 h. The resulting crude product was filtered off and recrystallized from methanol to give the tetrazole derivatives **14** and **15** respectively.

4,5-diphenyl-3-(1-H-tetrazol-5-yl)-2(5H)-furanone, (14).

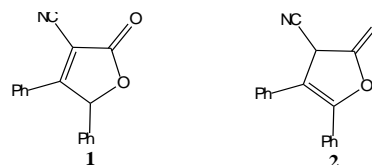
Grey powder; m.p: 125-127 °C, yield 92 %. IR (KBr) (ν_{\max} , cm^{-1}): 3213 (NH), 1758 (C=O lactone), 1614, 1600 (C=N, C=C). $^1\text{H-NMR}$ (DMSO- d_6): 6.13 (s, 1H, CHPh), 7.14-7.63 (m, 10H, ArH), 15.17 (weak br.s, 1H, NH, exchangeable). MS, m/z (%): 304 (M^+ , 100), 260 (89), 232(23), 91(25), 77(95). Anal. Calcd. For $\text{C}_{17}\text{H}_{12}\text{N}_4\text{O}_2$ (304): C, 67.10; H, 3.97; N, 18.41. Found: C, 66.97; H, 3.78; N, 18.23.

4,5-diphenyl-3-(1-H-tetrazol-5-yl)-2(3H)-furanone, (15).

Faint brown powder; m.p: 112-114 °C, yield 90 %. IR (KBr) (ν_{\max} , cm^{-1}): 1767 (C=O lactone), 1623, 1600 (C=N, C=C). $^1\text{H-NMR}$ (DMSO- d_6): 4.35 (s, 1H, CHCO), 7.08-7.47 (m, 10H, ArH), 15.32 (weak br.s, 1H, NH, exchangeable). MS, m/z (%):337 (M^+ +2, 3), 335 (M^+ , 51), 304 (23), 263(75), 240(43), 180(87), 161(31), 77(100). Anal. Calcd. For $\text{C}_{17}\text{H}_{12}\text{N}_4\text{O}_2$ (304): C, 67.10; H, 3.97; N, 18.41. Found: C, 66.02; H, 4.05; N, 18.57.

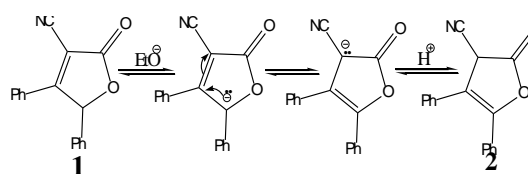
Results and discussion

In this investigation, we wish to report on the synthesis and reactions of two furanones derivatives, one of 2(3H)-type and the other of the 2(5H)- type as a comparative study, in an attempt to show the effect of the position of the double bond on their behavior. McRae and Kuehner,¹³ reported that the condensation of benzoin with ethyl cyanoacetate in the presence of sodium ethoxide led to formation of the lactone of α -cyano- β,γ -diphenyl- γ -hydroxy crotonic acid (m.p. 141 °C), whose currently present name is 3-cyano-4,5-diphenyl-2(5H)-furanone **1**. Perhaps due to the lack of spectroscopic tools at this earlier time, this compound was not characterized spectroscopically. Its structure was assigned based on chemical transformations. Our interest in the chemistry of furanones, led us to reinvestigate this reaction. On carrying this reaction under the same conditions reported,¹³ we were able to isolate the furanone **1** together with another product (m.p 175 °C) to which structure **2** was assigned on the bases of spectroscopic data.



The infrared spectrum of compound **1** showed absorption bands at 2235 cm^{-1} and 1770 cm^{-1} characteristic of the νCN and $\nu\text{C=O}$ respectively. Compound **2** showed νCN and $\nu\text{C=O}$ at 2252 cm^{-1} and 1782 cm^{-1} respectively. The $^1\text{H-NMR}$ of the above two compound showed the characteristic signals of the different protons (cf. Experimental part).

We believe that the formation of **2**, namely 2-cyano-4,5-diphenyl-2(3H)-furanone is not unexpected under the basic conditions at which the reaction was carried out. Thus, the formation of **2** may be explained on the basis of isomerization of **1** in the presence of the strong base ethoxide ion. Such isomerization might involve the intermediate formation of resonance stabilized carbanions as previously reported by our research group.¹⁴ Therefore, the formation of the 2(3H)-furanone **2** may be represented by Scheme 1.

**Scheme 1.**

The formation of the 2(3H)-furanone **2** in a relatively smaller yield compared with 2(5H)-isomer **1** (cf. the experimental part), reflects the higher stability of the latter. This led us to determine the relative stabilities of these two isomers applying the UMPW1K/6-31+g(d) method, of calculation.¹⁵ The results of these calculations revealed that **1** is more stable than **2** by 24.5 kJ mol⁻¹. Border et al,¹⁶ reported that generally 2(5H)-furanones are thermodynamically more stable than their tautomers, the 2(3H)-furanones. SCF- MO calculations showed that the energy of **3** is less than that of its tautomer **4** by 53 kJ/mole.¹⁶



The lower energy difference obtained in our case may be attributed to the presence of two phenyl groups attached to the ring double bond of **2** which impart some degree of stability to this isomer.

The study was extended to explore the effect of the relative positions of the double bond and the carbonyl group in **1** and **2** on their behavior towards some nitrogen nucleophiles. The 2(5H)-furanone **1** reacted with hydrazine hydrate in ethanol at room temperature to give its tautomer **2**. However, when the reaction was carried out at 80°C the propionic acid hydrazide **5** was obtained as the only isolable product. On the other hand, the reaction of the furanone **1** with hydrazine hydrate in refluxing ethanol, led to the formation of the pyridazinone derivative **6**.

The same two products **5** and **6** were obtained from the reaction of the 2(3H)-furanone **2** under the same reaction conditions. This behavior led us to believe that the reaction of the 2(5H)-furanone **1** with hydrazine follows the following sequence:

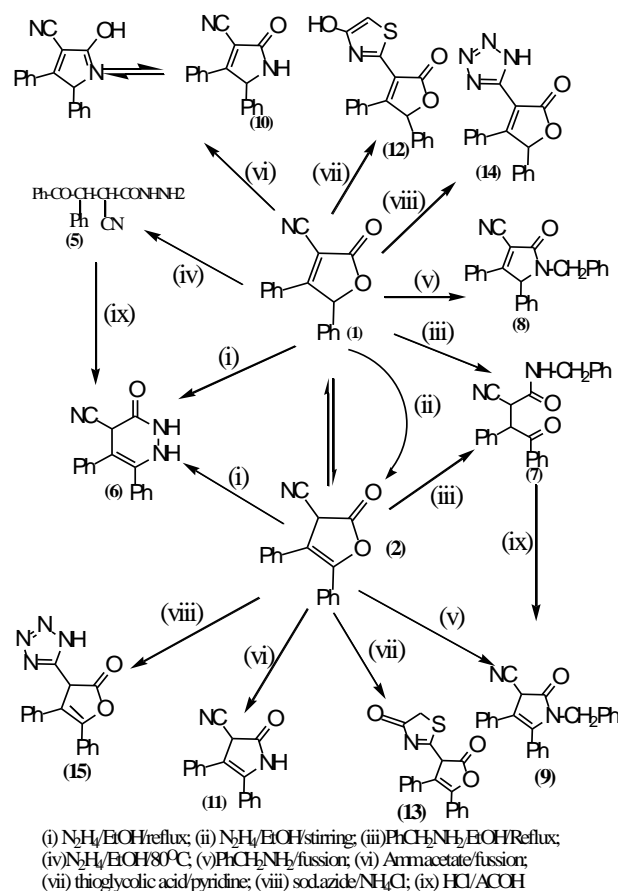
Firstly, the furanone isomerizes to the its 2(3H)-isomer, followed by ring opening to give the open chain hydrazide **5**, which undergoes ring closure to give the pyridazinone **6**. The latter was obtained also by cyclization of **5** in HCl/AcOH mixture. Benzylamine reacted with **1** in refluxing benzene to give the benzylamide derivative **7**. The same product **7** was obtained from the reaction of the 2(3H)-isomer **2** with benzylamine under the same reaction conditions.

This behavior again indicates that under these conditions, the 2(5H)- isomer **1** isomerizes firstly to its tautomer **2** before ring opening by benzylamine. On fusion of the furanone **1** with benzylamine in neat, the pyrrolone derivative **8** was obtained as the only isolable product. Under the same reaction conditions, the 2(3H)-isomer **2** gave another pyrrolone derivative **9**. This behavior excludes the possibility of isomerization of **1** into **2** under these reaction conditions. The compound **9** was also obtained by cyclization of **7** in HCl/AcOH mixture.

The reaction of the furanones **1** and **2** with ammonium acetate was also tried. On refluxing **1** or **2** and ammonium acetate in acetic acid, the reaction failed to give any product.

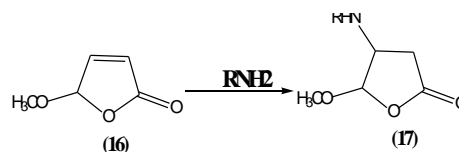
However, fusion of **1** and **2** with ammonium acetate led to the formation of the pyrrolone derivatives **10** and **11** respectively.

The presence of cyano group at position-3 in both the 2(5H)- and 2(3H) furanones promoted our interest to construct thiazolidinone and tetrazole rings at this position. Thus, **1** and **2** reacted with thioglycolic acid to give the thiazolidinone derivatives **12** and **13** respectively. The tetrazolyl derivatives **14** and **15** were obtained by reacting the 2(5H)- and 2(3H)- furanones respectively with sodium azide in the presence of ammonium chloride. The structures of all the products obtained were elucidated from their spectral analyses (cf. experimental part). All the foregoing reactions are illustrated by scheme (2).

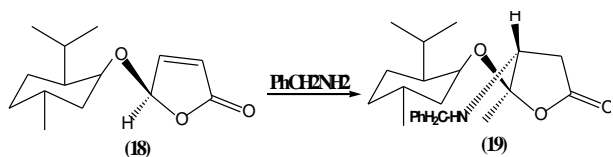


Scheme 2

De lange et al.,¹⁷ reported that the addition of amines to 5-methoxy-2(5H)-furanone **16** led to the formation of the aminolactone **17** which was formed by 1,4-addition to the α,β-unsaturated carbonyl moiety with the furanone ring remaining intact.



Also, the enantioselective synthesis of the N-benzyl substituted β-lactam **19**. A precursor for carbapenem antibiotics was synthesized by 1,4 addition of benzylamine to the chiral synthon 5(R)-methoxy-2(5H)-furanone **18**.¹⁸



It is evident that the 2(5H)-furanone **1** behaved differently towards the nitrogen nucleophiles studied. The unfavored 1,4 addition in our case may be attributed to the presence of a phenyl group at position 4 which exerts a combination of steric and electronic effects retarding the approach of the nucleophile at this position.

References

- ¹Hashem, A. I., Senning, A., *Adv. Heterocycl. Chem.* **1999**, *43*, 275.
- ²Hashem, A. I., Kleinpeter, E., *Adv. Heterocycl. Chem.* **2001**, *81*, 107.
- ³El-Kousy, S. M., El-Torgoman, A. M., EL-Bassiouny, A. A., Hashem, A. I., *Pharmazie*, **1988**, *43*(2), 80.
- ⁴Sayed, H. H., Hashem, A. I., Youssef, N. M., El-Sayed, W. A., *Arch. Pharm. Chem.*, **2007**, *340*, 315.
- ⁵Hashem, A. I., Shaban, M. E., *J. Prakt. Chem.*, **1981**, *323*, 164.
- ⁶Kandeel, K. A., Yossef, A. S., Abou-Elmagd, W. S. I., Hashem, A. I., *J. Heterocycl. Chem.*, **2006**, *43*, 957.
- ⁷Hashem, A. I., Yossef, A. S., Kandeel, K. A., Abou-Elmagd, W. S. I., *Eur. J. Med. Chem.*, **2007**, *42*, 934.
- ⁸Derbala, H. A., Hamad, A. S., EL-Sayed, W. A., Hashem, A. I., *Phosphorus, Sulfur and Silicon*, **2001**, *175*, 153.
- ⁹Hamad, A. S., Hashem, A. I., *Molecule*, **2000**, *5*, 895.
- ¹⁰Hamad, A. S., Hashem, A. I., *J. Heterocycl. Chem.*, **2002**, *39*, 1325.
- ¹¹Yassin, S., Abdel-Aleem, H. A., El-Sayed, I. E., Hashem, A. I., *Rev. Roum. Chim.*, **1996**, *41*, 989.
- ¹²El-Kafrawy, A. F., Yossef, A. S., Hamad, A. S., Hashem, A. I., *Egypt. J. Pharm. Sci.*, **1993**, *34*, 159.
- ¹³McRae, J. A., Kuehner, A. L., *J. Am.chem.soc.*, **1930**, *2*,337.
- ¹⁴Hamad, A. S., Derbala, H. A., El-Sayed, W. A., Hashem, A. I., *Acta Chim. Slov.*, **2001**, *48*, 417.
- ¹⁵Lynch, B. J., Fast, P. L., Harris, M., Truhlar, D. O., *J. Phys. Chem. A*, **2000**, *104*(21), 4811.
- ¹⁵Bordor, N., Dewar, M. J. S., Harget, A. M. J., *J. Am. Chem. Soc.*, **1970**, *92*, 2929.
- ¹⁶De Lange, B., Bolhuis, F. V., Feringa, B. L., *Tetrahedron*, **1989**, *45*, 6799.
- ¹⁷Collis, M. P., Hockless, D. C. R., Perlmutter, P., *Tetrahedron Lett.*, **1995**, *36*, 7133.

Received: 20.10.2014.
Accepted: 05.12.2014.



SYNTHESIS AND ANTIMICROBIAL ACTIVITY OF SOME NEW 3-(4-FLUOROPHENYL)BENZO[g]INDAZOLES AND 1-PYRAZOLYLTHIAZOLES

Bakr F. Abdel-Wahab^[a], Hanan A. Mohamed^[a] and Ghada E. A. Awad^[b]

Keywords: benzo[g]indazoles, pyrazole, thiazole, antimicrobial activity, minimal inhibitory concentration

A new series of 3-(4-fluorophenyl)benzo[g]indazoles derivatives have been synthesized by simple, high yielding routes. The key step in the construction of the 3-(4-fluorophenyl)benzo[g]indazoles nucleus involves the reaction of α -tetralone with 4-fluorobenzaldehyde followed by reaction with hydrazine or thiosemicarbazide. The newly synthesized compounds were evaluated for their antimicrobial activity and compounds **5**, **6b**, **12d** and **16b** demonstrated inhibitory effects on the growth of a wide range of microbes.

* Corresponding Authors

Fax: +202 2 760-1877

E-Mail: Bakrfatehy@yahoo.com

[a] Applied Organic Chemistry Department, National Research Centre, Dokki, 12622 Giza, Egypt

[b] Chemistry of Natural and Microbial Products, National Research Center, Dokki, 12622 Giza, Egypt

INTRODUCTION

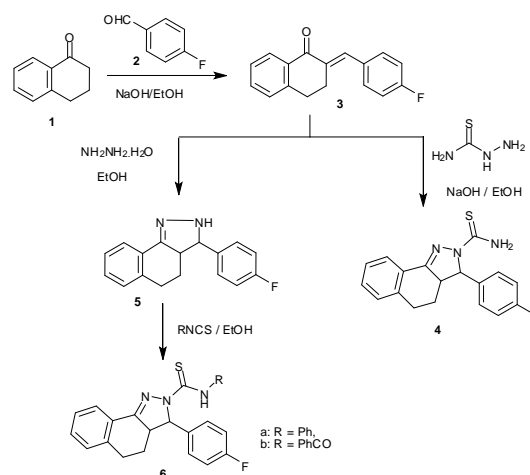
Literature survey revealed that many compounds bearing five membered rings such as pyrazoles and thiazoles show significant biological activity. Compounds containing pyrazole nucleus exhibit antibacterial,¹ antifungal,² anti-tubercular,³ anti-inflammatory activities.⁴ The thiazole nucleus is also present in various molecules with diverse pharmacological properties, such as antimicrobial.⁵ Also, pyrazolylthiazoles showed excellent antimicrobial activities.⁶⁻⁸ Keeping this observation in view and in continuation of our research on the synthesis of heterocyclic compounds containing nitrogen, sulfur and bicyclic systems with expected biological activity,^{6,9} this paper presents the synthesis of several new heterocyclic compounds which contain diphenylsulfone 3-(4-fluorophenyl)benzo[g]indazole moiety and the study of their antibacterial and antifungal activities.

RESULTS and DISCUSSION

The compound (*E*)-2-(4-fluorobenzylidene)-3,4-dihydronaphthalen-1(2*H*)-one **3** was prepared by the Claisen-Schmidt condensation reaction of α -tetralone **1** and 4-fluorobenzaldehyde **2** (Scheme 1).¹⁰

The target compounds 3-(4-fluorophenyl)-3,3a,4,5-tetrahydro-2*H*-benzo[g]indazoles **4-6** were prepared from **3** by reaction with thiosemicarbazide or hydrazine followed by isothiocyanates in anhydrous ethanol.

The structures **4-6** were fully supported by elemental analysis and spectral analysis.



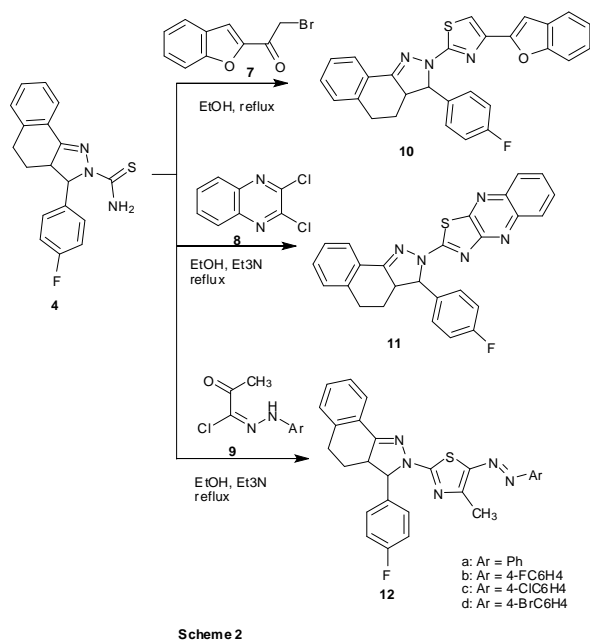
Scheme 1

In the ¹H NMR spectrum of **4** the NH₂ proton appears at δ 11.02 ppm. In the mass spectra of **4**, **6a** and **6b** showed the molecular ion peaks at *m/z* 325, 401 and 429, respectively, in agreement with the calculated masses.

The reaction sequences employed for synthesis of title compounds **10-12** are shown in Scheme 2. A one pot synthesis of benzo[g]indazol-2-ylthiazole derivatives **10-12** was achieved when 3-(4-fluorophenyl)-3,3a,4,5-tetrahydro-2*H*-benzo[g]indazol-2-ylthioamide **4** and 2-bromoacetylbenzofuran **7** or 3,4-dichloroquinoxaline **8** were refluxed in ethanol. Also, benzo[g]indazol-2-yl-4-methyl-5-(phenyldiazenyl)thiazoles **12a-d** were produced in good yields by reaction of **4** with hydrazonoyl chlorides **9** in refluxing ethanol and in the presence of a catalytic amount of triethylamine.

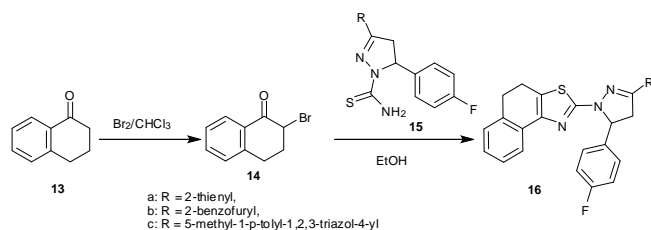
The ¹H NMR spectrum of **10**, a singlet at δ 8.02 was due to the thiazole-H. The protons of furan proton of benzofuran moiety resonated as singlet at δ 6.93 ppm. A characteristic singlet was observed at δ 2.49 due to the proton of the methyl group in **12**. Further evidence for the formation of benzo[g]indazol-2-ylthiazole derivatives were obtained by

recording its mass spectra. The mass spectra of compounds **10**, **11** and **12b** showed molecular ion peaks at m/z 465, 451 and 485, respectively, in conformity with their molecular formulas.



Scheme 2

Scheme 3 reports the reactions which led to pyrazol-1-yl-4,5-dihydronaphtho[1,2-*d*]thiazoles **16a-c**. Derivatives of pyrazol-1-yl-4,5-dihydronaphtho[1,2-*d*]thiazole series **16a-c** were obtained by a direct reaction between 2-bromo-3,4-dihydronaphthalen-1(2*H*)-one **14** and the appropriate 4,5-dihydro-1*H*-pyrazole-1-carbothioamides **15** by refluxing in neutral medium.



Scheme 3

Evidence for the formation of the pyrazol-1-yl-4,5-dihydronaphtho[1,2-*d*]thiazoles is found in the mass spectra of the **16a-c**. The molecular ion peaks of **16a-c** appeared at m/z 431, 465 and 520 respectively, which fit exactly with their calculated masses.

Antimicrobial activity

All the synthesized compounds were screened for their antibacterial and antifungal activities at 100 $\mu\text{g/mL}$ concentration against four *Gram positive bacteria* (*Staphylococcus Aureus* ATCC 29213; *B. subtilis* ATCC6633; *B. megaterium* ATCC 9885 and *Sarcinalutea*), three *Gram negative bacteria* (*Klebseillapneumoniae* ATCC13883; *Pseudomonas. Aeruginosa* ATCC27953; *E. coli* ATCC 25922) and two yeast (*Saccharomyces cervesia* and *Candida Albicans* NRRL Y-477).

Table 1. Characteristic data of the synthesized compounds

Entry	Mol. Formula (M. Wt)	Calcd./Found		
		C%	H%	N%
4	C ₁₈ H ₁₆ FN ₃ S (325.40)	<u>66.44</u>	<u>4.96</u>	<u>12.91</u>
		66.62	4.88	12.93
5	C ₁₇ H ₁₅ FN ₂ (266.31)	<u>76.67</u>	<u>5.68</u>	<u>10.52</u>
		76.72	5.81	10.60
6a	C ₂₄ H ₂₀ FN ₃ S (401.50)	<u>71.80</u>	<u>5.02</u>	<u>10.47</u>
		71.91	5.12	10.36
6b	C ₂₅ H ₂₀ FN ₃ OS (429.51)	<u>69.91</u>	<u>4.69</u>	<u>9.78</u>
		70.02	4.77	9.88
10	C ₂₈ H ₂₀ FN ₃ OS (465.54)	<u>72.24</u>	<u>4.33</u>	<u>9.03</u>
		72.31	4.39	9.16
11	C ₂₆ H ₁₈ FN ₅ S (451.52)	<u>69.16</u>	<u>4.02</u>	<u>15.51</u>
		69.20	4.16	15.30
12a	C ₂₇ H ₂₂ FN ₅ S (467.56)	<u>69.36</u>	<u>4.74</u>	<u>14.98</u>
		69.40	4.86	15.12
12b	C ₂₇ H ₂₁ F ₂ N ₅ S (485.55)	<u>66.79</u>	<u>4.36</u>	<u>14.42</u>
		66.83	4.45	14.62
12c	C ₂₇ H ₂₁ ClFN ₅ S (502.01)	<u>64.60</u>	<u>4.22</u>	<u>13.95</u>
		64.71	4.31	13.81
12d	C ₂₇ H ₂₁ BrFN ₅ S (546.46)	<u>59.34</u>	<u>3.87</u>	<u>12.82</u>
		59.40	3.77	12.89
16a	C ₂₄ H ₁₈ FN ₃ S ₂ (431.55)	<u>66.80</u>	<u>4.20</u>	<u>9.74</u>
		66.89	4.13	9.80
16b	C ₂₈ H ₂₀ FN ₃ OS (465.54)	<u>72.24</u>	<u>4.33</u>	<u>9.03</u>
		72.36	4.42	9.00
16c	C ₃₀ H ₂₅ FN ₆ S (520.62)	<u>69.21</u>	<u>4.84</u>	<u>16.14</u>
		69.29	4.89	16.21

Ciprofloxacin and ketoconazole were respectively used as standard antibacterial and antifungal reference, respectively. The results of antimicrobial activities were shown in Tables 2. Data in Table 2 revealed that most of compounds have superior significant antifungal potency to antibacterial potency. Compounds **5**, **6b**, **12d** and **16b** exhibited the highest potency against most of the tested organisms with respect to reference drugs. Compound **5** inhibited the growth of all the tested microorganisms with inhibition zones 28-38 mm. While compound **16b** showed excellent activity with inhibition zone 22-31mm. Also, compound **16c** showed highest activity against *B. subtilis* ATCC6633 with inhibition zone 23 mm.

EXPERIMENTAL

All melting points were taken on Electrothermal IA 9000 series digital melting point apparatus. Elemental analytical data were carried from the microanalytical unit, Cairo University, Giza, Egypt. The IR spectra were recorded in potassium bromide disks on a JASCO FT/IR-6100. ¹H-NMR spectra were run on JOEL-ECA 500MHz in deuterated dimethylsulphoxide (DMSO-*d*₆). Chemical shifts values (δ) are given in parts per million (ppm). The mass spectra were performed using mass Varian MAT CH-5 spectrometer at 70eV. 1-(Benzofuran-2-yl)-2-bromoethanone **7**¹¹, 2,3-dichloroquinoxaline **8**¹², hydrazonoyl halides **9**,¹³ 2-bromo-3,4-dihydronaphthalen-1(2*H*)-one **14**,¹⁴ 4,5-dihydro-1*H*-pyrazole-1-carbothioamides **15a**,¹⁵ **15b**¹⁶ and **15c**⁶ were prepared according to literature.

Table 2. Antimicrobial activity expressed as inhibition diameter zones in millimeters (mm) of chemical compounds against the pathological strains based on well diffusion assay

No.	Gram positive bacteria				Gram negative bacteria			Yeast	
	<i>S. aureus</i> ATCC 29213	<i>B. subtilis</i> ATCC6633	<i>B. megaterium</i> ATCC 9885	<i>Sarcina lutea</i>	<i>K. pneumoniae</i> ATCC13883	<i>P. Aeruginosa</i> ATCC27953	<i>E. coli</i> , ATCC 25922	<i>S. cerevisiae</i>	<i>C. Albicans</i> NRRL Y-477
4	15	17	15	14	18	18	15	18	19
5	28	33	30	34	33	34	38	30	31
6a	19	29	18	19	16	14	15	16	19
6b	20	27	21	23	18	16	15	18	20
10	15	24	15	18	19	N.A.	14	17	15
11	15	19	15	19	N.A.	N.A.	16	19	16
12a	20	18	19	16	18	20	19	20	20
12b	15	24	15	15	19	18	20	19	18
12c	16	31	19	16	18	19	18	18	16
12d	29	17	25	23	N.A.	16	19	N.A.	N.A.
16c	18	23	17	13	14	16	15	16	15
16a	18	24	19	20	18	14	15	20	19
16b	22	29	30	31	31	30	28	31	33
16c	18	23	17	13	14	16	15	16	15
Ciprofloxacin	20	22	24	20	25	24	23	N.A.	N.A.
Ketoconazole	N.A.	N.A.	N.A.	N.A.	N.A.	N.A.	N.A.	23	22

The experiment was carried out in triplicate and the average zone of inhibition was calculated

Table 3. Minimum inhibitory concentration ($\mu\text{g mL}^{-1}$) against the pathological strains based on two fold serial dilution technique

No.	Gram positive bacteria				Gram negative bacteria			Yeast	
	<i>Staphylococcus aureus</i> ATCC 29213	<i>B. subtilis</i> ATCC6633	<i>B. megaterium</i> ATCC 9885	<i>Sarcina lutea</i>	<i>Klebsiellapneumoniae</i> ATCC13883	<i>Pseudomonas. Aeruginosa</i> ATCC27953	<i>E. coli</i> ATCC 25922	<i>Saccharomyces cerevisia</i>	<i>CandidaAlbicans</i> NRRL Y-477
4	-	200	-	-	200	200	-	200	200
5	28	50	50	25	50	25	25	50	25
6a	200	50	200	200	200	-	-	200	200
6b	200	50	100	100	200	200	-	200	100
10	-	100	-	200	200	-	-	200	-
11	-	200	-	100	-	-	200	200	200
12a	200	200	100	200	200	100	200	100	200
12b	-	100	-	-	200	200	200	100	200
12c	-	50	200	200	200	200	200	200	200
12d	50	200	50	100	-	200	200	N.A.	N.A.
16a	200	100	100	100	200	-	-	100	-
16b	100	50	50	50	50	50	50	50	50
16c	200	100	200	-	200	200	-	200	-
Ciprofloxacin	25	25	25	25	25	25	25	N.A.	N.A.
Ketoconazole	N.A.	N.A.	N.A.	N.A.	N.A.	N.A.	N.A.	25	25

3-(4-Fluorophenyl)-3,3a,4,5-tetrahydro-2H-benzo[g]indazole-2-carbothioamide (4)

To a suspension of chalcone **3** (10 mmol, 2.52 g) and sodium hydroxide (25 mmol, 1.0 g) in ethanol (50 mL), thiosemicarbazide (12 mmol, 1.1 g) was added. The mixture was refluxed for 12 h, then left to cool; the solid product was filtered off, washed with ethanol and dried. Yield 58 %; m.p. 228-9°C; IR (KBr) $\nu_{\max}/\text{cm}^{-1}$ 3465, 3325 (NH₂); ¹H NMR (DMSO-d₆) δ 1.97 (m, 2H, CH₂), 2.10 (m, H, CH), 2.95 (m, 2H, CH₂), 5.48 (dd, 1H, CH, J= 8.45 Hz, J= 8.45 Hz), 7.20-7.89(m, 8H, Ar-H), 11.02 (s, 2H, NH₂, D₂O-exchangeable); MS m/z (%): 325 (M⁺, 36), 95 (100).

3-(4-Fluorophenyl)-3,3a,4,5-tetrahydro-2H-benzo[g]indazole (5)

To a solution of chalcones **3** (2 mmol, 0.5 g) in ethanol (30 mL), hydrazine hydrate 80 % (5 mmol) was added. The reaction mixture was refluxed for 6 h. Left to cool to room temperature, and the white solid product was filtered and washed with ethanol. Yield 61 %; m.p. 108-9 °C; IR (KBr) $\nu_{\max}/\text{cm}^{-1}$, 3220 (NH); ¹H NMR (DMSO-d₆) δ 1.92 (m, 2H, CH₂), 2.12 (m, 1H, CH), 2.92 (m, 2H, CH₂), 5.44 (dd, 1H, CH, J= 8.45 Hz, J= 8.45 Hz), 7.20-7.89(m, 8H, Ar-H), 10.12 (s, 1H, NH, D₂O-exchangeable); MS m/z (%): 266 (M⁺, 22), 95(100).

Benzo[g]indazole-2-carbothioamides (6a,b)

A mixture of **5** (2 mmol, 0.53 g) and phenylisothiocyanate (2 mmol, 0.27 g) {or benzoylisothiocyanate (2 mmol, 0.33 g) in case of **6b**} in dry ethanol (30 mL) was refluxed for 5 h. Cool to the room temperature and the formed solid product was collected by filtration to give products **6a,b**.

3-(4-Fluorophenyl)-N-phenyl-3,3a,4,5-tetrahydro-2H-benzo[g]indazole-2-carbothioamide (6a)

Yield 73 %; m.p. 158-9 °C; IR (KBr) $\nu_{\max}/\text{cm}^{-1}$, 3198 (NH); ¹H NMR (DMSO-d₆) δ 1.96 (m, 2H, CH₂), 2.28 (m, H, CH), 2.99 (m, 2H, CH₂), 5.42 (dd, 1H, CH, J= 8.45 Hz, J= 8.45 Hz), 7.20-7.89(m, 13H, Ar-H), 9.88 (s, 1H, NH, D₂O-exchangeable); MS m/z (%): 401 (M⁺, 28), 77 (100).

N-(3-(4-Fluorophenyl)-3,3a,4,5-tetrahydro-2H-benzo[g]indazole-2-carbonothioyl)benzamide (6b)

Yield 70 %; m.p. 184-6°C; IR (KBr) $\nu_{\max}/\text{cm}^{-1}$, 3198 (NH); ¹H NMR (DMSO-d₆) δ 1.95 (m, 2H, CH₂), 2.28 (m, H, CH), 2.98 (m, 2H, CH₂), 5.41 (dd, 1H, CH, J= 8.45 Hz, J= 8.45 Hz), 7.21-7.88(m, 13H, Ar-H), 10.21 (s, 1H, NH, D₂O-exchangeable); MS m/z (%): 429 (M⁺, 33), 77 (100).

Synthesis of 10-12*General procedure*

To a suspension of compound **4** (1 mmol, 0.33 g) in ethanol (20 mL) the 1 mmol of appropriate reagent {(2-bromoacetylbenzofuran, **7**) or (3,4-dichloroquinoxaline, **8**)

or hydrozonoyl chlorides, **9** + Et₃N} was added and heated under reflux for 2.5 h. After cooling, the precipitate was collected by suction filtration.

4-(Benzofuran-2-yl)-2-(3-(4-fluorophenyl)-3,3a,4,5-tetrahydro-2H-benzo[g]indazol-2-yl)thiazole (10)

Yield 45 %; m.p. 218-9 °C; ¹H NMR (DMSO-d₆) δ 1.84 (m, 2H, CH₂), 2.28 (m, H, CH), 2.98 (m, 2H, CH₂), 5.95 (dd, 1H, CH, J= 8.45 Hz, J= 8.45 Hz), 6.96 (s, 1H, benzofuryl-CH), 7.17-7.97 (m, 12H, Ar-H), 8.02(s, 1H, thiazolyl-CH); MS m/z (%): 465 (M⁺, 11), 85 (100).

2-(3-(4-Fluorophenyl)-3,3a,4,5-tetrahydro-2H-benzo[g]indazol-2-yl)thiazolo[4,5-b]quinoxaline (11)

Yield 42 %; m.p. 192-3°C; ¹H NMR (DMSO-d₆) δ 1.84 (m, 2H, CH₂), 2.28 (m, H, CH), 2.98 (m, 2H, CH₂), 5.95 (dd, 1H, CH, J= 8.45 Hz, J= 8.45 Hz), 7.20-7.95(m, 12H, Ar-H); MS m/z (%): 451 (M⁺, 23), 187 (100).

2-(3-(4-Fluorophenyl)-3,3a,4,5-tetrahydro-2H-benzo[g]indazol-2-yl)-4-methyl-5-(phenyldiazenyl)thiazole (12a)

Yield 66 %; m.p. 178-9 °C; ¹H NMR (DMSO-d₆) δ 1.79 (m, 2H, CH₂), 2.28 (m, H, CH), 2.49(s, 3H, CH₃), 2.93 (m, 2H, CH₂), 5.96 (dd, 1H, CH, J= 8.45 Hz, J= 8.45 Hz), 7.11-7.97(m, 13H, Ar-H); MS m/z (%): 467 (M⁺, 19), 95 (100).

2-(3-(4-Fluorophenyl)-3,3a,4,5-tetrahydro-2H-benzo[g]indazol-2-yl)-5-((4-fluorophenyl)diazenyl)-4-methylthiazole (12b)

Yield 66 %; m.p. 220-1°C; ¹H NMR (DMSO-d₆) δ 1.79 (m, 2H, CH₂), 2.28 (m, H, CH), 2.45(s, 3H, CH₃), 2.93 (m, 2H, CH₂), 5.93 (dd, 1H, CH, J= 8.45 Hz, J= 8.45 Hz), 7.11-7.97(m, 12H, Ar-H); MS m/z (%): 485 (M⁺, 60), 95 (100).

5-((4-Chlorophenyl)diazenyl)-2-(3-(4-fluorophenyl)-3,3a,4,5-tetrahydro-2H-benzo[g]indazol-2-yl)-4-methylthiazole (12c)

Yield 69 %; m.p. 244-5°C; ¹H NMR (DMSO-d₆) δ 1.79 (m, 2H, CH₂), 2.28 (m, H, CH), 2.51(s, 3H, CH₃), 2.93 (m, 2H, CH₂), 5.93 (dd, 1H, CH, J= 8.45 Hz, J= 8.45 Hz), 7.11-7.97(m, 12H, Ar-H); MS m/z (%): 501 (M⁺, 56), 95 (100).

5-((4-Bromophenyl)diazenyl)-2-(3-(4-fluorophenyl)-3,3a,4,5-tetrahydro-2H-benzo[g]indazol-2-yl)-4-methylthiazole (12d)

Yield 73 %; m.p. 250-1°C; ¹H NMR (DMSO-d₆) δ 1.79 (m, 2H, CH₂), 2.28 (m, H, CH), 2.50(s, 3H, CH₃), 2.94 (m, 2H, CH₂), 5.93 (dd, 1H, CH, J= 8.45 Hz, J= 8.45 Hz), 7.11-7.97(m, 12H, Ar-H); MS m/z (%): 546 (M⁺, 66), 95 (100).

Synthesis of dihydronaphtho[1,2-d]thiazoles 16*General procedure*

A mixture of 2-bromo-3,4-dihydronaphthalen-1(2H)-one **14** (1mmol) and appropriate pyrazoline-1-carbothioamide **15** (1mmol) dissolved in ethanol (30 mL) was refluxed for 4 h. The formed solid was filtered off and dried.

2-(5-(4-Fluorophenyl)-3-(thiophen-2-yl)-4,5-dihydro-1H-pyrazol-1-yl)-4,5-dihydronaphtho[1,2-d]thiazole (16a)

Yield 53 %; m.p. 180-1 °C; ¹H NMR (DMSO-d₆) δ 2.87-2.89 (m, 4H, 2CH₂), 4.09 (m, 1H, CH), 6.05 (dd, 2H, CH₂, J=10.8 Hz, J=10.8 Hz), 7.15-7.75 (m, 11H, Ar-H); MS m/z (%): 431 (M⁺, 19), 187 (100).

2-(3-(Benzofuran-2-yl)-5-(4-fluorophenyl)-4,5-dihydro-1H-pyrazol-1-yl)-4,5-dihydronaphtho[1,2-d]thiazole (16b)

Yield 45 %; m.p. 170-1 °C; ¹H NMR (DMSO-d₆) δ 2.87-2.89 (m, 4H, 2CH₂), 4.09 (m, 1H, CH), 6.05 (dd, 2H, CH₂, J=10.8 Hz, J=10.8 Hz), 7.15(s, 1H, benzofuryl), 7.18-7.75 (m, 12H, Ar-H); MS m/z (%): 465 (M⁺, 19), 187 (100).

2-(5-(4-Fluorophenyl)-3-(5-methyl-1-p-tolyl-1H-1,2,3-triazol-4-yl)-4,5-dihydro-1H-pyrazol-1-yl)-4,5-dihydronaphtho[1,2-d]thiazole (16c)

Yield 61 %; m.p. 185-6 °C; ¹H NMR (DMSO-d₆) δ 2.40 (s, 3H, CH₃), 2.46 (s, 3H, CH₃), 2.86-2.88 (m, 4H, 2CH₂), 4.05 (m, 1H, CH), 6.05 (dd, 2H, CH₂, J= 10.8 Hz, J= 10.8 Hz), 7.15 (s, 1H, benzofuryl), 7.18-7.75 (m, 12H, Ar-H); MS m/z (%): 520 (M⁺, 12), 187 (100).

Antimicrobial activity

Chemical compounds were individually tested against a panel of gram positive and gram negative bacterial pathogens, yeast and fungi. Antimicrobial tests were carried out by the agar well diffusion method,¹⁷ using 100 µL of suspension containing 1x10⁸ CFU/mL of pathological tested bacteria and 1 x10⁶ CFU/ml of yeast spread on nutrient agar (NA) and Sabouraud dextrose agar (SDA) respectively. After the media had cooled and solidified, wells (10 mm in diameter) were made in the solidified agar and loaded with 100 µL of tested compound solution prepared by dissolving 100 mg of the chemical compound in one ml of dimethyl sulfoxide (DMSO). The inoculated plates were then incubated for 24 h at 37 °C for bacteria and 48 h at 28 °C for fungi. Negative controls were prepared using DMSO employed for dissolving the tested compound. Ciprofloxacin (50 µg mL⁻¹) and Ketoconazole (50 µg mL⁻¹) were used as standard for antibacterial and antifungal activity respectively. After incubation time, antimicrobial activity was evaluated by measuring the zone of inhibition against the test organisms and compared with that of the standard. The observed zone of inhibition is presented in Table 1. Antimicrobial activities were expressed as inhibition diameter zones in millimeters (mm). The experiment was carried out in triplicate and the average zone of inhibition was calculated.

Minimal inhibitory concentration (MIC) measurement

The bacteriostatic activity of the active compounds (having inhibition zones (IZ) ≥ 16 mm) was then evaluated using the two fold serial dilution technique.¹⁸ Two fold serial dilutions of the tested compounds solutions were prepared using the proper nutrient broth. The final concentration of the solutions was 200, 100, 50 and 25 µg

mL⁻¹. The tubes were then inoculated with the test organisms, grown in their suitable broth at 37 °C for 24 hours for bacteria (about 1x10⁸ CFU/ml), each 5 ml received 0.1 ml of the above inoculum and incubated at 37 °C for 24 h. The lowest concentration showing no growth was taken as the minimum inhibitory concentration (MIC).

Minimal inhibitory concentration (MIC)

The minimum inhibitory concentration (MIC) of the synthesized compounds against highly inhibited organisms is reported in Table 3.

Compounds **5** revealed the lowest MIC (25 µg mL⁻¹) against *Sarcina Lutea*, *Pseudomonas Aeruginosa* ATCC27953 and *E. coli* ATCC 25922. On the other hand, compounds **16b** exhibited high MIC (50 µg mL⁻¹) against all the tested microorganisms except *Staphylococcus Aureus* ATCC 29213. Compound **6a**, **6b**, **12a** and **16c** showed the lowest MIC 200 µg mL⁻¹ against most of the tested organisms (Table 3).

CONCLUSION

Novel 3-(4-fluorophenyl)-benzo[g]indazoles derivatives, with potential antimicrobial activity, were prepared from available α-tetralone. The new compounds were tested for their antimicrobial activity; some of them showed significant activities, probably due to the presence of some moieties such as benzo[g]indazoles and thiazole.

REFERENCES

- Mitchell, R. E., Greenwood, D. R., Sarojini, V. *Phytochemistry*, **2008**, *69*, 2704-7.
- Zhang, C. Y., Liu, X. H., Wang, B. L., Wang, S. H., Li, Z. M. *Chem. Biol. Drug. Des.*, **2010**, *75*, 489-93.
- Pandit, U.; Dodiya, A. *Med. Chem. Res.*, **2013**, *22*, 3364-71.
- Tewari, A. K., Srivastava, P., Singh, V. P., Singh, A., Goel, R. K., Mohan, C. G., *Chem. Pharm. Bull.*, **2010**, *58*, 634-8.
- Pucci, M. J., Bronson, J. J., Barrett, J. F., Den Bleyker, K. L., Discotto, L. F., Fung-Tomc, J. C., Ueda, Y. *Antimicrob. Agents Chemother.*, **2004**, *48*, 3697-701.
- Abdel-Wahab, B. F., Sediek, A., Mohamed, H. A., Awad, G. E. A. *Lett. Drug Des. Discov.*, **2013**, *10*, 111-8.
- Abdel-Wahab, B. F., Mohamed, H. A., Farahat, A. A., Dawood, K. M., *Heterocycles*, **2011**, *83*, 2731-67.
- Abdel-Wahab, B. F., Shaaban, S., *Synthesis*, **2014**, *46*, 1709-1716.
- Abdel-Wahab, B. F., Abdel-Gawad, H., Awad, G. E. A., Badria, F. A., *Med. Chem. Res.*, **2012**, *21*, 1418-1426.
- Feng, Y., Ding, X., Chen, T., Chen, L., Liu, F., Jia, X., Luo, X., Shen, X., Chen, K., Jiang, H., Wang, H., Liu, H., Liu, D., *J. Med. Chem.*, **2010**, *53*, 3465-79.
- Shriner, R. L., Anderson, J., *J. Am. Chem. Soc.*, **1939**, *61*, 2705-8.
- Krishnan, V. S. H., Chowdary, K. S., Dubey, P. K., *Indian J. Chem.*, **1999**, *38B*, 45-51.
- Czollner, L., Szilagyi, G., Lango, J., Janaky, J., *Arch. Pharm.*, **1990**, *323*, 225-7.

- ¹⁴Prokopowicz, M., Młynarz, P., Kafarski, P., *Tetrahedron Lett.*, **2009**, *50*, 7314-7.
- ¹⁵Fun, H. K., Suwunwong, T., Chantrapromma, S., *Acta Cryst.*, **2012**, *68*, 259-60.
- ¹⁶Mohamed, H. A., Abdel-Latif, E., Abdel-Wahab, B. F., Awad, G. E. A., *Int. J. Med. Chem.*, **2013**, 1-6.
- ¹⁷Scott, A. C., *Laboratory Control of Antimicrobial Therapy*. In: Collee, J. G., Duguid, J. P., Fraser, A. G., Marmion, B. P., *Mackie and MacCartney Practical Medical Microbiology*, 13th Ed, Churchill Livingstone. **1989**, *2*, 161–181.
- ¹⁸Perez, C., Pauli, M., Bazevque, P., *Acta Biol. Med. Exp.*, **1990**, *15*, 113–115.

Received: 20.09.2014.

Accepted: 07.12.2014.



DESIGN, SYNTHESIS AND BIOLOGICAL EVALUATION OF STEROIDAL TETRAZOLES AS ANTIPROLIFERATIVE AND ANTIOXIDANT AGENTS

Shamsuzzaman,^[a]* Mohd Asif,^[a] Abad Ali,^[a] Ashraf Mashrai,^[a] Hena Khanam,^[a] Asif Sherwani^[b] and Mohammad Owais^[b]

Keywords: Tetrazoles, steroids, anti-tumour activity, antioxidants, DPPH.

A series of steroidal tetrazole derivatives (**7-9**) has been obtained by facile and convenient method in a two-step process. All the newly synthesized compounds were characterized by means of elemental analyses, IR, ¹H NMR, ¹³C NMR and MS. The mean surface roughness value (*R_a*) of compound **9** was found to be 10.32 measured with AFM. Lipinski's 'Rule of Five' analysis and biological score predicted higher intrinsic quality and revealed that these compounds possess good passive oral absorption. The antiproliferative activity was tested *in vitro* against HeLa (cervical cancer), KCL-22 (myeloid leukemia), MDA-MBA-231 (breast cancer) and normal cell lines, blood peripheral mononuclear (PBMC) by MTT assay. The synthesized compounds exhibited moderate to good activity against the three human cancer cell lines and were found to be nontoxic to the normal cell lines. In addition, the synthesized compounds were tested for their *in vitro* antioxidant activity by DPPH method in which compound **9** exhibited good antioxidant activity.

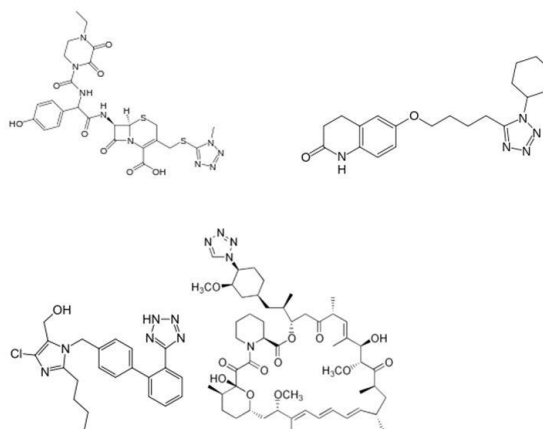
*Corresponding Authors

Phone: +91-9411003465

E-Mail: shamsuzzaman9@gmail.com

[a] Steroid Research Laboratory, Department of Chemistry, Aligarh Muslim University, Aligarh 202 002, India

[b] Interdisciplinary Unit of Biotechnology, Aligarh Muslim University, Aligarh 202 002, India



Introduction

Nitrogen heterocycles form a fundamental core of numerous pharmacophores and occupy a prominent position in medicinal chemistry.¹⁻³ They demonstrate diverse biological and pharmacological activities due in part to the similarities with many natural and synthetic molecules with known biological activity.⁴ Furthermore, compounds that contain heterocyclic moieties illustrate improved solubilities and can facilitate salt formation properties, both of which are known to be important for oral absorption.⁵ A large number of drugs contain these scaffolds.⁶ Tetrazoles are one of the most stable nitrogen rich heterocyclic compounds among other systems. These heterocyclic systems are studied extensively due to their wide range of biological and commercial applications.⁷ Tetrazoles have gained wide attention due to their use in drug design as an isosteric replacement for carboxylic acids.⁸ Applications of tetrazole includes its use in pharmaceuticals, explosives and as a precursor for a variety of nitrogen containing heterocyclic compounds.⁹ In addition they have been successfully used in the field of material science and synthetic organic chemistry as analytical reagents and synthons.¹⁰ Some well known tetrazoles having various synthetic and pharmacological properties are given in **Figure 1**.¹¹⁻¹⁴

Steroids due to their diverse properties have gained much focus among the researchers, as they constitute an important class of biologically active molecules that comprises of tetra-cyclic cyclopenta[a]phenanthrene arrangement constituting ABCD ring system and also compounds where extra rings are annulated to the main skeletal framework.¹⁵

Figure 1. Some well-known tetrazoles having synthetic and pharmacological properties

The steroids are well known for promoting growth, sexual development and regulating metabolism.¹⁶⁻¹⁸ In addition, steroids are also part of plasma membrane, thus modifying the permeability of membrane in animals.¹⁹ In recent time a lot of attention have been paid on structural modification of steroid compounds through incorporation of heteroatoms probably due to reason that various advantages associated with steroid based drug therapies.^{20,21} These hetero atoms may be present in the main ring system or in the additional fused ring. The incorporation of different types of heteroatoms to steroid skeleton enhanced their various biological activities.²² Some of the modified steroid derivatives have also been reported as active pharmacophores.²³ As a part of our extensive research program to develop facile and convenient route for the synthesis of steroid based compounds containing heteroatoms and screening their biological activities²⁴ and keeping in view the importance of tetrazole scaffolds, herein we report the synthesis, characterization and biological evaluation of steroidal tetrazole derivatives as antiproliferative and antioxidant agents.

Experimental

General

Chemicals and solvents used in this study were of ACS grade and used directly without further purification. Melting points were determined on a Biogen digital auto melting point apparatus. The IR spectra were recorded on KBr pellets with Perkin Elmer FT-IR Spectrometer spectrum Two and values are given in cm^{-1} . ^1H and ^{13}C NMR spectra were run in CDCl_3 on a Bruker Avance II 400 NMR Spectrometer (operating at 400 MHz for ^1H and at 100 MHz for ^{13}C NMR) with tetramethylsilane (TMS) as internal standard and values are given in parts per million (ppm) (δ). Mass spectra were recorded on a JEOL D-300 mass spectrometer. Elemental analyses were recorded on Perkin Elmer 2400 CHN Elemental Analyzer. Topographical images of the synthesized compounds were taken using AFM, with a uniform thin film in acetonitrile on a 10-2.5 cm glass slide. To evaporate excess solvent, the slide was kept in vacuum at room temperature for 24 h. Thin layer chromatography (TLC) plates were coated with silica gel and exposed to iodine vapours to check the homogeneity as well as the progress of reaction. Sodium sulphate (anhydrous) was used as a drying agent.

General procedure for the synthesis of steroidal cyanoacetylhydrazone derivatives (4-6)

To a solution of cholest-6-one **1-3** (1 mmol) in ethanol (20 mL), cyanoacetylhydrazine (1 mmol) was added. The reaction mixture was refluxed for 8-10 h. The progress of reaction was monitored by TLC. After completion of reaction, the excess solvent was removed to three-fourths of the original volume under reduced pressure. The reaction mixture was taken in diethyl ether, washed with water and dried over anhydrous sodium sulfate. Removal of solvents gave the crude product which was recrystallized from methanol to afford respective products (**4-6**).

General procedure for the synthesis of steroidal tetrazole derivatives (7-9)

To a solution of steroidal cyanoacetylhydrazones **4-6** (1 mmol) in DMF (20 mL), sodium azide (1 mmol) and two equimolar amount of ammonium chloride were added. The reaction mixture was refluxed for 12-15 h. The progress as well as completion of the reaction was monitored by TLC. After completion of the reaction, the excess solvent was removed under reduced pressure. The reaction mixture was then taken in diethyl ether, washed with water and dried over anhydrous sodium sulphate. Evaporation of solvents and recrystallization from methanol afforded the respective products **7-9**.

3 β -Acetoxy-5 α -cholestane-6-ylidene-tetrazol-5-yl-acetylhydrazone (7)

Yield (80 %); solid m.p. 162-164 °C; IR (KBr cm^{-1}): 3325 (NH), 1735 (OCOCH_3), 1669 (C=O), 1625 (C=N), 1325 (C-N); ^1H NMR (400 MHz, CDCl_3): δ 8.6 (brs, 2H, NH, exchangeable with D_2O), 4.7 (m, 1H, $\text{C}_3\alpha\text{-H}$, $W_{1/2}=15$ Hz),

2.7 (dd, 1H, $\text{C}_5\alpha\text{-H}$, $J=12$ Hz, 4 Hz), 2.03 (s, 3H, OCOCH_3), 1.18 (s, 3H, $\text{C}_{10}\text{-CH}_3$), 0.70 (s, 3H, $\text{C}_{13}\text{-CH}_3$), 0.97 & 0.83 (other methyl protons); ^{13}C NMR (100 MHz, CDCl_3): δ 172.3 (NHCO), 171.3 (OCOCH_3), 160.3 (N-C=N), 158.1 (C_6), 72.5 (C_3), 46 (C_{14}), 44 (C_{13}), 42 (C_4), 39 (C_{10}), 35 (C_5), 26 (C_{19}), 24 (C_{11}), 22 (C_{18}), 20 (C_{15}), 17 (C_{16}); Anal. Calc. for $\text{C}_{32}\text{H}_{52}\text{N}_6\text{O}_3$: C, 67.60, H, 9.21, N, 14.78 % found: C, 67.64, H, 9.17, N, 14.74 %. ESI MS: m/z 568 [M^+].

3 β -Chloro-5 α -cholestane-6-ylidene-tetrazol-5-yl-acetylhydrazone (8)

Yield (73 %); solid m.p. 174-176 °C; IR (KBr cm^{-1}): 3328 (NH), 1670 (C=O), 1627 (C=N), 1328 (C-N), 741(C-Cl); ^1H NMR (400 MHz, CDCl_3): δ 8.4 (brs, 2H, NH, exchangeable with D_2O), 3.8 (m, 1H, $\text{C}_3\alpha\text{-H}$, $W_{1/2}=17$ Hz), 2.6 (dd, 1H, $\text{C}_5\alpha\text{-H}$, $J=12.05$ Hz, 4.1 Hz), 1.18 (s, 3H, $\text{C}_{10}\text{-CH}_3$), 0.70 (s, 3H, $\text{C}_{13}\text{-CH}_3$), 0.97 & 0.83 (other methyl protons); ^{13}C NMR (100 MHz, CDCl_3): δ 171.2 (NHCO), 161.8 (N-C=N), 157.8 (C_6), 57.7 (C_3), 45.3 (C_{14}), 43.3 (C_{13}), 42.6 (C_4), 39 (C_{10}), 35 (C_5), 26 (C_{19}), 24.2 (C_{11}), 22.1 (C_{18}), 20 (C_{15}), 17 (C_{16}); Anal. Calc. for $\text{C}_{30}\text{H}_{49}\text{N}_6\text{ClO}$: C, 66.09; H, 9.06; N, 15.41 % found C, 66.05, H, 9.10, N, 15.45 %. ESI MS: m/z 544/546 [M^+].

5 α -Cholestane-6-ylidene-tetrazol-5-yl-acetylhydrazone (9)

Yield (70 %); solid m.p. 141-142 °C; IR (KBr cm^{-1}): 3337 (NH), 1673 (C=O), 1635 (C=N), 1330 (C-N); ^1H NMR (400 MHz, CDCl_3): δ 8.4 (brs, 2H, NH, exchangeable with D_2O), 2.4 (dd, 1H, $\text{C}_5\alpha\text{-H}$, $J=12.01$ Hz, 4.2 Hz), 1.18 (s, 3H, $\text{C}_{10}\text{-CH}_3$), 0.70 (s, 3H, $\text{C}_{13}\text{-CH}_3$), 0.97 & 0.83 (other methyl protons); ^{13}C NMR (100 MHz, CDCl_3): δ 171.8 (NHCO), 161.5 (N-C=N), 157.8 (C_6), 42.2 (C_{14}), 42.2 (C_4), 39 (C_{10}), 35 (C_5), 26 (C_{19}), 24 (C_{11}), 22 (C_{18}), 20 (C_{15}), 17 (C_{16}); Anal. Calc. for $\text{C}_{30}\text{H}_{50}\text{N}_6\text{O}$: C, 70.55; H, 9.87; N, 16.45 % found: C, 70.51, H, 9.83, N, 16.49 %. ESI MS: m/z 510 [M^+].

Physicochemical properties

The physicochemical parameters including octanol partition coefficients (miLogP), Mw, HBD, HBA and TPSA were determined. The bioactivity scores were calculated using molinspiration server (<http://www.molinspiration.com/cgi-bin/properties>) and ChemAxon (chemicalize.org).

Antiproliferative assay

The anti-tumor potential of steroidal derivatives against three cancer cell lines, viz. HeLa (cervical cancer), KCL-22 (myeloid leukemia) and MDA-MBA-231 (breast cancer) obtained from NCCS Pune, Maharashtra and normal cells was assessed by determining the number of viable cells surviving after their incubation with drug for set time period using MTT (3-(4,5-Dimethylthiazol-2-yl)-2,5-diphenyl tetrazolium bromide) method. The cancer cell lines and normal cells (PBMC) were maintained in RPMI-1640 culture medium supplemented with 10% heat-inactivated fetal calf serum (FCS). The cells were plated at a density of 5×10^4 cells per well in a 96-well plate, and cultured for 24 h at 37 °C. Stock solutions of the synthesized compounds were prepared in 1:1 mixture of DMSO and THF.

The cells were later exposed to drugs. The plates were incubated for 48 h, and cell proliferation was measured by adding 20 μL of MTT dye 5 mg mL^{-1} in phosphate-buffered saline (PBS) per well. Further the plates were incubated for more 4 h at 37 $^{\circ}\text{C}$ in a humidified chamber containing 5 % CO_2 . Formazan crystals formed due to reduction of dye by mitochondrial dehydrogenase activity of viable cells in each well were dissolved in 150 μL DMSO, and absorbance was read at 570 nm with a microplate reader (Bio-Rad Instruments). The absorption values were expressed as the cell viability (%), according to the control group as 100 %. (IC_{50}) was calculated using the software “Prism 3.0”

Blood peripheral mononuclear cell isolation

Fresh blood (20-15 mL) was kindly provided by Blood bank Jawahar Lal Nehru Medical College, AMU Aligarh. The blood sample was diluted with the same volume of PBS. Then, diluted blood was layered on Ficoll-Histopaque. The mixture was centrifuged under at 400g for 30 min at 20-22 $^{\circ}\text{C}$. The undisturbed lymphocyte layer was transferred out. The lymphocyte was washed and pelleted down with three volumes of PBS for twice and resuspended RPMI-1640 media with antibiotic and antimycotic solution 10 %, v/v (FCS). Cell counting was performed to determine the PBMC cell number with equal volume of trypan blue.

Antioxidant activity

The synthesized compounds were evaluated for their antioxidant property by 2, 2-diphenyl-1-picryl-hydrazyl (DPPH) method. Stock solution of the drug (1 mg mL^{-1}) was diluted to final concentration of 2, 4, 6, 8, 10 and 12 mg mL^{-1} in methanol. After that Methanolic DPPH solution (1 mL, 0.3 mmol) was added to 3.0 mL of drug solution of different concentrations. The tube was kept at an ambient temperature for 30 min and the absorbance was recorded at 517 nm. The radical scavenging activity of the compounds so synthesized was calculated by the following formula where A_{control} is the absorbance of the L-ascorbic acid (Standard) and A_{sample} is the absorbance of different compounds. The methanolic DPPH solution (1 mL, 0.3 mM) was used as control.

$$\%(\text{inhibition}) = 100 \frac{A_{\text{control}} - A_{\text{sample}}}{A_{\text{control}}} \quad (1)$$

Results and Discussion

Chemistry

Synthesis of highly potent molecules from simpler ones always gained attention among the chemists. So herein, we report the synthesis of new steroidal tetrazole derivatives (**7-9**) using literature method.²⁵ All target compounds **7-9** as shown in (Scheme 1) were obtained by two-step process by reaction of compounds **4-6** with sodium azide in presence of ammonium chloride and DMF as solvent under refluxed condition for about 12-15 h, on the completion of the reaction, the products were obtained in good yields (70-

80 %). The structures of the compounds were established by means of their IR, ^1H NMR, ^{13}C NMR, MS and analytical data. The selected diagnostic bands in IR spectra of synthesized products provide useful information for determining structures of the tetrazole derivatives. The absorption bands at 3325-3337 cm^{-1} , 1625-1635 cm^{-1} and 1325-1330 cm^{-1} confirmed the presences of NH, C=N and C-N groups, respectively, while a strong absorption band at 1669-1673 cm^{-1} attributed to amide group in compounds **7-9**. The ^1H NMR spectra of the synthesized compounds, besides the expected signals of cholestane moiety, exhibited broad singlet at δ 8.6-8.4 (exchangeable with D_2O) was ascribed to NH proton. The singlets at δ 1.18 and 0.70 were assigned to three protons of the methyl group attached to ‘ C_{10} ’ and three protons of the methyl group attached to ‘ C_{13} ’ respectively. In ^{13}C NMR spectra, the signals at δ 172.3-171.8, 161.8-160.3 and 158.1-157.8 confirmed the presence of NHCO, N-C=N and C=N, respectively. Finally the presence of distinct molecular ion peak [M^+] at m/z : 568, 544/546 and 510 also proved the formation of compounds (**7-9**).

Atomic force microscopy study

Morphological study of the compounds is generally important to understand their physicochemical role, topology and size distribution, which play crucial role in drug studies. Topographical images of compound **9** were taken using AFM, with a uniform thin film. The sample was scanned using non-contact tapping mode and obtained 3D topological image (Figure 2).

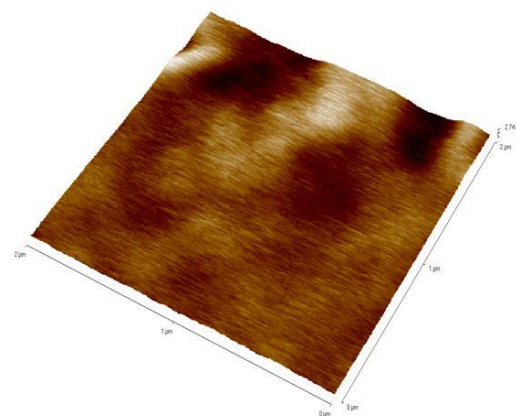


Figure 2. Topographic image of **9** using atomic force microscopy

The vertical and horizontal line analysis of images showed roughness parameters such as minimum and maximum surface value. Mean roughness (R_a) values which was found to be 10.32 nm. The other roughness parameters like mid-value (average of maximum and minimum), mean, peak to valley of the line (R_{pv} , difference between minimum and maximum), root-mean-squared roughness, ten point average roughness area (R_z , is the arithmetic average of the five highest and five lowest valleys peaks in the line calculated by ten point average), skewness (R_{sk}) and kurtosis (R_{ku}) values of line are given in Table 1.

Table 1. AFM topographical mean surface parameters (nm) for compound **9**.

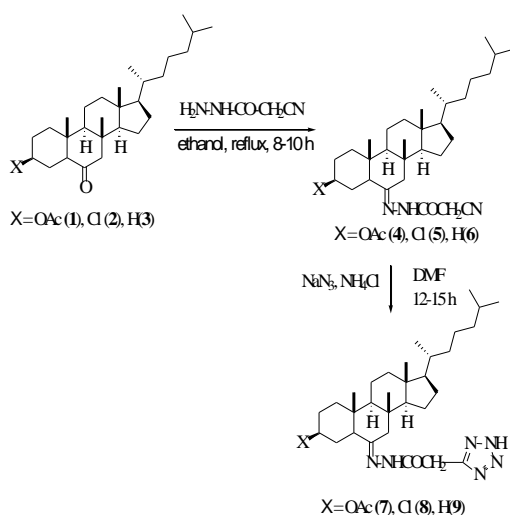
Line	Min	Max	Mid	Mean	R_{pv}	R_q	R_a	R_z	R_{sk}	R_{ku}
Horizontal	-20.14	14.10	-3.11	0.00	42.45	10.32	11.45	22.51	0.25	2.21
Vertical	-11.12	10.11	-1.10	0.00	22.60	5.90	4.12	22.45	0.69	3.34

Table 2. Calculated physicochemical properties of steroidal derivatives (**4-9**).

Compounds	Mw	C_{logP}	HBD	HBA	TPSA	No. of violations
4	511.75	6.207	0	1	91.559	2
5	488.16	6.740	0	1	65.254	1
6	453.715	6.887	0	1	65.250	1
7	554.78	5.971	0	2	122.234	2
8	531.189	6.505	0	2	95.929	2
9	496.744	6.652	0	2	95.929	1

Table 3. Bioactivity score of steroidal derivatives (**4-9**).

Compounds	GPCR ligand	Ion channel	Modulator kinase	Protease inhibitor	Nuclear receptor ligand	Enzyme inhibitor
4	-0.17	-0.37	-0.68	-0.10	-0.16	0.20

**Scheme 1.** Synthesis of steroidal tetrazoles **7-9**

In silico study

Rule of Five and bioactivity score

The use of Lipinski's rule as a filter to choose the reasonable scaffolds for biological activity is well known. The rule states that most molecules with good membrane permeability have $\log P \leq 5$, molecular weight ≤ 500 , number of hydrogen bond acceptors ≤ 10 , number of hydrogen bond donors ≤ 5 and polar surface area less than 140 \AA^2 . Synthesized compounds showed two violations of Lipinski's rules due to a calculated C_{logP} value above the limit of 5 and the molecular weight above 500 (**Tables 2**). Based on the above results we can say that the synthesized compounds adhere to Lipinski's "Rule of Five".

The exceptions to the Lipinski's rule are recognized and involve anticancer drugs such as Doxorubicin. The physicochemical properties of these new scaffolds suggest that the synthesized compounds are reasonable starting points for a drug discovery effort. The bioactivity scores of the synthesized compounds were also calculated for six criteria, GPCR ligand activity, ion channel modulation, kinase inhibition activity, protease inhibitor, enzyme inhibitor and nuclear receptor ligand activity.

For organic molecules if the bioactivity score is more than 0.00 then the compound is active but if it is between -0.50 to 0.00 then the compound is moderately active and if the compound has less than -0.50 then it is inactive compound.²⁶ As we can see in **Table 3**, the synthesized compounds show good bioactivity score.

Antiproliferative activity

The IC_{50} values (concentration required to inhibit tumor cell proliferation by 50%) for the synthesized steroidal compounds against three human cancer cell lines including HeLa, KCL-22 and MDA-MBA-231 were determined using the MTT assay, while PBMCs were used as normal cells. A period of 48 h of drug exposure was chosen to test cytotoxicity. The well known anticancer drugs 5-Fluorouracil (5-Fu) and Doxorubicin (Dox) were used as references.

As shown in **Table 4**, all of the synthesized compounds showed moderate to good antiproliferative activities against the cancer cell lines. From the antiproliferative screening data (**Table 4**) it was found that compounds **4-6** were less active than compounds **7-9** as they exhibit much higher IC_{50} values and this could be explained on basis of the fact that compounds **7-9** contain heterocyclic moiety which

results in better activity. During the cytotoxic screening of steroidal tetrazoles **7-9**, their potential behaviour against given cancer cells was depicted: compound **7** showed $IC_{50} = 18.01 \mu\text{M}$ (HeLa), $19.14 \mu\text{M}$ (KCL-22), $17.12 \mu\text{M}$ (MDA-MBA-231). Compound **8** also showed IC_{50} value in the range of $15.15 \mu\text{M}$ (HeLa), $17.22 \mu\text{M}$ (KCL-22), $18.14 \mu\text{M}$ (MDA-MBA-231). While compound **9** demonstrated improved anti-proliferative activities with the $IC_{50} = 11.18 \mu\text{M}$ (HeLa), $14.24 \mu\text{M}$ (KCL-22), $21.03 \mu\text{M}$ (MDA-MBA-231).

The compound **9** was found to be the most active among all synthesized compounds, and showed marked inhibitory effect against Hela. To confirm the result of cytotoxicity the synthesized compounds **4-9** were evaluated against non cancerous cell line PBMC, and none of the synthesized compounds were found to be toxic, all compounds showed $IC_{50} > 60 \mu\text{M}$. Further modifications and derivatization may lead to the development of more active antiproliferative agents.

Antioxidant activity

The *in vitro* antioxidant activity and scavenging effects of steroidal derivatives **4-9** were evaluated by using different reactive species assay containing DPPH radical scavenging activity. The free radical scavenging activity of the synthesized compounds was evaluated through their ability to quench the DPPH. using ascorbic acid as a reference.

Table 4. Antiproliferative activity of steroidal derivatives (**4-9**).

Compounds	HeLa	KCL22	MDA-MBA-231	PMBC
4	38.27±0.1	39.15±0.2	45.03±0.5	67
5	39.21±2.5	49.11±0.8	47.24±0.2	68
6	36.61±1.8	23.22±0.2	37.34±0.8	69
7	18.01±1.2	19.14±0.6	17.12±0.2	64
8	15.15±0.4	17.22±0.6	18.14±2.5	69
9	11.18±0.7	14.24±0.6	21.03±1.5	64
Dox	4.1±0.1	3.1±0.3	4.12±0.6	-
5-Flu	8.1±0.3	6.5±0.2	9.04±0.4	-

Value represent the mean ± standard error mean (SEM) of three experiment.

Table 5. The antioxidant activity data of steroidal derivatives (**4-9**)^a

Compounds	Inhibition (in %) at various doses in $\mu\text{g mL}^{-1}$			
	25	50	75	100
4	14.1±1.4	12.5±0.3	15.6±0.3	20.2±0.4
5	16.8±0.2	14.8±0.5	14.6±0.5	15.1±0.8
6	17.2±0.7	13.1±0.3	11.2±0.9	15.5±0.2
7	19.3±0.2	19.5±0.4	16.6±0.7	22.9±0.9
8	20.1±0.5	25.7±0.2	12.6±0.1	21.8±0.7
9	22.2±0.5	21.1±0.2	28.4±0.4	27.7±0.2
Standard	36.0±0.3	37.0±0.2	44.0±0.3	50.0±0.5

^aValue represent the mean ± standard error mean (SEM) of three experiment. Standard: ascorbic acid.

Potencies for the antioxidant activity of the synthesized compounds to the reference drug are shown in **Table 5**. In general, all the synthesized compounds were less potent than the reference. Among the synthesized compounds, compound **9** exhibited a slightly more antioxidant activity.

Conclusion

In summary, we have developed a facile and expedient approach for the synthesis of new steroidal tetrazole derivatives which involves the reaction of steroidal cyanoacetylhydrazone with sodium azide in DMF as solvent. The reaction completed in 12-15 h and on completion, better yields (70-80 %) were obtained. This approach offered a very straight forward and efficient method for access to steroidal tetrazoles. From *in vitro* antiproliferative screening, it is clear that compound **9** showed better cytotoxic behaviour among all synthesized compounds with minimum IC_{50} value against HeLa cell line. All synthesised compounds were also screened for their *in vitro* antioxidant activity and compound **9** was found to be slightly more active. In conclusion, the present study showed that synthesized compounds can be used as a template for future development through modification and derivatization to design more potent and selective antiproliferative as well as antioxidant agents.

Acknowledgments

The authors thank the Chairman, Department of Chemistry, A.M.U. Aligarh, for providing the necessary research facilities. MA and AA acknowledge UGC, New Delhi India for providing research fellowship.

References

- Polshettiwar, V., Varma, R. S., *Curr. Opin. Drug Discover Dev.*, **2007**, *10*, 723-737.
- Padwa, A., Bur, S. K., *Tetrahedron*, **2007**, *63*, 5341-5378.
- D'Souza, D. M., Muller, T. J., *Chem. Soc. Rev.*, **2007**, *36*, 1095-1108.
- DeSimone, R. W., Currie, K. S., Mitchell, S. A., Darrow, J. W., Pippin, D. A., *Comb. Chem. High Throughput Screening*, **2004**, *7*, 473-494.
- Leeson, P. D., Springthorpe, B., *Nat. Rev. Drug Discov.*, **2007**, *6*, 881-890.
- McGrath, N. A., Brichacek, M., Njardarson, J. T., *J. Chem. Educ.*, **2010**, *87*, 1348-1349.
- Butler, R. N., Katritzky, A. R., Rees, C. W., Scriven, E. F.V., *Comprehensive Heterocyclic Chemistry*, Pergamon Oxford, **1996**.
- Herr, R. J., *Bioorg. Med. Chem.*, **2002**, *10*, 3379-3393.
- (a) Ostrovskii, V.A., Pevzner, M. S., Kofmna, T.P., Shcherbinin, M. B., Tselinskii, I.V., *Targets Heterocycl. Syst.*, **1999**, *3*, 467-526; (b) Hiskey, M., Chavez, D. E., Naud, D. L., Son, S.F., Berghout, H. L., Bolme, C. A., *Proc. Int. Pyrotech. Semin.*, **2000**, *27*, 3-14.

- ¹⁰Moskvin, L. B., Bulatov, A.V., Griogorjev, G. L., Koldobkij, G. I., *Flow. Inject. Anal.* **2003**, *20*, 53.
- ¹¹Mohite, P. B., Bhaskar, V. H., *Int. J. Pharm Tech. Res.*, **2011**, *3*, 1557-1566.
- ¹²Osheroff, N., Zechiedrich, E. L., Gale, K. C., *BioEssays*, **1991**, *13*, 269-275.
- ¹³Issell, B. F., *Cancer Chemother. Pharmacol.*, **1982**, *7*, 73-80.
- ¹⁴Beers, S. A., Imakura, Y., Dai, H. J., Li, D. H., Cheng, Y. C., Lee, K. H., *J. Nat. Prod.*, **1988**, *5*, 901-905.
- ¹⁵Turner, C. I., Williamson, R. M., Turner, P., Sherburn, M. S., *Chem. Commun.*, **2003**, 610-1611.
- ¹⁶Issemann, I., Green, S., *Nature*, **1990**, *347*, 645-650.
- ¹⁷Ahtiainen, J. P., Hulmi, J. J., Kraemer, W. J., Lehti, M., Nyman, K., Selänne, H., *Steroids*, 2011, *76*, 183-192.
- ¹⁸Evans, R. M., *Science*, **1988**, *240*, 889-895.
- ¹⁹Morzycki, J. W., *Steroids*, **2014**, *83*, 62-79.
- ²⁰Zhang, B. L., Zhang, E., Pang, L. P., Song, L. X., Li, Y. F., Yu, B., Liu, H. M., *Steroids*, **2013**, *78*, 1200-1208.
- ²¹Elmegeed, G. A., Khalil, W. K. B., Mohareb, R. M., Ahmed, H. H., Abd-Elhalim, M. M., Elsayed, G. H., *Bioorg. Med. Chem.*, **2011**, *19*, 6860-6872.
- ²²Singh, H., Jindal, D. P., Yadav, M. R., Kumar, M., *Heterosteroids and Drug Rresearch*, in *Progr. Med. Chem.*, Elsevier, Amsterdam, **1991**, *28*, 233-315.
- ²³Morand, P., Lyall, J., *Chem. Rev.*, **1968**, *68*, 85-124.
- ²⁴(a)Shamsuzzaman, Khanam, H., Mashrai, A., Sherwani, A., Owais, M., Siddiqui, N., *Steroids*, **2013**, *78*, 1263-1272; (b) Shamsuzzaman, Ali, A., Asif, M., Mashrai, A., Khanam, H., *Eur. Chem. Bull.*, **2014**, *3*, 939-945.
- ²⁵Faria, J. V., Santos, M. S. D., Bernardino, A. M. R., Becker, K. M., Machado, G. M. C., Rodrigues, R. F., Canto-Cavalheiro, M. M., Leon, L. L., *Bioorg. Med. Chem. lett.*, **2013**, *23*, 6310-6312.
- ²⁶Utrecht, J., *Curr. Opin. Drug Discover Dev.*, **2001**, *4*, 55-59.

Received: 30.09.2014.

Accepted: 08.12.2014.



KINETICS AND MECHANISM OF THE OXIDATION OF ALIPHATIC ALCOHOLS BY TETRAAMMINECOPPER(II) BIS(PERMANGANATE)

Gifty Sharma,^[a] Jayshree Banerji,^[a] Priyanka Purohit,^[a] Pradeep K. Sharma^[a] and Kalyan K. Banerji^{[b]*}

Keywords: tetraamminecopper(II) permanganate; alcohol; oxidation; kinetics; mechanism; correlation analysis

The oxidation of aliphatic alcohols by tetraamminecopper(II) bis(permanganate) (TACP) in aqueous acetic acid leads to the formation of corresponding carbonyl compounds. The reaction is first order with respect to TACP. A Michaelis-Menten type kinetics is observed with respect to alcohols. The reaction shows a first order dependence on hydrogen ions. The oxidation of $[1,1-^2H_2]$ ethanol and $[2-^2H]$ propan-2-ol exhibits the presence of a substantial primary kinetic isotope effect ($k_H/k_D = 3.52$ and 3.96 respectively at 298 K). The rate of disproportionation of the intermediate is susceptible to both polar and steric effects of the substituents. A suitable mechanism has been proposed.

* Corresponding Authors

Fax: +912912577540

E-Mail: banerjikk@rediffmail.com

[a] Chemical Kinetics Laboratory, Department of Chemistry, J.N.V. University, Jodhpur 342005, India

[b] Faculty of Science, National Law University, Jodhpur 342304, India

Introduction

Derivatives of permanganic acid have been used as mild and selective oxidizing reagents in synthetic organic chemistry.¹⁻⁵ Tetraamminecopper(II) bis(permanganate) (TACP) is also one of such compounds used for the oxidation of organic compounds.⁶ We have been interested in the kinetic and mechanistic aspects of the oxidation by derivatives of permanganic acid and several reports on permanganate derivatives have already reported from our laboratory.⁷⁻¹¹

In continuation of our earlier work with Mn(VII), we report here the kinetics and mechanism of oxidation of some aliphatic alcohols by TACP in aqueous acetic acid as solvent. The mechanistic aspects are discussed. A suitable mechanism has also been proposed.

Experimental

Materials

TACP was prepared by the reported method¹² and its purity was checked by an iodometric method. The procedures used for the purification of alcohols have been described earlier.¹³ $[1,1-^2H_2]$ Ethanol¹⁴ and $[2-^2H]$ propan-2-ol¹⁵ was prepared by reported methods. Their isotopic purity, as ascertained by their NMR spectra, was 96 ± 2 % and 95 ± 3 %. Perchloric acid (Merck) was used as a source of hydrogen ions. Acetic acid was refluxed for 3 h with acetic anhydride and chromic oxide and then distilled.

Product analysis

The product analysis was carried out under kinetic conditions. In a typical experiment, ethanol (4.60 g, 0.10 mol) and TACP (1.88 g, 0.01 mol) were made up to 50 cm³ in 1:1 acetic acid-water (v/v) and kept in dark for *ca.* 15 h to ensure the completion of the reaction. The solution was then treated with an excess (200 cm³) of a saturated solution of 2,4-dinitrophenylhydrazine in 2 mol L⁻¹ HCl and kept overnight in a refrigerator. The precipitated 2,4-dinitrophenylhydrazone (DNP) was filtered off, dried, weighed, recrystallized from ethanol and weighed again. The yield of DNP before and after recrystallization was 2.02 g (91 %) and 1.79 g (79 %), respectively. The DNP was found identical (m.p. and mixed m.p.) with the DNP of acetaldehyde. Similar experiments with other alcohols led to the formation of DNP of the corresponding carbonyl compounds in yields ranging from 70 to 94%, after recrystallization.

Kinetic Measurements

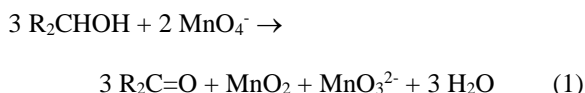
The reactions were followed under pseudo-first-order conditions by keeping a large excess ($\times 10$ or greater) of the alcohol over TACP. The temperature was kept constant to ± 0.1 K. The solvent was 1:1 acetic acid-water (v/v), unless specified otherwise. The reactions were followed by monitoring the decrease in the concentration of TACP spectrophotometrically at 529 nm for 80 % of the reaction. The pseudo-first-order rate constants, k_{obs} , were evaluated from the linear ($r^2 > 0.995$) plots of $\log [TACP]$ against time. Duplicate kinetic runs showed that the rate constants were reproducible to within ± 3 . Preliminary experiments showed that the reaction is not sensitive to changes in ionic strength, therefore, no attempt was made to keep the ionic strength constant. Simple and multivariate regression analyses were carried out by the least-squares method. We have used standard deviation (*sd*), coefficient of determination (R^2 or r^2) and Exner's¹⁶ parameter, ψ , as measures of the goodness of fit in correlation analysis.

Results

Kinetic data were obtained for all the alcohols studied. Since the results are similar, only representative data are reproduced here.

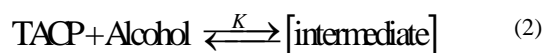
Stoichiometry

The oxidation of alcohols results in the formation of corresponding carbonyl compounds. The overall reaction may be represented as equation (1)



Rate Law

The reactions are of first order with respect to TACP. Further, the pseudo-first order rate constant, k_{obs} is independent of the initial concentration of TACP. The reaction rate increases with increase in the concentration of the alcohols but not linearly (Table 1). A plot of $1/k_{\text{obs}}$ against $1/[\text{alcohol}]$ is linear ($r^2 > 0.995$) with an intercept on the rate-ordinate. Thus, Michaelis-Menten type kinetics is observed with respect to the alcohols. This leads to the postulation of following overall mechanism (2) and (3) and rate law (4). The reaction showed a first order dependence on hydrogen ions (Table 1).



$$\text{Rate} = \frac{Kk_2[\text{Alcohol}][\text{TACP}]}{1 + K[\text{Alcohol}]} \quad (4)$$

The dependence of reaction rate on the alcohol concentration was studied at different temperatures and the values of K and k_2 were evaluated from the double reciprocal plots. The thermodynamic parameters of the formation of the intermediate and activation parameters of its disproportionation were calculated from the values of K and k_2 respectively at different temperatures (Tables 2 and 3).

Test for free radicals

The oxidation of alcohols, in an atmosphere of nitrogen, failed to induce polymerisation of acrylonitrile. Further, the addition of acrylonitrile did not affect the rate (Table 1). This indicates that a one-electron oxidation, giving rise to free radicals, is unlikely in the present reaction. To further confirm the absence of free radicals in the reaction pathway, the reaction was carried out in the presence of 0.05 mol L^{-1} of 2,6-di-*t*-butyl-4-methylphenol (butylated hydroxytoluene or BHT). It was observed that BHT was recovered unchanged, almost quantitatively.

Kinetic Isotope Effect

To ascertain the importance of the cleavage of the $\alpha\text{-C-H}$ bond in the rate-determining step, oxidation of $[1,1\text{-}^2\text{H}_2]\text{ethanol}$ (MeCD_2OH) and $[2\text{-}^2\text{H}]\text{propan-2-ol}$ ($[\text{Me}_2\text{CDOH}]$) was studied. The results (Table 3) showed that the disproportionation of the alcohol-TACP intermediate exhibited the presence of a primary kinetic isotope effect.

Effect of Solvents Composition

The oxidation of ethanol was studied in solvents containing different amounts of acetic acid and water. The rate of oxidation increases with an increase in the amount of acetic acid in the solvent (Table 4).

Discussion

A good linear correlation ($r^2 = 0.9894$; $\psi = 0.11$; $sd = 5.19$; slope = 434 ± 27) between the values the activation enthalpies and entropies of the oxidation of the fourteen aliphatic alcohols indicated the operation of compensation effect in this reaction.¹⁷ The reaction also exhibited an excellent isokinetic effect, as determined by Exner's criterion.¹⁸ An Exner's plot between $\log k_2$ at 288 K and at 318 K was linear ($r^2 = 0.9972$; $sd = 0.11$; $\psi = 0.05$; slope = 0.6804 ± 0.0104). The value of isokinetic temperature is $408 \pm 15 \text{ K}$.

Table 1. Rate constants of the oxidation of 2-propanol by TACP at 298 K

10^3 [TACP], mol L^{-1}	[2-Propanol], mol L^{-1}	$[\text{H}^+]$, mol L^{-1}	$10^4 k_{\text{obs}}$ s^{-1}
1.0	0.01	1.0	2.13
1.0	0.04	1.0	7.55
1.0	0.08	1.0	12.8
1.0	0.12	1.0	17.0
1.0	0.20	1.0	22.8
1.0	0.25	1.0	25.4
1.0	0.30	1.0	27.4
1.0	0.40	1.0	30.6
2.0	0.20	1.0	22.7
3.0	0.20	1.0	22.5
4.0	0.20	1.0	23.0
5.0	0.20	1.0	23.1
6.0	0.20	1.0	22.7
1.0	0.30	0.1	2.68
1.0	0.30	0.2	5.50
1.0	0.30	0.4	10.8
1.0	0.30	0.6	16.5
1.0	0.30	1.2	33.0
1.0	0.30	1.2	32.8*

*contained 0.01 mol dm^{-3} acrylonitrile

Table 2. Formation constants and thermodynamic parameters of alcohol-TACP intermediate

S.No.	Alcohol	$K, \text{dm}^{-3} \text{mol}^{-1}$				ΔH kJ mol ⁻¹	ΔS J mol ⁻¹ K ⁻¹	ΔG kJ mol ⁻¹
		288 K	298 K	308 K	318 K			
1.	Methanol	3.27	3.00	2.73	2.46	-9.7±0.4	-16±0.8	-5.2±0.2
2.	Ethanol	3.52	3.21	2.91	2.66	-9.6±0.1	-15±0.3	-5.4±0.2
3.	1-Propanol	3.94	3.61	3.26	2.98	-9.6±0.5	-14±0.5	-5.7±0.1
4.	1-Butanol	4.00	3.62	3.23	2.87	-10.9±0.3	-18±0.9	-5.7±0.2
5.	2-Methyl-1-propanol	4.89	4.43	3.97	3.52	-10.8±0.3	-16±1.0	-6.2±0.2
6.	1-Pentanol	2.45	2.25	2.07	1.87	-9.3±0.2	-17±0.8	-4.5±0.2
7.	2-Chloroethanol	4.02	3.63	3.26	2.89	-10.8±0.3	-18±0.9	-5.7±0.2
8.	2-Methoxyethanol	3.23	2.97	2.73	2.47	-9.3±0.2	-14±0.5	-5.2±0.2
9.	2,2-Dimethylethanol	3.44	3.14	2.85	2.60	-9.6±0.1	-15±0.4	-5.3±0.1
10.	2-Propanol	5.25	4.75	4.26	3.77	-10.9±0.3	-16±1.0	-6.3±0.2
11.	2-Butanol	2.95	2.71	2.49	2.26	-9.2±0.2	-15±0.6	-5.0±0.1
12.	2-Pentanol	4.53	4.11	3.68	3.26	-10.8±0.3	-17±1.0	-6.0±0.2
13.	1-Chloro-2-propanol	3.49	3.20	2.94	2.66	-9.3±0.2	-14±0.7	-5.4±0.2
14.	2-Methoxy-2-propanol	4.52	4.15	3.72	3.36	-10.1±0.3	-14±0.7	-6.0±0.2
15.	MeCD ₂ OH	3.66	3.33	3.03	2.77	-9.6±0.1	-14±0.2	-5.5±0.1
16.	Me ₂ CDOH	5.04	4.56	4.09	3.62	-10.9±0.3	-16±1.0	-6.2±0.2

Table 3. Rate constants and activation parameters for the disproportionation of alcohol-TACP intermediate

Alcohol ^a	$10^5 k_2 (\text{s}^{-1})$				ΔH^* kJ mol ⁻¹	ΔS^* J mol ⁻¹ K ⁻¹	ΔG^* kJ mol ⁻¹
	288 K	298 K	308 K	318 K			
1	0.21	0.84	3.40	11.6	99.7±0.9	- 8±1	102±2
2	6.61	19.5	52.3	128	72.7±1.0	- 73±2	94.2±0.8
3	11.1	30.4	77.8	188	69.3±1.1	- 80±2	93.1±0.8
4	17.3	45.6	103	240	63.8±0.8	- 96±2	92.2±0.6
5	27.4	66.8	156	346	61.9±0.8	- 99±1	91.1±0.8
6	20.2	50.4	122	274	63.8±1.0	- 95±3	91.8±1.8
7	0.36	1.42	4.88	14.5	91.4±0.9	- 32±1	101±2
8	1.81	6.02	18.2	48.8	81.1±0.8	- 54±2	97.1±1.1
9	240	425	745	1300	40.3±0.6	- 157±2	86.5±0.7
10	260	467	830	1410	40.5±0.5	- 154±2	86.3±0.8
11	386	677	1140	1940	38.2±0.4	- 158±2	85.4±0.5
12	678	1080	1670	2700	32.3±0.7	- 175±2	84.2±0.5
13	15.7	36.0	79.2	177	58.8±0.8	- 114±2	92.6±0.5
14	71.2	143	271	537	48.5±0.7	- 137±3	89.3±0.7
15	1.82	5.54	15.3	38.4	74.9±0.5	-76±2	97.3±0.4
k_H/k_D	3.64	3.52	3.42	3.33			
16	63.1	118	217	380	43.1±0.1	-157±1	89.7±0.8
k_H/k_D	4.12	3.96	3.82	3.71			

^aFor the identity of compounds see table 2

The linear isokinetic correlation implies that all the alcohols are oxidized by the same mechanism and the changes in rate are governed by the changes in both the enthalpy and entropy of the activation.

Table 4. Effect of solvent composition on the rate of oxidation of 2-propanol by TACP at 298 K

% AcOH (v/v)	25	40	50	60	70
$10^4 k_{\text{obs}} (\text{s}^{-1})$	10.3	14.6	23.0	34.7	50.4

[2-Propanol] 0.20 mol dm⁻³; [TACP] 0.001 mol dm⁻³; [H⁺] 1.0 mol dm⁻³

Correlation Analysis of Reactivity

A perusal of the data of Tables 2 and 3 showed that the formation constants of the alcohol-TACP intermediate do not vary much with the structure of alcohol, however, the rate of disproportionation exhibited wide variation with structure. Therefore, the rate of disproportionation was subjected to correlation analysis. The rates of disproportionation failed to yield any significant correlation separately with either Taft's¹⁹ σ^* or E_s values.

$$\log k_2 = -1.72(\pm 0.27) \Sigma \sigma^* - 2.44 \quad (5)$$

$$r^2 = 0.7766; \text{sd} = 0.47; \psi = 0.49; n = 14; T = 298 \text{ K}$$

$$\log k_2 = -0.98(\pm 0.18) \Sigma E_s - 2.73 \quad (6)$$

$$r^2 = 0.7035; sd = 0.54; \psi = 0.57; n = 14; T = 298 \text{ K}$$

The rates were, therefore, correlated in terms of Pavelich-Taft's²⁰ dual substituent-parameter (DSP) equation (7).

$$\log k_2 = \rho^* \sigma^* + \delta E_s + \log k_0 \quad (7)$$

The values of substituent constants were obtained from the compilation by Wiberg.¹⁹ The correlations are excellent; the reaction constants being negative (Table 5). There is no significant collinearity ($r^2 = 0.2322$) between σ^* and E_s values of the fourteen substituents.

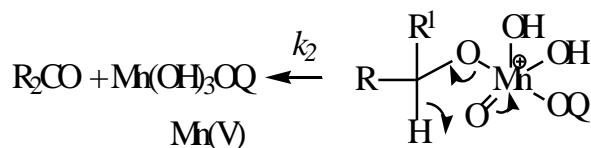
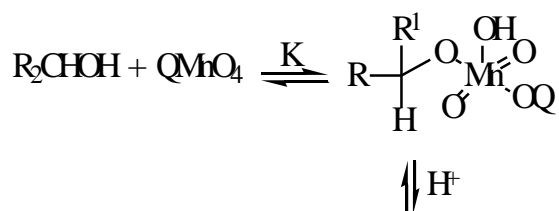
Table 5. Temperature dependence of the reaction constants

Temp., K	ρ^*	δ	R^2	sd	ψ
288	-1.35±0.01	-0.75±0.01	0.9998	0.01	0.02
298	-1.22±0.02	-0.63±0.02	0.9988	0.03	0.04
308	-1.10±0.02	-0.53±0.01	0.9994	0.03	0.03
318	-0.99±0.01	-0.45±0.02	0.9996	0.02	0.02

The negative polar reaction constant indicates an electron-deficient carbon centre in the transition state of the rate-determining step. The negative steric reaction constant shows a steric acceleration of the reaction. This may be explained on the basis of high ground state energy of the sterically crowded alcohols. Since the crowding is relieved in the product carbonyl compound as well as in the transition state leading to it, the transition state energies of the crowded and uncrowded alcohols do not differ much and steric acceleration, therefore, results.

Mechanism

The presence of a substantial primary kinetic isotope effect confirms the cleavage of $\alpha\text{-C-H}$ bond in the rate-determining step. The Michaelis-Menten kinetics indicates the formation of an intermediate in a rapid pre-equilibrium. This may well be the formation of a permanganate ester. Formation of such esters is known in several oxidation reactions.²¹ The observed acid-catalysis suggest that the intermediate is protonated in a fast reversible reaction, prior to the slow step. The observed solvent composition effect may be attributed to the change in the acidity of the medium with a change in the amount of acetic acid. Wiberg and Evans²² have determined the Hammett's acidity function, H_0 , for low concentration of perchloric acid in a series of acetic acid-water mixtures. They observed that the acidity increases as the concentration of acetic acid increases. The present reaction is an acid-catalyzed one and with an increase in the acidity of the solution, the rate is expected to increase. The mechanism depicted in Scheme 1 explains all the observed data.



Scheme 1

The low negative values of the polar reaction constant support the proposed mechanism. In an oxidation reaction, the net flow of the electrons is from the reductant to the oxidant. Therefore, an electron-deficiency is created, in the transition state, in the reductant moiety. The low magnitude of the primary kinetic isotope effect is also in accord with the non-linear transition state implied in the unimolecular decomposition of the intermediate.

Acknowledgements

Thanks are due to UGC (India) for financial support for BSR, a one-time grant (to PKS) and a start-up Grant (to PP).

References

- Vimala, D. C., Nagendrappa, G., *J. Saudi Chem. Soc.*, **2010**, *14*, 147.
- Dash, S, Patel, S., Mishra, B. K., *Tetrahedron*, **2009**, *65*, 707.
- Lee, D. G., Brown, K. C., *J. Am. Chem. Soc.*, **1982**, *104*, 5074.
- Firouzabadi, H., Naderi, M., Saradarian, A., Vessel, V., *Synth. Commun.*, **1983**, *13*, 611.
- Hajipour, A. R., Arbabian, M., Ruoho, A. E., *J. Org. Chem.*, **2002**, *67*, 8622.
- Klobb, M. T., *Bull. Soc. Chim. Fr.*, **1890**, *3*, 508
- Banerji, J., Kotai, L., Sharma, P. K., Banerji, K. K., *Eur. Chem. Bull.*, **2012**, *1*, 1310.
- Bohra, A., Sharma, P. K., Banerji, K. K., *J. Org. Chem.*, **1997**, *62*, 3562.
- Shukla, R., Sharma, P. K., Kotai, L., Banerji, K. K., *Proc. Indian Acad. Sci. (Chem. Sci.)*, **2003**, *115*, 129.
- Shukla, R., Kotai, L., Sharma, P. K., Banerji, K. K., *J. Chem. Res. (S)*, **2003**, 184
- Kumar, A., Mishra, P., Kotai, L., Banerji, K. K., *Indian J. Chem.*, **2003**, *42A*, 72.

- ¹²Kotai, L., Banerji, K. K., Sajo, I., Kristof, J., Sreedhar, B., Holly, S., Keresztury, G., Rockenbauer, A., *Helv. Chem. Acta*, **2002**, 85, 2316.
- ¹³Grover, A., Varshney, S., Banerji, K. K., *Indian J. Chem.*, **1996**, 35A, 206.
- ¹⁴Kalpan, L., *J. Am. Chem. Soc.*, **1958**, 80, 2639.
- ¹⁵Srinivasan, N. S., Venkatasubramanian, N., *Tetrahedron*, **1974**, 30, 419.
- ¹⁶Exner, O., *Collect. Chem. Czech. Commun.*, **1966**, 31, 3222.
- ¹⁷Liu, L., Q-X Guo, *Chem. Rev.*, **2001**, 101, 673.
- ¹⁸Exner, O., *Collect. Chem. Czech. Commun.*, **1964**, 29, 1094.
- ¹⁹Wiberg, K. B., *Physical Organic Chemistry*, Wiley, New York, **1963**, 416.
- ²⁰Pavelich, W. A., Taft, R. W., *J. Am. Chem. Soc.*, **1957**, 79, 4835.
- ²¹Rocek, J., Rudkowsky, A. E., *J. Am. Chem. Soc.*, **1973**, 95, 7123; Mukherjee, J., Banerji, K. K., *J. Org. Chem.*, **1981**, 46, 2323.
- ²²Wiberg, K. B., Evans, R. J., *J. Am. Chem. Soc.*, **1958**, 80, 3019.

Received: 26.11.2014.

Accepted: 07.12.2014.



WHITHER GENOME SEQUENCING OF PASSER?

Prashanth Suravajhala^[a,b] and Kshitish Acharya^[c,d]

Keywords: House sparrow; genome sequencing; evolution; comparative genomics; agriculture

Passer domesticus or the common house sparrow is a passerine with a world-wide distribution. The species do not show an obligatory commensal relationship with human beings. House sparrows have lived successfully around human beings for a long time, often competing well with other birds. In fact, these birds were considered a menace in the past, particularly in the USA. House sparrows may be occasional pollinators of flowers and edible crops, and despite being perceived as anti-farmers, they might actually be assisting in pest control. But in the recent times, the numbers of this bird have been declining in many urban areas because of electromagnetic radiations and other anthropogenic activities. *Passer domesticus* may suite as one of the models for studies influencing human technological advances on life and commensal life-forms in human habitats. Keeping in view of the good level of interest of obtaining better insights into evolutionary lineages of these birds and in particular understanding the genetics in various contexts (such as MHCs, SNPs, microsatellites, gene expressions and epigenetics), we discuss the challenges in genome sequencing of this bird.

* Corresponding Authors

E-Mail:

- [a] Bioclues.org, India and Denmark.
- [b] Bioinformatics Organization, Inc., 28 Pope Street, Hudson, MA 01749 USA.
- [c] Shodhaka Life Sciences Pvt. Ltd., Electronics City Phase 1, Electronics City, Bangalore, Karnataka 560100, India.
- [d] Institute of Bioinformatics and Applied Biotechnology, Electronics City Phase 1, Electronics City, Bangalore, Karnataka 560100, India.

Introduction

Passer domesticus or the common house sparrow is a passerine with a world-wide distribution. The species does not show an obligatory commensal relationship with human beings. It is rare in grasslands, forests and woodlands. House sparrows have lived successfully around human beings for a long time, often competing well with other birds. In fact, these birds have been considered a menace in the past, particularly in the USA. House sparrows may be occasional pollinators of flowers and edible crops, and despite being perceived as anti-farmers, they might actually be assisting in pest control. But in the recent times, the numbers of this bird have been declining in many urban areas owing to reduction in population-sizes that may be associated with electromagnetic radiations besides other recent anthropogenic activities.^{1,2} In the recent-past, there have been a few efforts initiated to conserve this species.³ *Passer domesticus* may suite as one of the models for studies on the influence of human technological advances on life in general and commensal life-forms in human habitats in particular.

Discussion

House sparrows have already been used for research on various other topics. Information from this species may provide clues for the fight against infectious diseases including avian influenza virus and west Nile virus. The bird has been used for studying digestive flexibility, senescence,

avian circadian system and anthropogenic pollution effects on wildlife. *Passer domesticus* may also offer a chance to study the *ecological* and *evolutionary* aspects of species invasions.⁴ Thus, the species might in fact form a perfect model to study the interplay between multiple aspects such as the infectious diseases in birds around human settlements, inter-bird-species conflicts, population dynamics, and sensitivity of wildlife and adaptation to the rapidly changing parameters within human-made habitats. There is also a lot that needs to be understood about the genetics and genomics of this species. Research in all such directions would be accelerated if the house sparrow genome sequence is established.

There is already a good level of interest in the genetics of *Passer domesticus* in various contexts such as MHCs, SNPs, microsatellites, gene expressions and epigenetics.⁵⁻⁹ For example, a few attempts have been to study the some of the transcriptomes and SNPs using the next generation sequencing technologies. Transcriptome of bursa, blood and spleen have been deposited in SRA in 2012. Some genomic sequences derived using the Roche 454 machine is also available but the total amount of read regions is minimal. Thus, unfortunately this species needs a dedicated project for obtaining a reliable reference sequence to begin with! A few avian genomes have also been sequenced allowing us to speculate the features of the genome of the related species to some extent.¹⁰ Studies on mitochondrial DNA suggest that speciation in the *Passer* genus might have occurred even before Pleistocene era.¹¹ While similar proportions of the genes have been predicted in zebra finch and chickens,^{12,13} possibly the *P. domesticus* genome is comparable to the genome biology of Chicken, where an approximate 23000 genes seem to translate the entire repertoire of proteins.¹⁴ Thus, an approximate one billion base pairs of nuclear genome and about 20,000 genes may be present in Passerines.

After sequencing the sparrow genome, it would be possible to address issues related to its genome structure. It should be interesting to compare genomes of house sparrows, zebra finch and chicken using sequence analysis and experiments. For example, evolutionary distances

among these bird species can be quantified, including variations across the coding and non-coding regions. The distinctive properties of avian micro-chromosomes can also be better inferred eventually, and crosschecked towards syntenic conservation, after the house sparrow genome is sequenced. Song bird genomics and comparison with other birds indeed form essential challenges that must be confronted to identify potential genetic limitations associated with their recent and sudden debility. The comparative genomics analysis nevertheless can be the foundation for further studies to explore specific questions. For example, it is worth attempting to discern what genetic aspects might have earlier helped some of the species to dominate other birds and whether or not any aspects of these dominating species would be causing sudden endangerment in multiple places. For biologists concerned with faunal biodiversity, it would be a special impetus to investigate the loss or gain of genes, or sequence changes in specific regions; this may have resulted in unique responses to recent environmental changes. Furthermore, the house sparrow genome sequence can also assist research on many other fronts including comparative genomics, structural and gene dynamic studies for many bird species. We firmly believe that the chances of obtaining better insights into evolutionary lineages would increase with every new genome sequence known and studied. In conclusion, there is a need to establish reliable nuclear and mitochondrial reference genomes of birds, particularly the house sparrow, by employing high depth and good quality sequencing from multiple individuals is the key for multiple active research areas.

References

- ¹Chamberlain, D. E., Toms, M. P., Cleary-McHarg, R., Banks, A. N., *J. Ornithol.*, **2007**, *148*, 453-462.
- ²Balmori, A. and Hallberg, O., *Electromagn. Biol. Med.*, **2007**, *26*(2), 141-51.
- ³The House Sparrow Project at Lund University: http://canmove.lu.se/research/conservation/house_sparrow
- ⁴Lima, M. R., Macedo R. H., Martins T. L., Schrey, A. W., Martin, L. B., Bensch, S., *PLoS One.*, **2012**, *7*(12), e53332
- ⁵Borg, A. A., Pedersen, S. A., Jensen, H., Westerdahl, H., *Ecol. Evol.*, **2011**, *1*(2), 145-59.
- ⁶Dawson, D. A., Horsburgh, G. J., Krupa, A. P., Stewart, I. R., Skjelseth, S., Jensen, H., Ball, A. D., Spurgin, L. G., Mannarelli, M. E., Nakagawa, S., Schroeder, J., Vangestel, C., Hinten, G. N., Burke, T., *Mol. Ecol. Resour.*, **2012**, *12*(3), 501-23.
- ⁷Schrey, A. W., Coon, C. A., Grispo, M. T., Awad, M., Imboma, T., McCoy, E. D., Mushinsky, H. R., Richards, C. L., Martin, L. B., *Genet. Res. Int.*, **2012**, 979751.
- ⁸Hagen, I. J., Billing, A. M., Rønning, B., Pedersen, S. A., Pärn, H., Slate, J., Jensen, H., *Mol. Ecol. Resour.*, **2013**, *13*(3), 429-39.
- ⁹Ekblom, R., Wennekes, P., Horsburgh, G. J., Burke, T., *Mol. Ecol. Resour.*, **2014**, *14*(3), 636-46.
- ¹⁰Songbird Science: <http://songbirdscience.com/resources/genomics/Comparative>
- ¹¹Allende, L. M., Rubio I., Ruíz-Del-Valle V., Guillén J., Martínez-Laso J., Lowy E., Varela P., Zamora J., Arnaiz-Villena A., *J. Mol. Evol.*, **2001**, *53*(2), 144-154.
- ¹²Warren, W. C., Clayton, D. F., Ellegren, H., Arnold, A. P., Hillier, L. W., Künstner, A., Searle, S., White, S., Vilella, A. J., Fairley, S., Heger, A., Kong L., Ponting, C. P., Jarvis, E. D., Mello, C. V., Minx, P., Lovell, P., Velho, T. A., Ferris, M., Balakrishnan, C. N., Sinha, S., Blatti, C., London, S. E., Li, Y., Lin, Y. C., George, J., Sweedler, J., Southey, B., Gunaratne, P., Watson, M., Nam, K., Backström, N., Smeds, L., Nabholz, B., Itoh, Y., Whitney, O., Pfenning, A. R., Howard, J., Völker, M., Skinner, B. M., Griffin, D. K., Ye, L., McLaren, W. M., Flicek, P., Quesada, V., Velasco, G., Lopez-Otin, C., Puente, X. S., Olender, T., Lancet, D., Smit, A. F., Hubley, R., Konkel, M. K., Walker, J. A., Batzer, M. A., Gu, W., Pollock, D. D., Chen, L., Cheng, Z., Eichler, E. E., Stapley, J., Slate, J., Ekblom, R., Birkhead, T., Burke, T., Burt, D., Scharff, C., Adam, I., Richard, H., Sultan, M., Soldatov, A., Lehrach, H., Edwards, S. V., Yang, S. P., Li, X., Graves, T., Fulton, L., Nelson, J., Chinwalla, A., Hou, S., Mardis, E. R., Wilson, R. K., *Nature*, **2010**, *1*, 464(7289):757-62.
- ¹³International Chicken Genome Sequencing Consortium, *Nature*, **2004**, *9*, 432(7018), 695-716
- ¹⁴Fulton, J. E., *BMC Genomics*, **2009**, *14*(10), Suppl 2, S1.

Received: 18.11.2014.
Accepted: 08.12.2014.



POLYVINYL ALCOHOL - MELAMINE FORMALDEHYDE RESIN COMPOSITE AND NANOCOMPOSITES WITH Ag, TiO₂, ZnO NANOPARTICLES AS ANTIMICROBIAL FILMS, COATINGS AND SPRAYS

Rita Kakkar^{1*}, Kalpana Madgula^{1*}, Y. V. Saritha Nehru, ¹ Raj M. Shailaja,² and B. Sreedhar³

Keywords: PVA-MFR composite films; Nanocomposites films, Nanoparticles of Ag, ZnO, TiO₂; Characterization; Antimicrobial activity

Melamine formaldehyde resin, MFR, is generally formed in a two stage process by the reaction of melamine and formaldehyde. The first stage reaction is carried out at about 70° - 80°C and pH 9-10; and the second stage involves subsequent polycondensation of the products in an acid medium. In this work, reaction is carried out till the first stage only. Thus, prepared MFR when blended in small proportion into PVA matrix, in-solubilises PVA, forming a well defined PVA-MFR composite. The blend can be cast into films of desired thickness and strength. Nanoparticles of Ag, ZnO and TiO₂ were prepared and characterised. Each of the prepared nanoparticles was first blended into aqueous PVA, then blended with MFR, and nanocomposite films obtained. The films were subjected to TGA, FTIR and antimicrobial studies. The PVA-MFR composite films are found to have a high level of antimicrobial activity. Nanocomposites have enhanced antimicrobial activity due to antimicrobial property of nano Ag/ZnO/TiO₂ in them. The activity is high, especially against highly resistant gram positive bacteria like *Staphylococcus Aureus* and *Bacillus*. The composite has good binding properties, forming stable, chemically resistant, coatings on fabric, paper, glass, polyester etc, rendering them antimicrobial. These films and coatings retain their antimicrobial activity over long period of time. Nano silver immobilised on antimicrobial PVA-MFR, could probably be an effective patch for wound dressings, and surgical mask, which are in great demand. A fine coating of the composite on medical devices can decrease the incidence of medical device related infections.

* Corresponding Authors

Fax: 914023544240

E-Mail: kakkarrita@yahoo.co.in kalpanasekhar@yahoo.com

- [1] Department of Chemistry, St. Francis College for Women, Begumpet, Hyderabad 500016, India
- [2] Department of Microbiology, St. Francis College for Women, Begumpet, Hyderabad 500016, India
- [3] Inorganic and Physical Chemistry Division, CSIR-Indian Institute of Chemical Technology, Hyderabad, India

INTRODUCTION

There has been a growing interest in developing polymeric materials with antimicrobial properties for biomedical, food packaging and storage applications.¹ As most of the types of commonly applied polymers have no antibacterial action, they have to be modified to obtain polymer materials with desired properties.² The modification of virgin polymer with a bioactive agent is a possible method where the polymer is a carrier, providing transport and controlled release of bioactive substances into the environment where they are needed.³⁻⁵ Numerous methods have also been used to develop polymeric materials⁶ with inherent antimicrobial properties. Poly (vinyl alcohol), PVA, belongs to the group of polymers which can be used in combination with other non-biodegradable polymers for tuning the required properties in the resultant composite blend. It is one of the synthetic, biodegradable, biocompatible, water-soluble

polymers utilized in medical applications such as wound dressings,⁷ artificial skin,⁸ coatings,⁹ Transdermal patches,¹⁰ cardiovascular devices,¹¹⁻¹⁴ and drug delivery systems.¹⁵ Moreover, it has good barrier properties against scents, oils, and fats. The physical characteristics of PVA are dependent on its method of preparation by hydrolysis or partial hydrolysis of Poly (vinyl acetate).¹⁶ PVA complexed with iodine to get polymeric broad spectrum coatings working on the principle of slow release of incorporated iodine have been reported in U.S. Pat. No.5,071,648.^{17,18} The patent also discloses effective antimicrobial polyvinyl acetal sponge wipes and coatings for non-wiping applications. Our emphasis is towards achieving water insoluble PVA films that show characteristic antimicrobial application which can help reduce complications, caused by bacteria commonly found in households, and resistant microbes acquired from hospitals. There are reports²⁰⁻²² of attempt, to in-solubilise PVA by treatment with sulphuric acid, formaldehyde, borax, boric acid, glutaraldehyde. Other methods in the literature report highly in-solubilised polyamide epoxy cured PVA coating; methylated melamine formaldehyde cured PVA coating; ammonium chloride/formaldehyde cured PVA and in solubilised starch/PVA mixes.

We herein report in-solubilisation of PVA by reaction with Melamine-formaldehyde, MFR. The two component system (PVA-MFR) form well defined molecular composite with antimicrobial properties. The blend can be cast into antimicrobial films of desirable thickness and strength. The

composite has been found to have good binding properties on fabric, paper, glass, polyester etc and thus can render them antimicrobial. MFR a hard thermosetting plastic was prepared from melamine and formaldehyde. Gong and Zhang¹⁹ have reported mechanical properties of MFR-PVA composites, where the matrix is MFR and effect of varying composition of PVA on the resulting composite is studied. In contrast, in the present study, MFR is blended in smaller proportion into PVA matrix to get water insoluble and chemically resistant composite films with antimicrobial properties.

Silver has been used as an antimicrobial since the 1800s. But since the discovery of systemic antibiotics in the early 20th century, the use of silver had declined. In the last two decades, with advent of nanotechnology, interest in silver for wound treatment resurged, since silver is efficacious for killing the antibiotic resistant bacteria strains. Silver releasing dressings and patches are increasingly in demand for treatment of infected wounds.²³ Along with Silver, ZnO and TiO₂ nanoparticles also have high level of antimicrobial activity and have been included in this study. Nanocomposites of PVA-MFR with ZnO/TiO₂/Ag as films and coatings that promise to be good polymeric material with wide range of antimicrobial applications are being reported. This gives us the advantage of using lesser concentration of nanoparticles in an inherent antimicrobial material PVA-MFR, so as to reach a desired level of antimicrobial efficacy, yet minimizing possibility of any toxicity by using lower concentrations of nanoparticles.²⁴ Bacterial infection from medical devices is a major problem in hospitals,²⁵ and so these polymeric antimicrobial coatings could probably be exploited to modify the surface of medical devices.

EXPERIMENTAL

Materials and Methods

Materials - Silver nitrate (extra pure-grade), Tri sodium citrate dihydrate (AR grade), Titanium trichloride (LR grade), Polyvinyl alcohol M.W. 85,000-1,24,000 (LR grade), Zinc acetate (LR grade), and Formaldehyde (37% w/v, LR) were purchased from S.D. Fine Chemicals Limited, Mumbai. Starch from Merck, Mumbai. Melamine powder (AR grade) was purchased from Gujarat Natural Fertilisers Limited (GNFC). All the solutions were made by using double distilled water. Nutrient broth and Nutrient agar was purchased from Himedia laboratories, Mumbai.

Characterization - TEM samples were prepared by the placement of the sample mixture drops directly on Formvar polymer-coated grids with a micropipette. The morphology, size and shape distribution of the nanoparticles were recorded with a TECNAI FE12 TEM (Eindhoven, The Netherlands) instrument operating at 120 kV. All TGA thermograms were recorded on TGA/SDTA Mettler Toledo 851^o system (Zurich, Switzerland) using open alumina crucibles containing samples weighing about 8–10 mg with a linear heating rate of 10 °C min⁻¹ between 25 to 800 °C. Nitrogen was used as purge gas for all these measurements. UV-Vis spectra were recorded on Systronics model 2201.

Antimicrobial studies

Disc diffusion method - Antimicrobial studies of PVA-MFR composite and PVA-MFR nanocomposite films were conducted by Kirby-Bauer disc diffusion method.²⁶ The nutrient agar media autoclaved at 15 lbs for 10 min and was poured in the petri dishes and allowed to solidify. 0.1ml of the inoculum of overnight cultures of the test organisms used such as *E.coli*, *Staphylococcus Aureus*, *Pseudomonas*, *Proteus*, and *Bacillus* was plated by spread plate technique on the nutrient agar plates. Different polymer composite films were cut into small pieces and were placed in their respective positions with the help of a sterile forceps onto the nutrient agar plates. The films were pressed gently with forceps to ensure contact with the agar surface. The plates were incubated at 37° C for 24 hours and later checked for antimicrobial activity by measuring zone diameter of inhibition.

Optical density method - Nanocomposite coatings inside glass beakers were subjected to turbidity method for their antimicrobial studies. Glass beakers coated with the nanocomposites were incubated with 20 ml of nutrient broth and 0.1 ml of microbial culture for 24 h at 37°C. After incubation the media from the above beakers was taken under sterile conditions and absorbance measured turbidimetrically in a spectrophotometer at 450 nm.

Preparation of Nanoparticles

Zinc oxide Nanoparticles were prepared using 20 ml of 0.2 M Zinc acetate in dimethylsulphoxide²⁷ and stirred in a typical chemical reactor for 30 min. To this 1.2 M KOH in 10 ml ethanol was added drop by drop. Solution was stirred for 5 min and then 0.12 ml thioglycerol was added. Thioglycerol acts as a capping reagent and has been used to prevent the agglomeration of nanoZnO particles. The solution was stirred for 1 h and it turned milky white. The residue was collected and washed three times with methanol and allowed to dry on a Petri dish.

Titanium dioxide nanoparticles were prepared by mixing 20 ml of TiCl₃ solution with 60 ml of 0.1 M ammonium hydroxide solution and stirred for 48 h at room temperature on a magnetic stirrer²⁸. A white coloured solution indicates the formation of titanium dioxide particles. The solution was centrifuged and the precipitate was washed with double distilled water, dried in isopropyl alcohol at room temperature. Organic molecules 'cap' the outer surface of core semiconductor²⁵ and prevent aggregation, oxidation, and also stabilize nanoparticles

Silver nanoparticles synthesis was carried with silver nitrate, starch and sodium citrate by following the procedure as reported in our earlier work.²⁹ 50 ml of 0.008M AgNO₃ was stirred for 15 minutes under reflux condition with a magnetic stirrer (Spinot Model MC_02), followed by addition of a solution of 200 mg starch powder dissolved in 100 ml of double distilled water, and then 50 ml of 0.08 M Sodium citrate solution was added, under continuous stirring and heating for 2 hours at 95°C. The silver content of this solution is 2x10⁻⁶ mol mL⁻¹.

Preparation of Melamine Formaldehyde Resin (MFR)

These are primarily oligomers and are formed in a two stage process by melamine – formaldehyde reaction with a 1: (2–12) molar ratio of melamine to formaldehyde. The first stage reaction is carried out at about 70° - 80°C and pH 9-10; and the second stage involves subsequent polycondensation of the products in an acid medium. In our study the reaction has been carried to the first stage only. Melamine-formaldehyde used in the study is prepared by well-known industrial method,³⁰ where formaldehyde and melamine are reacted under base catalyst and it's polymeric molecular weight increased by addition process. 57g of (37%) formaldehyde was taken in a double necked RB flask and brought to pH 9.5-10 by the addition of few drops of 2N -NaOH solution. The RB flask was kept on a magnetic stirrer and 50g of melamine powder slowly added under stirring followed by 15ml of distilled water. The reaction mixture was heated with continuous stirring till the temperature increased to about 60°C and then gradually allowed the temperature to rise to about 95°C. Refluxation and stirring at this temperature was continued till a clear liquid was obtained. Further heating was carried while checking the water tolerance of the reaction mixture after every 10 min., until the water tolerance at 30°C dropped to 1:4. The mixture was allowed to cool to room temperature. Final properties of the resin like viscosity and water tolerance³¹ were standardized to viscosity @ 32°C is 30 - 40 seconds; water tolerance @ 30°C is 1:2 to 1:4, and gel time @ 150°C is 210-230 sec. Under these conditions the reaction mixture is partially cured, and is a clear viscous liquid with the shelf life of 4-5 days at room temperature and about a month when stored in refrigerator. The prepared resin mixture however can be diluted with methanol if necessary for storage at room temperature.

Preparation of polymer films/coatings and sprays

PVA films - A very simple method was used to cast thin PVA polymer film.³² A homogenous solution of PVA powder M.W.85,000 - 1,24,000 (10 wt %) in water as plasticizer was prepared under stirring and heated to 100 °C for about 30 minutes. Hot aqueous homogenous solution was poured on to a plastic Petri dish and spread uniformly with a glass rod and dried in a hot air oven at 70°C. Film could not be obtained for compositions below 5 wt % of PVA. The PVA films dried in a hot air oven at 70°C for 2 hrs could be easily lifted and stored in Ziploc pouches.

PVA-MFR composites films/coatings/sprays - Various methods of synthesizing PVA-MFR are well documented in US 4461858 Patent¹⁶⁻¹⁸ wherein the material is primarily prepared to be used in paper industry as a binder as well as to improve the strength of paper because of its high absorption and binding capacity onto cellulose. The prepared PVA and melamine formaldehyde solutions were blended in various proportions as listed in Table.1, by using an electrical blender while heating at about 80°C. The PVA-MFR films with labels J1 to J8 were prepared by blending 20 ml of 10 wt% polyvinyl alcohol (PVA) and different volumes of melamine formaldehyde resin(MFR) i.e., 1 ml(J1), 1.5 ml(J2), 2 ml(J3), 2.5 ml(J4), 3 ml(J5), 3.5 ml(J6), 4 ml(J7) and 6 ml(J8).

Table 1. PVA–MFR films prepared with different composition by volume of MFR added to 20 ml of 10 wt.% aqueous PVA solution

Film label	J1	J2	J3	J4	J5	J6	J7	J8
MFR added in ml	1	1.5	2	2.5	3	3.5	4	6

The reaction mixture changed from colourless to white and its viscosity increased as the reaction proceeded. To cast a film the PVA-MFR - active blend was poured and spread uniformly on a plastic Petri dish before it forms a thick ball like mass, while for sprays and storage applications the blend was immediately diluted with methanol to the desired consistency and stored in air tight containers. The films were dried in hot air oven at about 70 – 80°C for 2 hours. After evaporation of the solvent at ambient temperature, film was peeled off and rinsed in benzene followed by water to remove any volatile unreacted materials and dried in oven and stored in Ziploc bags. It was noted that cross linking of PVA begins with even the smallest addition of MFR. As the concentration of MFR was increased the films were harder to tear and water resistance of the film increased. The opacity of the films obtained changed from transparent colourless to white opaque films with reduced elasticity as the composition changed from J1 to J8.

Active blend as prepared above was coated on paper strips, cloth strips, inner surfaces of plastic as well as glass beakers, and earthen clay pots each one dried in oven as described above. The glass beakers and clay pots had to be heated overnight to get hardened inner lining. The lining so prepared on a plastic beaker could be dislodged as a moulded cup. The paper strips had greater tear strength in one direction and retained shape even in boiling water. At the same time the PVA-MFR–active blend obtained was diluted four times with methanol and sprayed on food grade Aluminum foil and food wrapping films and dried by suspending freely in hot air oven for two hours to get thin antimicrobial coating on them.

Preparation of PVA–MFR nanocomposite films/coating and sprays - Repeat experiments showed that it is possible to get PVA–MFR composite films of desired thickness and strength and these films are antimicrobial. Synthesised ZnO, Ag, or TiO₂ nanoparticles were first blended into aqueous PVA and then allowed to condense with MFR. PVA–MFR–silver composite films were obtained using 20 ml of as prepared nano silver solution (silver content of 2 x 10⁻⁶ moles/ml or 2 milli moles/lit). 2g PVA powder was added directly and dissolved by heating over a water bath with constant stirring ensuring a homogeneous solution. To this 2 ml MFR was added and blended and films were prepared by the method similar to that of PVA-MFR composite films and about 100 sq.cm of the film were obtained. Thus, the film had 4 x 10⁻⁷ moles of silver/sq.cm of film area. These silver nanocomposite films obtained was brownish in colour. Similar nanocomposite films were obtained by incorporating TiO₂ or ZnO nanoparticles, the difference being the prepared nanoparticle powder was first dispersed in water using a sonicator, followed by addition of PVA and MFR in same proportion and following the same method as for nanosilver composites. The concentration of ZnO and TiO₂ in the composite was 25 mmol/lit of each. Nanocomposite sprays and coatings were made in the same manner as the corresponding composites.

Reactivity of the films - PVA-MFR-polymeric films were found to be un-reactive towards solvents like boiling water, dilute acids, sodium hydroxide, benzene, chloroform, methanol, ethanol and hexane etc., though it disintegrated on heating in concentrated hydrochloric acid and charred in sulphuric acid. The material is thus very stable towards various applications.

Results and discussion

FTIR studies of pure PVA and crosslinked PVA-MFR films

The interaction of PVA-MFR was indicated by the FTIR spectral data³³ as reported, where the disappearance of 1000 cm⁻¹ peak for methylol (-CH₂OH) group in MFR indicating its reaction with -OH group of PVA leading to the formation of C-O-C linkage between PVA and MFR.

This is further supported by the suppression of -OH absorption band at 830 cm⁻¹ in PVA suggesting reaction of some of the free -OH groups of PVA with pre-polymerised MFR.

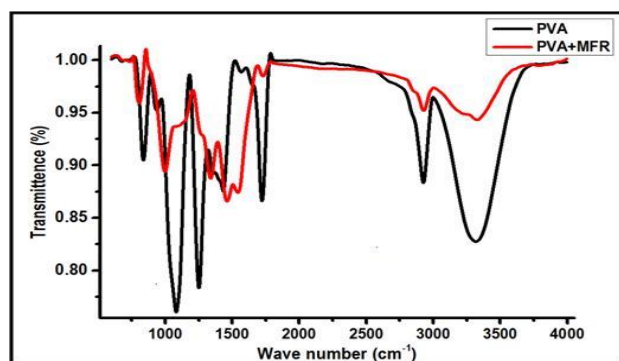


Figure 1. FTIR spectra of pure PVA and crosslinked PVA-MFR films

FTIR spectrum of PVA film shows typical strong hydroxyl bands for free alcohol (non bonded -OH stretching band at 3313cm⁻¹ and also PVA film reveals major peaks like C-H broad alkyl stretching band (2850-3000 cm⁻¹).³⁴ Intramolecular and intermolecular hydrogen bonding are expected to occur among PVA chains due to high hydrophilic forces, where strong intramolecular hydrogen bonded band 3200-3570 cm⁻¹ may occur. An important absorption peak was verified at 1245 cm⁻¹ for -C-O str bond and 1090 cm⁻¹ for -C-O-H bending vibration. These bands have been used as characteristic bands for assessing the semi-crystalline nature of poly(vinyl alcohol) structure which is expected due to different process parameters.³⁵⁻³⁶

By crosslinking PVA with MFR (synthesized and restricted to oligomeric form only 1st stage, where there is only conversion of methylol groups to primary amine)³⁷ the -OH peaks have been reduced and became broad when compared to pure PVA that suggests hydrogen bonding becomes weak in crosslinked PVA as shown in the FTIR spectrum of PVA-MFR. In addition to that, the C-O stretching at 1090 cm⁻¹ is reduced in cross linked PVA to a broader absorption band PVA-MFR (1000-1300cm⁻¹) as can

be seen in Figure 1. The peak of 813 cm⁻¹ exists in all these IR spectra that is characteristic of triazinyl ring³⁸ of melamine moiety.

Characterisation of nanoparticles

The as-synthesized ZnO nanoparticles were characterized by the UV-Visible Spectroscopy and TEM. The size of the nanoparticles plays an important role in changing the entire properties of materials. Thus, size evolution of semiconducting nanoparticles becomes very essential to explore the properties of the materials. UV-visible absorption spectroscopy is widely being used technique to examine the optical properties of nano-sized particles. The absorption spectrum of ZnO nanopowder is shown in Figure 2. It exhibits a strong absorption band at about 336 nm. It is also evident that significant sharp absorption of ZnO indicating the monodispersed nature of the nanoparticle distribution.^{39, 40}

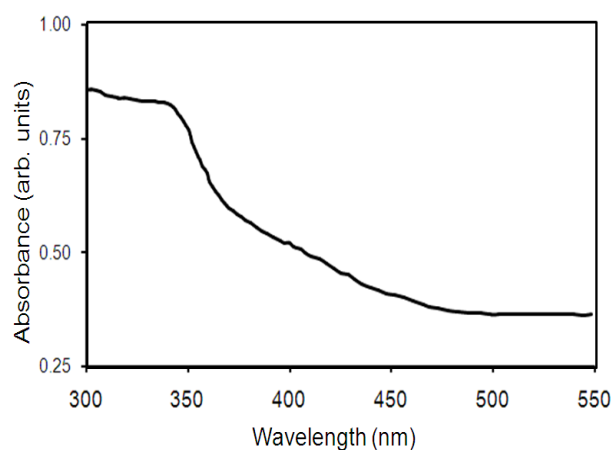


Figure 2. Absorption spectra of as-synthesized zinc oxide nanoparticles

To access the size and morphology of the samples, we performed TEM and the images are presented in Figure 3. As can be seen from the image, the size of the ZnO particles are below 5 nm with uniform morphology.

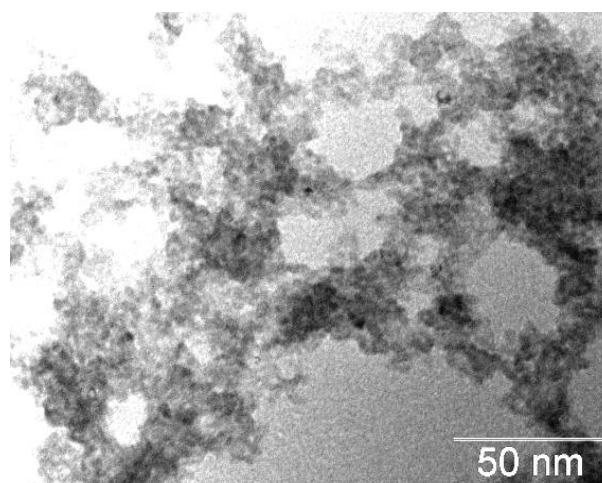


Figure 3. TEM image of the as synthesized zinc oxide nanoparticles

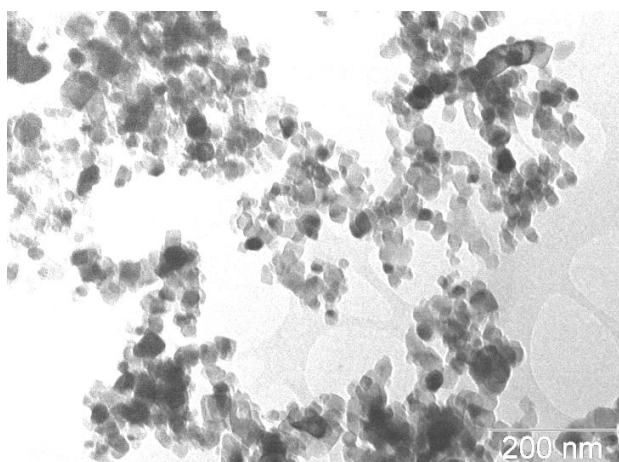


Figure 4. TEM image of as synthesized Titanium dioxide nanoparticles

The particle size of the TiO₂ prepared was found to be 15-20 nm by TEM (Figure 4).

Highly stabilised silver nanoparticles were characterised by TEM (Figure 5) and UV-Visible measurements (Figure 6).

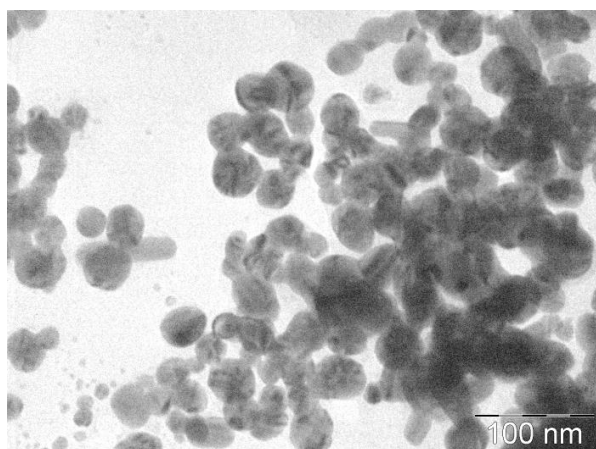


Figure 5. Characterization of silver nanoparticles by TEM

Silver nanoparticles show a small gap between the conduction band and valence band where electron moves freely that are responsible for Surface Plasmon peak.^{41,42} This absorption strongly depends on the particle size, dielectric medium and chemical surroundings.⁴³ The reduction of Ag⁺ ions was monitored by measuring the UV-Visible spectrum by diluting a small aliquot of the sample into distilled water shown in Figure 6.

UV-Vis spectral analysis was done in the range of 250-750 nm and the absorption (SPR) peaks obtained in the visible regions at 412 nm, that are identical to the characteristics UV-visible spectrum of metallic silver.⁴⁴

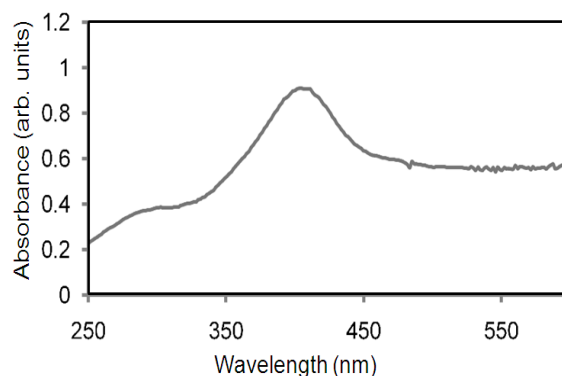


Figure 6. UV Visible spectra of nanosilver

TGA studies of PVA –MFR films - The polymeric PVA-MFR films labelled J1 to J8 listed in Table. 1 were prepared using different composition of PVA and MFR. Representative films J1, J3, J5, J6, were selected and subjected to thermal degradation for TGA studies as shown in Figure 7. The thermal stability of polymeric films plays an important role in determining the final film properties and is greatly influenced by the structure, chemical composition, monomer distribution, and different interaction parameters. The thermal properties of these films depend primarily on network structure and the stability is a function of more than one variable than just the extent of crosslinking with MFR, both the kind and concentration of remaining groups, cohesive energy between molecular chains, molecular chain rigidity, and other chemical structural factors such as, for example, steric strain and conformational arrangements of groups.

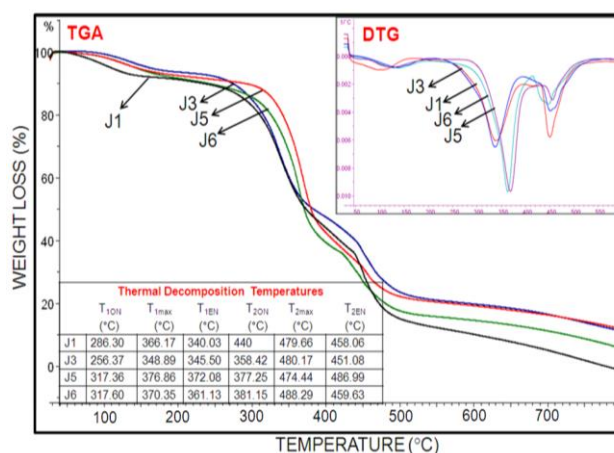


Figure 7. TGA Studies of polymer composite PVA-MFR films prepared with changing concentration of MFR in 10wt% PVA

Thermogravimetric (TG) curves of all the polymer composites show mainly two step decomposition. The initial step at temperature less than 200°C can be attributed to loss of loosely bound solvents that are accompanied by the formation of volatile disintegrated products. The decomposition at this temperature, which is closer to decomposition temperature of fully hydrolysed PVA at 230°C, is also due to loss of PVA component in the composite films.^{45,46} The weight loss is comparatively more

in J1 where lesser composition of MFR is used, as the concentration of MFR is increased the loss at this step is reduced indicating all the PVA is cross-linked with MFR, hence loss in weight from J3 to J6 is the same at this temperature. The residue in all the films after this initial step is predominantly PVA-MFR composite and shows a similar TGA profile. As can be seen from Figure 7, the onset of decomposition T_{1ON} of the first step at lower concentrations of MFR i.e., in J1 and J3 is at 285.3 and 256.37° C, respectively that is much lower than that observed for higher concentrations i.e., J5 and J6, at 317.36 and 317.60 °C showing an increase in thermal stability. Similar trend was observed in the temperature of maximum decomposition T_{2max} for the synthesized PVA-MFR films, whereas the second step has a temperature of maximum decomposition T_{2max} in a narrow range i.e. 474 – 488 °C.

TGA studies of PVA-MFR-Nanocomposite films - PVA-MFR composite corresponding to composition J3, (Table 1) were used to prepare organic-inorganic hybrid nanocomposites. In Figure 8, the film label J3 - stands for PVA-MFR composite film of composition J3. Labels ZnO, TiO₂, and Ag stand for corresponding nanocomposite films at nanoparticle concentration of 25, 25, 2 mmol/L, respectively and PVA-MFR composition corresponding to J3.

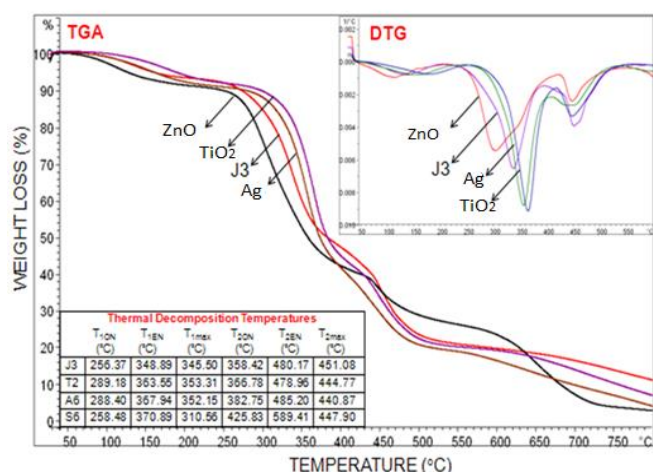


Figure 8. TGA Studies of PVA-MFR nanocomposite films. The film label J3-stands for PVA-MFR composite film of composition J3. ZnO, TiO₂, and Ag, stand for films at nanoparticle concentration of 25, 25, 2 mmol L⁻¹, respectively and PVA-MFR composition corresponding to J3.

Figure 8 compares the effect of inorganic nanoparticles on the decomposition profile of PVA-MFR composite, J3. The T_{1max} is lowered by the presence of ZnO, while it is increased with silver and TiO₂ in corresponding films. Except for film with ZnO all the samples show a similar thermogravimetry profile with mainly two steps of decomposition after 200°C. Film with ZnO on the other hand has a third decomposition peak at 600°C, with a reduced second step resulting to the third step, resulting in only 4 wt% of final residue mass, as compared to 6, 8.5, 10.5% for Ag, TiO₂ and J3 films, respectively. Generally during the initial stages of the decomposition, the strained bonds or the weakest bonds with low dissociation energy break resulting in the strain-free cross-linked intermediate (after the first stage of decomposition) that decompose at higher temperatures and correspond to second and third stages of degradation as in film ZnO.

Antimicrobial Studies

Antimicrobial properties of PVA-MFR films with varying MFR concentration

- A series of these composites were prepared by taking 20 ml of 10 wt % PVA solution and adding varying volumes (x - ml) of MFR liquid. Films ranging from KI-K10 (Table 2) are similar to films J1 to J6 in Table 1, except a wider range of compositions have been explored. Antimicrobial property of the films was studied by disc diffusion method. A zone of inhibition was seen around the polymer films to which the organism is sensitive. All the organisms were sensitive to the polymer films and hence, found to be having antimicrobial activity. The zone diameter of inhibition was measured and tabulated (Table 2). Film labelled K0, the blank, had no MFR and is only a plain PVA film and showed zero zone diameter of inhibition against all organisms, ascertaining that PVA by itself is not antimicrobial. All the PVA -MFR films from K1 to K10 are antimicrobial. Highest antimicrobial activity 3.9 cm of zone diameter of inhibition was observed with K5 against *S.aureus* and the least activity observed with *P.mirabilis* against K2. Table 2 shows an increase in the activity in films K1 to K5 with increase in MFR concentration, there after it levels off, so K4 can be taken as a representative composition, which is 20 ml of 10% PVA solution blended with 3 ml of MFR. The fact that antimicrobial activity does not continue to increase with increased concentration of MFR used in films K5-K10, shows that the activity is not brought in merely by addition of MFR to PVA. The antimicrobial activity is also not due to any free formaldehyde in the prepared MFR resin as the films were heated in oven for two hours at 70° C whereby the entire volatile component would have evaporated. The films have been found to retain the antimicrobial efficacy when studied even after a period of eight months, as can be seen from the results in Figure 9.

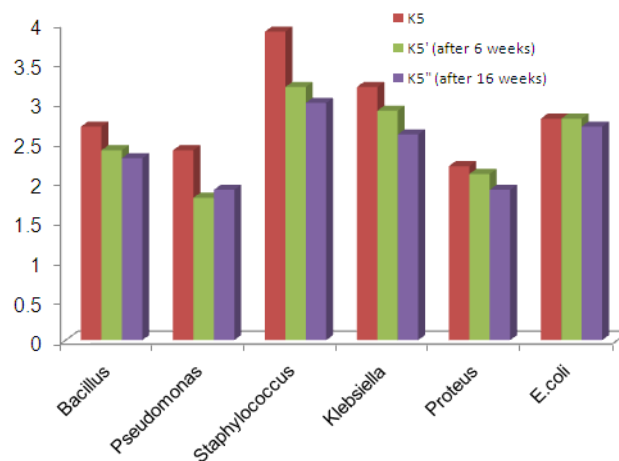


Figure 9. Antimicrobial activity – variation with time of PVA-MFR film composition K5. Zone diameter of inhibition in cm on immediate use, after six and sixteen weeks

PVA-MFR-Silver nanocomposite films - effect of increasing silver concentration

- Silver releasing dressings and patches are increasingly in demand for treatment of infected wounds. A small concentration of nano silver immobilised in antimicrobial PVA-MFR, can be a far cheaper version of silver dressing as far lesser quantity of nanosilver would be required to reach the required level of antimicrobial activity. Concentration of silver, MFR, and film thickness can be varied easily and studied.

Table 2. Antimicrobial properties of PVA-MFR films - varying MFR concentration composition of the films is - x-ml of MFR in 20 ml of 10 wt.% PVA solution

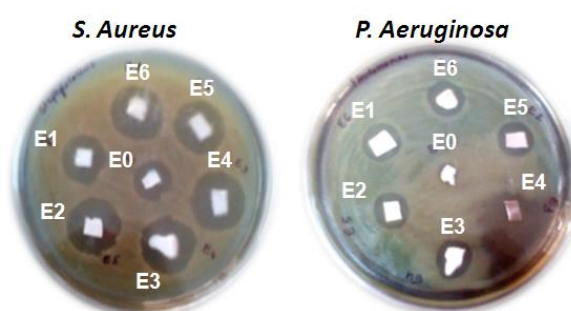
FILM LABEL	K ₀	K ₁	K ₂	K ₃	K ₄	K ₅	K ₆	K ₇	K ₈	K ₉	K ₁₀
Composition (X ml MFR)	0	1	2	2.5	3	3.5	4	4.5	5	5.5	6
ORGANISM	Zone of inhibition in diameter in cm										
<i>Bacillus subtilis</i>	0	0.9	2.4	2.6	2.2	2.7	2.4	2.3	2.4	2.3	2.8
<i>Pseudomonasaeruginosa</i>	0	0.4	1.9	1.7	2	2.4	2.2	2.1	3	2.9	3
<i>Staphylococcus aureus</i>	0	1	2.0	2.5	3.2	3.9	2.1	2	2	2.4	2.7
<i>Klebsiella pneumonia</i>	0	0.8	1	2	2.8	3.2	2.4	3	2.8	2.4	2.8
<i>Proteus mirabilis</i>	0	0	1.5	1.6	1.9	2.2	2.3	2.2	2.4	2.1	2.5

Table 3. Antimicrobial studies of PVA-MFR-silver nanocomposite films- effect of increasing silver concentration blank E0 with no silver and E1-E6 with increasing silver concentration

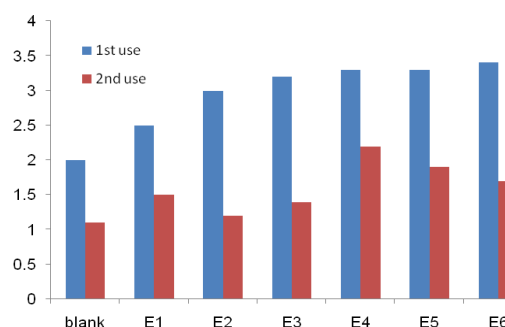
Nano-Ag film	10 ⁻⁷ mol AgNO ₃ cm ⁻² of film area	<i>S. aureus</i> / Zone inhibition diameter, cm	<i>P. Aeruginosa</i>
E0	0	2	1
E1	0.4	2.5	1.8
E2	0.8	3	2
E3	1.2	3.2	2.2
E4	2	3.3	2.3
E5	3	3.3	2.2
E6	4	3.4	2.3

As prepared nanosilver solution was diluted with double distilled water and PVA-MFR-silver nanocomposite films with different concentrations of silver were made. Listed in Table 3 are films E1 to E6, with different silver concentrations. The film E0 was a blank PVA-MFR film and contained no silver. All the films E0 to E6 had composition, 2ml of MFR in 20 ml of 10 wt. % PVA. This composition was chosen so as to use minimal amount of MFR yet get its antimicrobial contribution, while rest is to be contributed by silver. Concentration of silver, MFR, and film thickness can be varied easily and studied. Antimicrobial studies on the films were conducted in similar conditions. Results in Table 3 show antimicrobial property of the films and it is found to increase with increasing concentration of silver. All organisms studied for K-series showed activity, but for convenience only results *S. aureus* and *Pseudomonas* of are shown here. Antimicrobial activity for both the organisms in all the films containing silver (E1-E6) was more compared to the film E0 containing no silver, where the activity is only due to PVA-MFR. Antimicrobial activity due to silver is thus clearly superimposed over the activity due to PVA-MFR. Activity increased with increasing concentration of silver used in films E1 to E3 and levelled off thereafter in E4-E6. Thus, antimicrobial property of the film can be increased by using more of nanosilver concentration and less of MFR if so desired for any medical applications. At the same time if cost is a criteria and MFR has no harmful effect, concentration of MFR in the film can be increased with lesser or no silver at all. In this study, ideal example is E3, with a composition which was achieved by using 6 ml of as prepared nanosilver solution, containing 0.012 mmol of silver, diluting it to 20ml with double distilled water, and then dissolving 2g of PVA powder to get 10 wt. % PVA, 2 ml of MFR, and proceeding as described earlier.

This composite so prepared gave about 100 sq cm of film, having about 1.2×10^{-7} mol of silver cm⁻² of film so prepared.

**Figure 10.** Antimicrobial studies of PVA-MFR-silver nanocomposite films- effect of increasing silver concentration blank E0 with no silver and E1-E6 with increasing silver concentration in the case of *S. aureus* and *Pseudomonas/P. aeruginosa*

A study was conducted to ascertain the level of depletion of antimicrobial activity of the films after the first study, if the films have to find usage as a medicinal patch. The piece of film material which was used for the first round of antimicrobial studies was picked, thoroughly washed with water, dried in oven and resubjected to antimicrobial studies. All the samples used in Table 3, for *S. Aureus* studies were restudied in this way. *S. Aureus* was picked for reusability studies as it had shown maximum antimicrobial effect. Figure 11 shows a fall in activity in each film, yet a good level of activity is still found in each of the films on reuse, an encouraging result.

**Figure 11.** Reusability of silver nanocomposite films - Antimicrobial studies with *S. aureus* (Zone diameter of inhibition in cm) films

Although research indicates that silver nanoparticles are more effective to gram negative than gram positive bacteria, involving the charge of peptidoglycan molecules in the bacterial cell wall, our results show that they are equally effective against both gram-positive bacteria and gram negative bacteria, and showing highest activity against *S. Aureus*. The mechanism of the bactericidal effect of silver nanoparticles is not very well-known. It is believed that cellular proteins become inactive after treatment with silver nanoparticles.⁴⁴ Silver nanoparticles after penetration into the bacteria in-activate the enzymes, generating hydrogen peroxide and causing bacterial cell death.⁴³ Silver nanoparticles can be used as effective growth inhibitors in various micro-organisms, making them applicable to diverse medicines and antimicrobial control systems. It is thought that silver atoms bind to thiol groups (-SH) in enzymes and subsequently cause the deactivation of enzymes. The silver-catalyzed formation of disulfide bonds could possibly change the shape of cellular enzymes and subsequently affect their function.

Antimicrobial efficacy of films - variation with time -

Since the PVA-MFR composite has shown good adhesion property on paper, fabric, jute, as well as strong antimicrobial film making property, it can find application in dry grain storage and other packaging applications. A study was conducted to see the stability of film and how its antimicrobial property is affected over time period. A representative PVA-MFR film K5 from Table 2 was chosen and compared its antimicrobial properties on immediate use, after six and sixteen weeks. Very encouraging trend is that a slight fall in the activity is seen, for all the microbes and all the films, in first six weeks and then there is negligible change in next ten weeks, as seen in Figure 9. We recommend jute, raw cotton bags to be given a thin PVA – MFR film lining or else directly coat them with PVA-MFR, which will not only protect them from moisture but also from microbes, making a better grain storage, packaging material.

Similar antimicrobial studies were done on PVA-MFR and corresponding Ag, ZnO, TiO₂ nanocomposite films, observed in Figure 12. All the films with nanoparticles have higher antimicrobial activity than the plain PVA-MFR films. The nanocomposite films are stable and have retained a good level of antimicrobial activity even after eight months of their preparation. For convenience, only *S. Aureus* work is being reported here.

Table 4. *S. Aureus* - antimicrobial activity by turbidity method coating inside glass beaker and a suspended film

Sample	Absorbance	
	Composite coated inside glass beaker	Suspended composite as film
PVA polymer	0.21	0.21
PVA-MFR	0.16	0.06
PVA-MFR-ZnO nano	0.05	0.02
PVA-MFR-Ag nano	0.02	0.01
PVA-MFR-TiO ₂ nano	0.01	0.01
PVA-MFR-TiO ₂ commercial	0.1	0.1

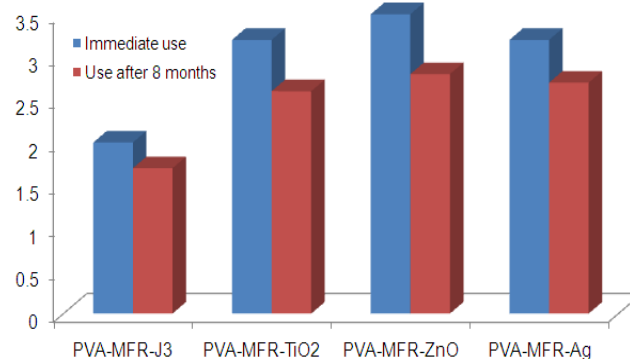


Figure 12. Antimicrobial activity (*S.Aureus*) – variation with time - Zone diameter of inhibition in cm - on immediate use and after eight months PVA-MFR, and nanocomposite films with TiO₂, ZnO, and silver nanoparticles.

PVA-MFR-nanocomposite coatings inside glass beakers

The nanocomposite coatings inside glass beakers, PVC beakers and clay pots were subjected to turbidity method for their antimicrobial studies. Though all the three coatings showed antimicrobial activity, only work on glass beakers is being reported. Corresponding films were also studied by the turbidity method by suspending them in the culture medium in the same manner. Near zero absorbance for all the nanocomposite coatings seen in Table 4, shows a very good level of antimicrobial property in these coatings, whereas the blank, a plain PVA coating showed maximum growth of microorganism and thus high absorbance value, indicative of negligible antimicrobial activity.

Similar results are seen with the suspended films in Table 4. It is thus concluded that MFR in solubilises PVA, with good adhering properties as well as renders it antimicrobial. The nanoparticles in the nanocomposite, superimpose the antimicrobial properties of the nanoparticle to the film or the coatings. Comparison of absorbance values for coatings with PVA-MFR-TiO₂ (commercial), and PVA-MFR- TiO₂(nano) particle showed large difference in absorbance indicating the efficacy of nanoparticle as an antimicrobial agent and confirm the presence of nanoparticles in the PVA-MFR-nanocomposites.

Spray coatings of PVA-MFR nanocomposite on food grade aluminium foil

It needs to be mentioned here that food grade foils, and the foil used in packaging industry are essentially a thin film of aluminium coated with a polymer, and hence it is possible to spray coat them or laminate them with PVA-MFR.

Antimicrobial studies on these films reported in Table. 5, show the aluminium foil by itself has zero activity, while films coated with PVA-MFR are antimicrobial and a higher level of enhancement of the antimicrobial activity when foil is coated with PVA-MFR- nanocomposites as can be seen in Figure 13.

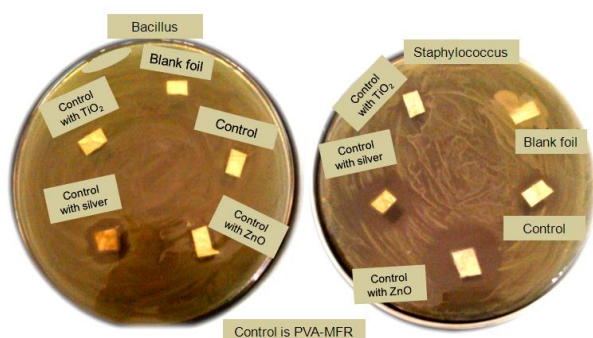


Figure 13. Antimicrobial studies of PVA-MFR Nanocomposite Coatings on food grade Aluminium foil - *Bacillus* and *Staphylococcus*.

Table 5. Antimicrobial studies of PVA-MFR Nanocomposite Coatings on food grade Aluminium foil- Zone of inhibition diameter in cm.

Composite	Microorganism	
	<i>Bacillus</i> / <i>B. subtilis</i>	<i>Staphylococcus</i> / <i>S. aureus</i>
PVA- MFR-Ag	2	2
PVA- MFR-TiO ₂	1.6	1.6
PVA- MFR-ZnO	2	2.3
PVA-MF blank	0.6	1
Blank foil	0	0

These were essentially very thin coatings, obtained by diluting the active composite with methanol before it is cured, hence have very low concentration of nanoparticle, yet antimicrobial efficacy is good with all the nanoparticles. Such prepared coatings can be explored for antimicrobial food packaging applications.

Conclusion

PVA -MFR films are antimicrobial, especially in the case of gram positive bacteria like *S. Aureus* and *Bacillus* that are generally persistent in hospitals, and are a major health hazard, these films sprays and coatings could probably make a cheap and effective material in the hospitals and diagnostic labs where the cultures are prepared. Since the material has good adhesion properties clay pots, glass, polypropylene lab containers, can be coated with PVA-MFR to render them antimicrobial. Paper, jute, raw fabric grain storage bags can be sprayed with or given PVA-MFR coating or else film lining which will not only protect them from moisture but also from microbes, making a better grain storage and food packaging material. The prepared films and coating are stable and retain their activity over a long period. The active composite can be diluted before curing to be used as a spray for uniform, fine antimicrobial coating on food grade aluminium foil and polyester films etc.

Though PVA-MFR films are antimicrobial but films where nanoparticles are immobilised in PVA-MFR matrix, have a large surface to volume ratio and more effective antimicrobial activity. These can be explored for surgical face masks and other medical applications. A very minimal concentration of silver was used in making these films as it remains to be determined if silver nanoparticles will be safe for patients in the long run. In the mean time, due to the evolution of antibiotic resistant bacteria silver nanoparticles remain a hot item and these are incorporated in a number of products ranging from device coatings and wound dressings to commercially available deodorants and cosmetics. Application of PVA-MFR- silver nanocomposite films and coatings as an antimicrobial patch for treatment of highly resistant wounds of diabetic foot diseased patients has been studied, and is being reported separately.

Acknowledgements

Authors would like to thank University Grants Commission (UGC), New Delhi, India for financial support under major research project No.F.40-91/2011 (SR)

References

- Sedlarik, V., Saha, N., Kuritka, I., Saha, P., *Int. J. Polym. Anal. Ch.*, **2006**, *11*, 253.
- Donelli, G., Francolini, I., Ruggeri, V., Guaglianone, E., D'Ilario, L., Piozzi, A., *J. Appl. Microbiol.*, **2005**, *100*, 615.
- Lee, K. Y., Yuk, S.H., *Prog. Polym. Sci.*, **2007**, *32*, 669.
- Elbahri, L., Taverder, J.L., *Polym. Bull.*, **2005**, *54*, 353.
- Kenawy, E.R., Worley, S.D., Broughton, R., *Biomacromol.*, **2007**, *8*, 1359.
- Hwang, M.R., Jong, O.K., Jeong, H.L., Kim, Y., Jeong, H.K., Chang, S.W., Sung, G.J., Jung, A.K., Lyoo, W.S., Sung, S.H., Ku, S.K., Yong, C.S., Choi, H.G., *AAPS. Pharm. Sci. Tech.*, **2010**, *11*(3), 1092-1103.
- Simões, M.M., de Oliveira, M.G., *J. Biomed. Mater. Res. B- Appl. Biomater.*, **2010**, *93* (2), 416-24.
- Rottmann, N., Cech, T., Schmeller, T., *Chimica Oggi / Chemistry Today- Focus on Excipients.*, **2009**, *27*, 5.
- Eisha, G., Kuldeep, G., Pathak, A.K., *Intl. J. Res. Pharm. Chem.*, **2011**, *1*(4).
- Wan, W.K., Campbell, G., Zhang, Z., Hui, A.J., Boughner, D.R., *J. Biomed. Mater. Res.*, **2002**, *63*, B: 854-861.
- Barry, B.W., *Eur. J. Pharm. Sci.*, **2001**, *14*, 101-14.
- Wade Hull, M.S., *J. Appl. Res.*, **2002**, *2*, 1-9.
- Chein, Y.W., "Transdermal drug delivery systems", 2nd ed. Marcel Dekker Inc., **1992**, 301.
- Libermann and Lachman., "Pharmaceutical dosage forms", 2nd ed. Lea and Febiger., **1990**, 265.
- Mohamed, A., Yasmin, S., Asgar, A., *Acta. Pharm.*, **2003**, *53*, 119-25.
- Robert, L. A., E. I. Du Pont De Nemours and Company, *US 4461858 A; Appl. No. US. 06/323,053*; **1984**
- Rosenblatt., *U.S. Pat. No. 6365169*, **2002**.
- Rosenblatt., *U.S. Pat. No. 5,071,648*, **2002**.

- ¹⁹Gong, K., Zhang, X., *MRS fall meeting.*, **1989**.
- ²⁰Gebben, B., Hans, W. A., Berg, V.D., Bargeman, D., Cees A. S., *Polymer.*, **1985**, Vol.26.
- ²¹Wu, K., Song, L., Wang, Z., Hu, Y., *Polymers for Adv. Technologies.*, **2008**, 19(12), 1914–21.
- ²²www.chemyq.com/Patentfmen/pt101/1009552_40132
- ²³Fong, J., and Wood, F., *Int. J. Nanomedicine.* **2006**, 1(4), 441–449.
- ²⁴Chaloupka, K., Yogeshkumar, Alexander, M., Seifalian, M., *Trends in Biotechnology.*, **2010**, 28(11), 580–588.
- ²⁵Menno, L. W., Knetsch and Leo, H., Koole., *Polymers.*, **2011**, 3(1), 340-366
- ²⁶Hewitt, W., “*Microbiological Assays for Pharmaceutical analysis- a rational approach*”, CRC press, Indian Edition, **2004**.
- ²⁷Sulabha. K. K. “*Nanotechnology-Principles and Practices*”, Capital Publishing Company, New Delhi, **2011**.
- ²⁸Vu, T.T., Mighri, F., Do T., Aji, A., *J. Nanosci. Nanotechnol.*, **2012**, 12(3), 2815-24.
- ²⁹Kakkar, R., Sherly, E. D., Kalpana, M., Keerthi Devi, D., and Sreedhar, B., *J. Appl. Poly. Sci.*, **2012**, 126, E154–E161.
- ³⁰Hwang, J.S., Kim, J.N., Wee, Y.J., Jang, J.S., Kim, H.G., Kim, S.H., Ryu, H.W., *Biotechnol. Bioprocess Eng.*, **2006**, 11(14), 332-6.
- ³¹Awang, B., Beng, Y.K., Noor, A., Fong, H. S., *Borneo Sci.*, **2001**, 10, 11-23.
- ³²Peppas, N.A., Tennenhouse, D., *J. Drug. Del. Sci. Tech.*, **2004**, 14 (4), 291-297.
- ³³Robert, L.A., US4461858 A, E.I. Dupont., **1985**.
- ³⁴Meyers, R.A., (ed.), “*Interpretation of Infrared Spectra, A Practical Approach, John Coates in Encyclopedia of Analytical Chemistry*”, John Wiley & Sons Ltd, **2000**, 10815-37.
- ³⁵Mansur, H.S., Oréfice, R.L., Mansur, A.A.P., *Polymer.*, **2004**, 45(21), 7193-202.
- ³⁶Mansur, H.S., Oréfice, R.L., Pereira, M.M., Lobato, Z.I.P., Vasconcelos, W.L., Machado L.J.C., *Spectroscopy - An International Journal.*, **2002**, 16 (3-4), 351-60.
- ³⁷Dyana, J., Merline, S.V., and Ahmed, A. A., *Polymer J.*, **2013**, 45, 413-19.
- ³⁸Wang, D., Zhang, X., Song, L., Li, S., *Advances in Materials Physics and Chemistry.*, **2012**, 2, 63-67
- ³⁹Taleb, A., Petit, C., and Pileni, M.P., *J. Phys. Chem. B.*, **1998**, 102, 2214–20.
- ⁴⁰Vu, T.T., Mighri, F., Do TO., Aji, A., *J. Nanosci. Nanotechnol.*, **2012**, 12(3), 2815-24
- ⁴¹Noginov, M.A., Zhu, G., Bahoura, M., Adegoke, J., Small, C., Ritzo, B.A., Drachev, V.P., and ShalaeV, V. M., *Appl. Phys. B.*, **2007**, 86, 458–60.
- ⁴²Das, R., Nath, S. S., Chakdar, D., Gope, G., Bhattacharjee, R., *J. Experimental Nanoscience.*, **2010**, 5(4), 357–62.
- ⁴³Kokkoris, M., Trapalis, C.C., Kossionides, S., Vlastou, R., Nsouli, B., Grotzschel, R., Spartalis, S., Kordas, G., Paradellis, T., *Nuclear Instruments and Methods B.*, **2002**, 188(1-4), 67-72.
- ⁴⁴Raffi, M., Hussain, F., Bhatti, T.M., Akhter, J.I., Hameed, A., and Hasan, M.M., *J. Mater. Sci. Techn.*, **2008**, 24(2), 192-196.
- ⁴⁵Nelson, G.L., “*ACS Symp. Ser.No. 599*”, Am. Chem. Soc., Washington DC, **1994**.
- ⁴⁶Osiris, W., G., Moselhey, M.T.H., *Natural Sci.*, **2012**, 4(1), 57-67.

Received: 27.11.2014.

Accepted: 12.12.2014.



DETERMINATION AND CORRELATION OF HERBICIDE RESIDUES IN WATER AND SEDIMENTS IN THE STREAMS FLOWING INTO THE CALEDON RIVER USING THE BUBBLE-IN-DROP SINGLE DROP MICRO-EXTRACTION METHOD

Mosotho J. George^[a]

Keywords: bubble-in-drop micro-extraction, hot-water extraction, herbicides monitoring, sediments, farming area, Lesotho

Environmental monitoring of metolachlor and atrazine herbicides in water samples has been reported recently with the use of the “bubble-in-drop single drop micro-extraction” (BID-SDME) method. This study reports the application of this method coupled with the hot-water extraction for the analysis of the residues of these herbicides from the water and sediment samples obtained in the streams running into the Caledon River in the eastern Free State – South Africa. The method was validated for several figures of merit before application to the real samples: it showed sufficient robustness (RSD < 7 % repeatability and reproducibility); sufficient linearity with $0.9991 > R^2 > 0.9978$, accuracy of 98 % using 5 ng mL⁻¹ atraton CRM in water. The results demonstrated that both these herbicides are widely used in the farms as all the streams had detectable levels of at least one herbicide with concentrations ranging from 5 ng mL⁻¹ to about 30 ng mL⁻¹ for water samples and 1 ng mL⁻¹ to 35 ng mL⁻¹ in the sediment samples with some positive correlation between the abundance in the two media ($R^2 = 0.8267$ for atrazine and 0.9012 for metolachlor). The analyte recoveries from the samples relative to HPLC grade water solutions were higher than 90 % demonstrating sufficient recovery. Some related compounds (simazine, terbutylazine and acetochlor) were also detected in some of these samples, although not quantified for lack of appropriate standards.

*Corresponding Authors

E-Mail: jm.george@nul.ls or maluti2005@gmail.com

[a] Department of Chemistry and Chemical Technology, National University of Lesotho, P.O. Roma 180, Lesotho, Southern Africa. Telephone: +266 5221 3502, Fax: +26 2234 0000,

Introduction

In the wake of herbicide pollution and its detrimental effect on biodiversity, there is a lot of research towards development of affordable and quick methods without compromising the effectiveness of such in detecting and monitoring of these herbicides. Some of the deleterious effects of herbicides include carcinogenicity,¹ endocrine activity² and a range of other ailments such as immune suppression, diminished intelligence and reproductive abnormalities.³ However, these chemicals are still very important in agro-industry for control of pests and weeds for increased agricultural and food production. Consequently, this poses a dilemma regarding food security on one hand and a threat to human life and biodiversity of not only amphibians but also of other natural flora and fauna, on the other.^{4,5} Due to these effects and many other associated issues, foods tainted with pesticides lose their competitiveness in the markets;⁶ this is especially so lately when attention seems to shift towards the so-called ‘organic’ foods.⁷ Other than the market related issues, herbicides monitoring could also aid in important issues such as planning crop rotation which sometimes could be dependent on the presence of traces of the herbicides applied in the previous season.^{8,9} There is also a fear that indiscriminate applications of pesticides could also unintentionally destroy

the beneficial pest predators as well as increasing the tolerance and the resulting virulence of some species of agricultural pests due to excessive exposure.¹⁰

A number of extraction techniques have been developed with reported improvements in any of the performance phenomena such as efficiency, degree of complexity, practicality, just to mention a few, prior to the most common analytical techniques – gas and/or liquid chromatography with various detectors.^{11,12}

In the advent of miniaturisation, solvent micro-extraction has also evolved from classical solvent extraction where copious amount of hazardous organic solvents are used to the drop-based methods all of which are reported to improve on any of their predecessors in terms of at least one of the attributes such as mass transfer rate, extraction efficiency, ease of handling, selectivity, automation, just to mention but a few as reported by the recent review.¹³ However this review seems to be oblivious of one of the simplest modification reported by Williams *et al.*¹⁴ where the intentional incorporation of the air-bubble into the droplet reportedly improved extraction rate hence efficiency by 150 % over a simple single-drop micro-extraction. The related air bubble modification was reported Farajzadeh *et al.*¹⁵ few months later, albeit for a different purpose - to aid dynamic extraction without stirring the mixture.

Agriculture production in South Africa is the highest regionally, with its associated use of these hazardous agro-chemicals for improved yields per unit area. As such herbicide monitoring in the streams in the agriculture dominated areas such as the Free State Province is very important.

The importance of monitoring in the streams flowing into the international rivers is reported as one of the critical issues, especially in the areas where there is scarcity of clean water resources with some predicting a third World war to be likely over water and not oil.^{16,17} The Caledon River, an international boundary between South Africa and Lesotho, is very important because it provides a source for municipal water supply in Maseru, a capital city of Lesotho, where pesticide application is very minimal owing to the lack of commercial farming and to some extent also lack of most agricultural pests. Assessment of the Caledon River water quality around the Maseru metropolis revealed presence of high levels of agro-based chemicals such as phosphates and nitrates which could only be attributed to the commercial farming in the South African side of the border.¹⁸

This manuscript reports the assessment of the herbicides (metolachlor, atrazine and their related herbicides) residues in the sediment and water samples in the streams running into the Caledon River on the eastern border of the Free State Province of South Africa with Lesotho (see Figure 1) using the bubble-in-drop single-drop micro-extraction method coupled to gas chromatography mass spectrometry. The samples used in this work included both sediments collected from some of the permanent streams as well as those that only run during rains, some of which seemed artificial for purposes of guiding water flow during heavy rains to avoid flooding.

Experimental

Reagents and chemicals

The pesticides, metolachlor (MET), atrazine (ATRZ) and their deuterated (²H) analogues (100 µg mL⁻¹ in 1 mL ampules each), were obtained from Dr Ehrenstorfer GmbH (Augsburg, Germany). Diphenylamine (DPA), and desethylatrazine (DEA) (100 µg mL⁻¹) were obtained from Chem Service (Pennsylvania, USA), while chloroform, methanol and water (all HPLC grade) were obtained from Riedel de Haën (Seelze, Germany). Sodium chloride (AR grade) was obtained from Sigma-Aldrich (Seelze, Germany).

Standard solutions

The H-standards of 100 µg mL⁻¹ atrazine and metolachlor, respectively, were mixed together and diluted to 1 µg mL⁻¹ in MeOH and kept in a freezer at -5 °C. The deuterated (²H) standards for the same herbicides were prepared and stored in the same manner. The breakdown product, DEA was also mixed with atrazine and metolachlor to prepare a 1 µg mL⁻¹ standard mixture in MeOH and the mixture was kept in the same freezer. The working solutions were prepared by dilution of these stock solutions. Reference solutions were prepared by dilution of the stock solution with methanol and injected directly (1 µL) into the instrument. For the extraction procedure, 0.1 g portions of NaCl were added to the aqueous solutions to make 10 % NaCl aqueous solutions. The 100 ng mL⁻¹ diphenylamine solution was prepared by dilution from the 100 µg mL⁻¹ solution with chloroform, used as the extracting solvent for the BID-SDME method with the diphenylamine employed as an internal standard.

Instrumentation

A calibrated gas-tight Hamilton GC syringe (Seelze, Germany) (10 µL) was used for sampling and injections. Analyses were carried out using a Shimadzu (Kyoto, Japan) QP2010 gas chromatograph coupled to mass spectrometry (GC-MS) equipped GC-MS Solution® was fitted with a Zebron 35MS column with 30 m x 0.25 mm x 0.25 µm dimensions. Pure helium (99.999 %, Afrox, South Africa) at a constant flow rate of 1 mL/min was used as the carrier gas. Injections (1 µL) were carried out in the splitless mode; after 2 minutes, a split ratio of 1:10 was maintained throughout the runs. The injection port and the transfer line were maintained at 250 °C. The oven programming included an initial temperature of 100 °C (held for 4 minutes), the temperature increased by 50 °C min⁻¹ to 200 °C, then ramped by 10 °C min⁻¹ to 280 °C and held for 5 minutes. The total time for one GC run was 17 minutes.

The mass spectrometer (EI 70 eV and 1.5 kV at 200 °C ion source temperature) was set up on the scanning mode with mass range 50-350 mass units for the monitoring experiments. The ions of interest were extracted out of the total ion chromatogram as follows: 162 (166), 169, 172 and 200 (205) for MET, DPA, DEA and ATRZ respectively (the values in the parentheses represent the ²H analogues). The MS was set on the selected ion monitoring SIM mode embedded in the GC-MS Solution® software of the QP2010 GC-MS instrument using the same ions as listed above together with their respective qualifying ions (215 and 238 for ATRZ and MET, respectively), otherwise the MS was always used on scanning mode using the extracted ion monitoring (EIM) facility. The detector was switched on between 5 and 13 minutes.

Sample collection, storage and preparation

Water samples were collected in the streams and paddles of water where the flow had stopped along the Caledon River on the South African side between Hobhouse and Ficksburg (see the highlighted area in Figure 1). The samples for Caledon River were collected over the Peka Boarder Post (upstream site) one site downstream around Mokhalinyane on the Lesotho side. The sediment samples were collected from excess run-off deposits just outside running water; alternatively they were collected in the middle of the streams that were no longer running.

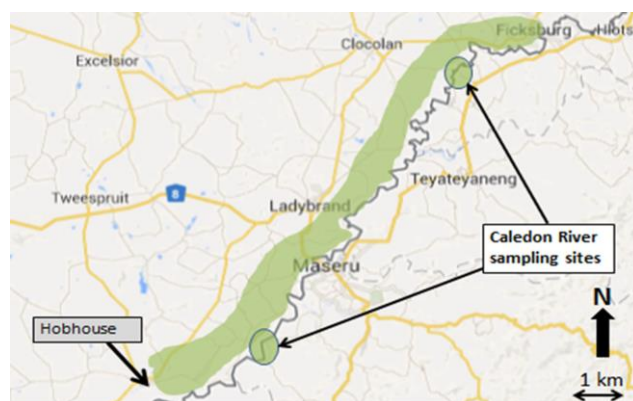


Figure 1. A map of the sampled area showing the Caledon River running from top right to bottom left

Where access was difficult, since most of the area is fenced for security of the farms, the samples were scooped with a Schott bottle attached to a 3 m long stick using a thin piece of wire. These samples were dried in the oven at 40 °C to a constant mass. There dried samples were ground uniformly and stored in a freezer at -5 °C until further use.

Portions of 2 g of air dried soil samples were transferred to sample bottles and doused with 50 µL of 100 ng mL⁻¹ of aqueous deuterated standards solution. Sufficient amount HPLC grade water was added to submerge the samples and shaken gently to avoid lodging too much soil on the sides of the bottle for about 15 minutes. This suspension dried in the oven at 40 °C. After complete dryness the samples were re-dissolved in 2 mL of near boiling HPLC grade water and shaken for about 15 seconds followed by centrifugation to settle the particulate matter, following the procedure outlined by Williams *et al.*¹⁹ A 1 mL aliquot of the clear supernatant liquid was transferred into a vial containing 0.1 g NaCl to make 10 % NaCl ready for the BID-SDME extraction process.

For the recovery the experiments, the relative responses of the deuterated standards of metolachlor and atrazine in the samples were compared to those obtained with that of the HPLC grade water spiked to the same concentration (25 ng mL⁻¹).

Three different solutions were prepared for each sample, and the extraction was performed in triplicates resulting in n = 9. Following assessment of recovery, quantitation of the amounts of the herbicides in the soil was calculated from the calibration curve using the extraction efficiency factor.

Micro-extraction procedure

The set-up for the BID-SDME extraction protocol is reported in detail elsewhere.¹⁴ An aliquot of 1 µL of the extracting solution was drawn into the syringe, followed by 0.5 µL air. These contents were introduced into the aqueous solution by gentle depression of the plunger, causing the air to form a bubble contained within the micro-droplet. Following a period of 20 minutes (under static conditions), the total solvent volume was carefully retracted into the syringe, and injected into the GC-MS.

Analytical performance and validation of the analytical method for the herbicides

The performance of the method was assessed using the aqueous solution of the ¹H-standards at the concentration range 0.5 to 10 ng mL⁻¹. These aqueous samples were extracted with the BID-SDME as previously described using diphenylamine as an internal standard. The linearity and LOD were evaluated from the analytical data obtained from the calibration curve.

The method was validated for accuracy using 5 ng mL⁻¹ atraton (a member of atrazine herbicides) certified reference material in water (Chem Service, Pennsylvania, USA).

Results and discussion

Validation of the method for the different herbicides

Table 1 presents the validation data for the different analytes using the optimised conditions as described in Williams *et al.*¹⁴ The method gave sufficient linearity with correlation coefficient *R*² ranging between the values 0.9979 (atrazine) and 0.9991 (metolachlor).

Table 1. The calibration data showing the intercepts, *R*², slopes and LOD values

Parameter	Metolachlor	Atrazine	Desethylatrazine
Retention time, min	11.98	9.80	9.31
BEF*	1.54	1.49	1.52
Intercept	2.198	0.619	0.974
Slope	44.717	53.978	51.346
<i>R</i> ²	0.9991	0.9979	0.9984
LOD, ng mL ⁻¹ #	0.024	0.013	0.054
Accuracy, % [§]	-	98	-
Reproducibility, % RSD	6.7	7.4	7.1
Repeatability, % RSD	5.8	4.9	6.4

BEF - bubble enrichment factor - ratio of extraction using BID-SDME to simple SDME; #LOD determined using LOD = 3 × Standard Error Intercept/Slope;²⁰ §Determined using atraton using 5 ng mL⁻¹ in water CRM

Determination of the BID-SDME extraction of recovery of the herbicides

The recovery rates of the herbicides were assessed using the deuterated ²H₅-atrazine and ²H₆-metolachlor standards spiked at 10 mg mL⁻¹ and compared to the HPLC grade water-based solutions. The use of DEA, break down product of atrazine, was necessitated by the fact that it was not detectable in the water and the sediment samples alike. The recovery rates are presented in Figure 2 depicted as a difference from the expected 100 % obtained using the HPLC grade aqueous solutions.

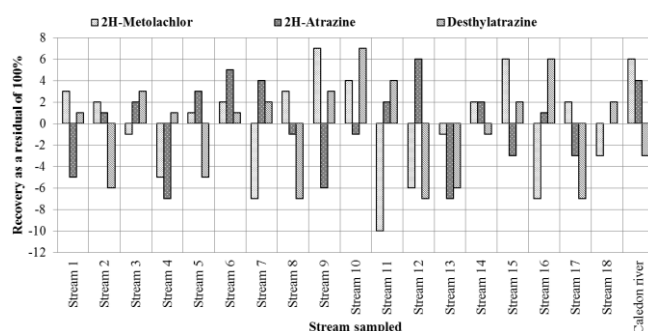


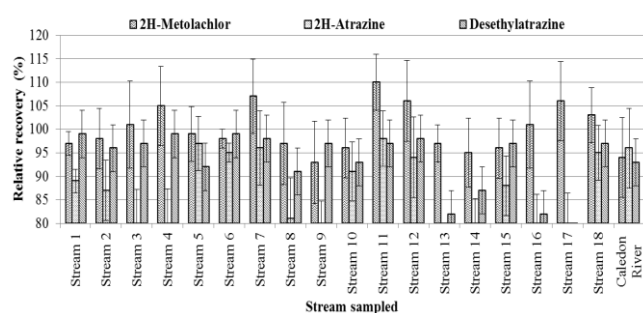
Figure 2. Obtained recoveries of the standards in water samples as residuals of 100 % from extracting HPLC grade aqueous solutions

Figure 3 depicts the relative recoveries (%) of the analytes from the sediment samples for the streams. As can be seen the average recovery for ²H-atrazine (93 %) are significantly better than those reported by Williams *et al.* (70 %).¹⁹ However, it is worth mentioning that the samples where these were collected were significantly different.

Table 2. Some herbicides detected from the water and sediment samples from the streams

Stream	Herbicide identified	Obtained ratio*	Concentration [§]	
			Water (ng mL ⁻¹)	Sediment (ng g ⁻¹)
1, 7 and 12	Metolachlor	1.53 - 1.56	12.5 - 34.0 (8.8)	15.1 - 31.4 (6.9)
	Atrazine	1.45 - 1.47	23.6 (8.9)	18.4 (9.1)
2, 3, 8	Metolachlor	1.49 - 1.53	6.8 - 38.9 (7.3)	12.2 - 23.6 (8.2)
	Acetochlor**	1.64 - 1.66	N/Q [€]	N/Q
	Simazine	1.53 - 1.56	N/Q	N/Q
4, 16, 17	Atrazine	1.43 - 1.47	17.3 - 28.5 (7.3)	21.4 - 18.7 (5.7)
	Simazine	1.52 - 1.55	N/Q	N/Q
5, 6, 9, 14	Atrazine	1.46 - 1.47	33.1 (6.4)	21.0 - 27.4 (8.4)
	Terbutylazine	2.54 - 2.58	N/Q	N/Q
	Metolachlor	1.47 - 1.51	27.7 (6.9)	18.2 - 21.8 (6.7)
	Acetochlor	1.64 - 1.67	N/Q	N/Q
10, 13, 15	Atrazine	1.44 - 1.48	8.7 - 35.2 (6.7)	5.9 - 19.7 (9.3)
	Terbutylazine	2.52 - 2.57	N/Q	N/Q
	Metolachlor	1.49 - 1.52	6.71 - 18.7 (8.9)	0.5 - 17.8 (5.2)
11, 18	Terbutylazine	2.54 - 2.56	N/Q	N/Q
Caledon river 1 & 2 [#]	Not detected	N/A	N/A	N/A

*Ratios obtained from reference to qualifying ions for different ions obtained in the streams; [§]Calculated using the percentage recovery of the deuterated standards and denoted as a range for streams in the entry (values in brackets indicate the average % RSD); [€]N/Q denotes not quantified, these analytes were not quantified due to absence of the appropriate standards; **Suspected from the detection of ions: 223, 162 and 146 with the Ref/Qual ion of 1.67 obtained using 146/223 compared to the standard reported in Findley *et al.*; [#] Collected at Peka/Gumtree Boarder Post (1) and downstream in the Mokhalinyane area (2).

**Figure 3.** Obtained recoveries of the standards in sediment samples relative to HPLC grade aqueous solutions

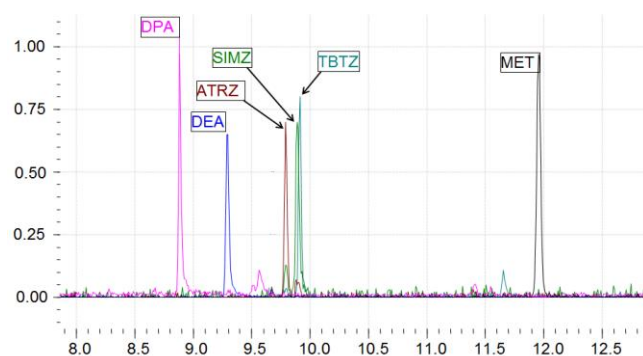
As can be seen the recoveries are significantly high (average 93 %) compared to the stream water samples that averaged 100 % with the combined average % RSD of 6.7.

Monitoring of herbicide residues in the streams and sediments

Figure 1 shows the map of the area where the sampling was carried out. As was stated earlier, all these streams flow into the Caledon River – an international border between South Africa and Lesotho. For identification of the analytes, the NIST Library incorporated into the GCMS Solution[®] of the instrument together with the retention times and the reference/qualifying ratios were used although the library matches resulted in much lower match accuracy as the background increased with the real samples.

The following reference/qualifying ion (Ref/Qual) ratios were used appropriately: atrazine 200/215 (1.43) at 9.80 min, simazine 201/214 (1.56) at 9.91 min, terbutylazine 214/229 (2.59) at 9.92 min (overlapping with simazine, but resolved

through the selected/extracted ion monitoring, see Figure 4) as obtained using the US-EPA mixture TP-619, as well as the addition of metolachlor 162/238 (1.51) at 11.98 min; Desethylazine and diphenylamine were used as atrazine breakdown product and an internal standard respectively as reported elsewhere.²¹

**Figure 4.** A chromatogram showing some of the herbicides detected in the sampled streams

Examination of Table 2 reveals no clear trend between the water and sediment samples. However the plot of the correlation between the water and sediment samples reveals significant correlation with $R^2 = 0.9012$ for metolachlor and $R^2 = 0.8267$ for atrazine (Figure 5). These correlation values indicate that the abundance in the sediment is directly proportional to the abundance in water as would be expected. However, due to the complexity of the dynamics, the correlation was expected to be more unpredictable than the correlation coefficients suggest.

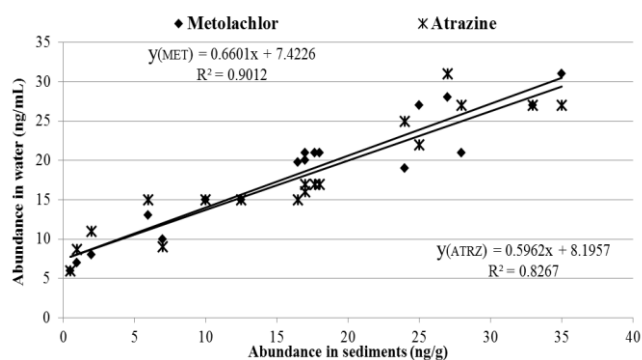


Figure 5. A figure showing the correlation of the abundances between the water and sediments samples

The water samples from the streams reported earlier have shown some decrease in the concentrations (33.1 - 21.7 ng mL⁻¹ compared to 27.7 - 18.7 mg mL⁻¹ for metolachlor and atrazine respectively). Interestingly, this time around some metolachlor related compounds, acetochlor was detected in some streams (2, 5, 6 and 9), although they could not be quantified. It must be mentioned that the intensity of the signals on the chromatograms were very low, although the Ref/Qual ion ratios were still satisfactory as compared to those calculated from Findley *et al.*²²

Discussions and conclusion

This work has complemented the earlier report where the BID-SDME method was applied for the monitoring of the water samples from the five streams flowing into the Caledon River.²² However there was no correlation between these results and those reported earlier as it was already argued therein that the abundance of these herbicides in the streams is dependent on a number of variables such as amount of herbicides applied, weather conditions, soil type, amounts of rain and co-application of other chemicals such as fertilisers that all could affect the herbicides' mobility. These results demonstrate the applicability of the hot-water extraction coupled with the BID-SDME as a highly efficient tool for application to the environmental monitoring of the herbicides (atrazine and metolachlor) in the sediment and soil samples with the sub-nano gram per millilitre (parts per billion) level LODs (0.013 - 0.054 ng mL⁻¹, respectively).

The correlation between the water and sediment samples is quite interesting given that most of the streams flow only during rainy seasons and dry up during dry season. These results in a way further confirm the observation that most agro-based chemicals such as phosphates and nitrates detected in the Caledon River could actually be as a result of run-off from these farms just across the river.¹⁸

The non-detectability of these herbicides in the Caledon River is worrisome given that the streams that feed into this river do contain these herbicides. This suggests that further experiments, possibly using passive samples would be necessary for the monitoring of these herbicides in this important river between the Lesotho and its sole neighbour South Africa.

References

- ¹ World Health Organisation (WHO), *Guidelines for Drinking-Water Quality*, vol. 1. 2nd ed. (Chapter 3). World Health Organization, Geneva **1993**.
- ² Special Report on Environmental Endocrine Disruption: An effects Assessment Analysis, **1997**, Vol. 62(50), 50J
- ³ Abhilash, P. C. and Singh, N., *J. Hazard. Mater.*, **2009**, 165, 1-12
- ⁴ Hayes, T., Haston, K., Tsui, M., Hoang, A., Haeffele, C. and Vonk, A. *Environ. Health Perspect.*, **2003**, 111, 568-575
- ⁵ McLaughlin, A. and Mineau, P., *Agric. Ecosyst. Environ.*, **1995**, 55(3), 201-212
- ⁶ Galt, R. E., *Geoforum*, **2008**, 39(3), 1378-1392
- ⁷ Williamson, S., Ball, A. and Pretty, J., *Crop Protection*, **2008**, 27, 1327-1334
- ⁸ Monks, C. D. and Banks, P. A., *Weed Science*, **1991**, 39(40), 629-633
- ⁹ Stougaard, B., *Northern Agricultural Research Center*, Montana State University, retri. on 14 Oct. 2014 from <http://www.montana.edu/cpa/news/wwwwpb-archives/ag/caryover.html>
- ¹⁰ Wilson, C. and Tisdell, C., *Ecol. Economics*, **2001**, 39(3), 449-462
- ¹¹ Andreu, V. and Picó, Y., *Trends Anal. Chem.*, **2004**, 23(10-11), 772-789
- ¹² Le Doux, M., *J. Chromatogr. A*, **2011**, 1218(8), 1021-1036
- ¹³ Prosen, H., *Molecules*, **2014**, 19(5), 6776-6808
- ¹⁴ Williams, D. B. G., George, M. J., Meyer, R. and Marjanovic, L., *Anal. Chem.*, **2011**, 83(17), 6713-6716
- ¹⁵ Farajzadeh, M. A., Afshar Mogaddam, M. R. *Anal. Chim. Acta* **2012**, 728, 31-38
- ¹⁶ Morissette, J. J. and Borer, D. A., *Parameters*, **2004**, 86-101
- ¹⁷ Gleick, P. H. and Heberger, M., *The World's Water*, **2011**, 175-214
- ¹⁸ Tanor, E. B., Ts'eni, S. and George, M. J., *Euro. Chem. Bull.*, **2014**, 3(8), 776-782
- ¹⁹ Williams D. B. G., George, M. J. and Marjanovic, L., *J. Agric. Food Chem.*, **2014**, 62(31), 7676-7681
- ²⁰ Ribani, M., Collins, C. H., and Bottoli, C. B. G., *J. Chromatogr. A*, **2007**, 1156, 201-205
- ²¹ George, M. J., *PhD Thesis*, University of Johannesburg, Johannesburg, South Africa, **2012**
- ²² George, M. J., *S. Afr. J. Chem.*, **2014**, 67, 56-60

Received: 23.10.2014.

Accepted: 26.12.2014.